The stochastic characteristics of geometric properties of sand waves in the North Sea

M.Sc thesis

M.F. de Koning

May 2007

CE&M research report 2007R-004/WEM-003
ISSN 1568-4652

University of Twente
Enschede - The Netherlands

The stochastic characteristics of geometric properties of sand waves in the North Sea

M.F. de Koning

May 2007

Committee:
Prof. Dr. S.J.M.H. Hulscher
Ir. C.F. van der Mark
Dr. Ir. A. Blom
Drs. A. Stolk

CE&M research report 2007R-004/WEM-003
ISSN 1568-4652

Preface

This report forms the completion of my study Civil Engineering & Management at the Department for Water Engineering and Management, which is part of the Faculty of Engineering Technology at the University of Twente, The Netherlands. The past half year I studied sand waves in the North Sea without actually seeing one and to finish this report I needed the guidance and support of various people.

First I would like to thank the members of my graduation committee dr. ir. Astrid Blom of Delft University of Technology, drs. Ad Stolk of RWS North Sea Directorate, prof. dr. Suzanne Hulscher of the University of Twente and especially ir. Rolien van der Mark of the University of Twente for their support, supervision and enthusiasm.

Further I want to thank the RWS North Sea Directorate for making bathymetry data available for this study. I also want to thank ir. Leendert Dorst of the Hydrographic Service for his help with the implementation of *digipol*.

I would like to thank my fellow students in the 'Aquarium' for the endless discussions, the fun during coffee breaks and of course their support in times of *'nood en ontbering'*. I would also like to thank my friends and team members of Harambee for making my years as a student in Enschede a great time.

Finally, I would like to thank my parents, brothers and my sister for supporting me. Most of all I would like to thank Renate, not only for her patience and kind support, but also for releasing me from the computer screen during weekends and holidays.

Michiel de Koning
Enschede, May 2007

Summary

In shallow shelf seas such as the North Sea several rhythmic patterns occur, among which sand waves are found. Sand waves occur as a result of the interaction between water and sediment. Sand waves can have lengths up to 500 metres and amplitudes up to 5 metres. In literature sand waves are sometimes schematised as regular idealised sinusoidal waves with a mean sand wave length and mean sand wave height. Existing models predict mean values for sand wave height and sand wave length. However, in reality sand waves are irregular in size and shape and three-dimensional in plan view.

For several economic activities, information on mean geometric properties of sand waves is not sufficient. Often additional knowledge is needed on the more extreme values of, for example, the sand wave height or the crest and trough elevations. For navigation for instance, information is needed on the highest sand waves. Knowledge on the variability in sand wave height contributes to a more efficient dredging program. Pipelines and cables, which are buried in the North Sea for transport of fossil fuels and electricity, should not get exposed to the flow and the occurrence of free spans, as a result of migrating sand wave troughs, should be avoided (Németh and Hulscher, 2003). Knowledge on the deepest troughs is therefore important.

In the present research the irregularity in geometric properties of sand waves is investigated by analysing field data from the North Sea. By looking at plan views of different areas, a difference between short crested sand wave fields and long crested sand wave fields is seen. In this study long crested sand waves from the Ecomorf 3 are analysed and also short crested sand wave fields from two areas (Noordhinder and TWIN) are analysed. In the TWIN area dredging takes place, which may affect the stochastics of the sand waves in that area. All the bathymetry data used was obtained in 2003 and the grid size is $5\,\mathrm{m} \times 5\,\mathrm{m}$.

First, the orientation of the sand wave field is determined with the use of the *digipol* method (RIKZ, 1997). In this method the value of the gradient in bed elevation is determined in every direction. The angle at which the highest gradient is found, is assumed to be the orientation of the sand wave field.

With the orientation for the sand waves, longitudinal bed elevation profiles (BEPs) can be taken from the data. The BEPs serve as input for the bedform tracking tool (BTT) developed by Van der Mark and Blom (2007). The longitudinal bed elevation profiles are detrended and filtered in order to determine zero level crossings. The geometric properties of sand waves (sand wave length, sand wave height, crest elevation, trough elevation and asymmetry) are determined for every individual sand wave in the profiles. The output of the BTT consists of

data sets with all the values found for the geometric properties of sand waves.

With the output of the BTT it is possible to plot probability density functions of the different geometric properties of sand waves. The Kolmogorov-Smirnov test is used in order to determine whether a data set is distributed according to a known probability distribution. As the Kolmogorov-Smirnov test cannot compare probability distribution, the total vertical difference between the cumulative density function of the data and a certain probability distribution is determined. The probability distribution with the lowest value is considered as the best fit. The long crested sand waves show a more symmetrical distribution of its geometric properties than the short crested sand waves. Some geometric properties seem to be well represented by one probability distribution, like the sand wave height and the crest elevation. The other geometric properties are closely followed by more probability distributions.

A relationship is found between the standard deviation σ and the mean μ of sand wave height, sand wave length, crest elevation and trough elevation as was found for the wave length and wave height of river dunes (Van der Mark et al., 2005). The standard deviation divided by the mean value equals the coefficient of variation C, which is more or less a constant for the short crested sand wave fields. This constant value means that, given this constant, the standard deviation in, for instance, sand wave height in a short crested area can be modelled by only predicting the mean sand wave height. Only one area with long crested sand waves could be analysed and therefore this relation is not found for the long crested sand waves.

For every data set and all the different geometric properties of the sand waves it is determined if the lowest 5% percent of the values or the highest 5% percent are analysed. First the distance between the extreme values and the mean was calculated and divided by the standard deviation. This results in the variables a and b for the distance between Δ_5 and the mean and the distance between Δ_{95} and the mean, respectively. A variable E is introduced as the relation between the a and b. For every geometric property it is determined if the highest values or the lowest values are more distant from the mean values.

The extreme values can be predicted for sand wave height with the mean value μ and standard deviation σ. This can be done for short crested sand waves and long crested sand waves. Given the constant variables a and b, the Δ_5 and Δ_{95} can be predicted. With the relation between the standard deviation and the mean value for sand wave height only the mean value is needed to predict the extreme values.

Contents

List of Figures

List of Tables

List of Symbols

a	[-]	the distance δ_5 expressed in the standard deviation, determined by δ_5/σ
A	[-]	asymmetry of sand wave
b	[-]	the distance δ_{95} expressed in the standard deviation, determined by δ_{95}/σ
B	[-]	bifurcation number
c	[-]	the distance δ_{99} expressed in the standard deviation, determined by δ_{99}/σ
C	[-]	coefficient of variation determined by $\lvert\sigma/\mu\rvert$
E	[-]	relationship between the high and the low extreme values
$\lvert\overrightarrow{G}\rvert$	[-]	gradient vector in a grid point
H	[m]	bed elevation
L	[-]	sum of all the gradient vectors
L_c	[m]	bedform length between crests
L_l	[m]	length of lee side
L_s	[m]	length of stoss side
L_t	[m]	bedform length between troughs
n	[-]	number of the quantity of a data set
$\mathbb{P}$	[-]	unknown distribution of a data set
$\mathbb{P}_0$	[-]	a particular probability distribution
$P(x)$	[-]	cumulative distribution function of a data set
$P_0(x)$	[-]	cumulative distribution function of a particular probability distribution
s	[-]	skewness of a probability distribution
S	[-]	the total positive difference between the CDF of the data $\mathbb{P}$ and the CDF of a probability distribution $\mathbb{P}_0$
x	[m]	coordinates in the bathymetry data sets in Eastern direction
y	[m]	coordinates in the bathymetry data sets in Northern direction
z	[m]	bed elevation in the bathymetry data sets
α	[°]	angle of the orientation of a sand wave field
β	[°]	angle between $\lvert\overrightarrow{G}\rvert$ and the line it is projected on
δ_5	[m]	distance between the value of Δ_5 and the mean value
δ_{95}	[m]	distance between the value of Δ_{95} and the mean value
δ_{99}	[m]	distance between the value of Δ_{99} and the mean value
Δ_5	[m]	value for which 5% of the values is smaller
Δ_{95}	[m]	value for which 95% of the values is smaller
Δ_{99}	[m]	value for which 99% of the values is smaller
Δ_l	[m]	bedform height from crest to the next trough
$\Delta y'$	[m]	step size in the BEPs drawn in the bathymetry data
η_c	[m]	crest elevation
η_t	[m]	trough elevation
μ	[m]	mean value of a data set
σ	[m]	standard deviation, a measure of the spread of the values in a data set

Chapter 1

Introduction

Beds in rivers or marine environments are hardly ever flat, as they are often covered with rhythmic bedforms. The occurrence and development of these bedforms are due to the interaction between water and sediment. Examples of these bedforms are river dunes in the Dutch Rhine branches and sand waves in the North Sea. Within this research only the marine environment is taken into account. This chapter gives an outline of sand waves in shallow shelf seas such as the North Sea. Sand wave formation, sand wave occurrence and the migration of sand waves in the North Sea are described. In most studies sand waves are considered as regular rhythmic bedforms. However in reality rhythmic bedforms such as sand waves show irregularity in size and space. Therefore the focus in this study is on a stochastic approach towards sand waves. In this chapter the relevance of this study is discussed. Furthermore the problem definition is determined and the objectives of this study are given. Finally the methodology of this study is described.

1.1 Sand waves

The rhythmic bedforms that cover the seabed have been investigated intensively. Table 1.1 shows the geometric properties of the patterns found in the North Sea as described by Morelissen et al. (2003): tidal sand banks, long bed waves, sand waves, megaripples and ripples. These bedforms are often considered to be regular patterns. They appear as patches of varying size that may overlay each other. Sand waves have wave lengths up to 500 metres and an amplitude up to 5 metres. The formation of sand waves takes up to a few years and sand waves are known to migrate up to 10 metres a year.

Table 1.1: Bedform patterns (Morelissen et al., 2003)

Pattern	Wave length (m)	Amplitude (m)	Migration	Timescale
Tidal sand banks	~ 5000	~ 10	~ 1 m/year	century
Long bed waves	~ 1500	~ 5	unknown	unknown
Sand waves	~ 500	~ 5	~ 10 m/year	years
Megaripples	~ 10	~ 0.1	~ 100 m/year	days
Ripples	~ 1	~ 0.01	~ 1 m/day	hours

1.1.1 Formation and occurrence

Sand waves are found where sand covers the seabed. Sand waves are not found at locations where the seabed is predominantly mud. Sand waves are generated by the interaction of the tidal motion and the sandy seabed. Sand waves and sandbanks only occur in areas where depth-averaged tidal velocities are higher than 0.6 m/s (McCave, 1971). Van der Veen et al. (2006) state that above the critical value of 0.5 m/s, sand waves are observed.

Sand wave fields are known to exist all over the world in tidal shallow seas. Within this research the focus will be on sand waves and their geometric properties in the North Sea. The North Sea is relatively shallow, having an average depth of about 100 m, but a large part is much shallower. The tidal currents have a great influence on the hydraulic conditions in a shallow sea. An area of 15.000 km^2 off the Dutch coast is covered with sand waves (McCave, 1971; Brown et al., 2002). Figure 1.1 shows the location of observed sand waves in the North Sea.

In this study data sets from the North Sea are analysed. Sand waves are also found in the Persian Gulf, the Korean Sea (McCave, 1971), the Bisanseto Sea in Japan (Knaapen and Hulscher, 2002), the Gulf of Cadiz in Spain (Nelson et al., 1993) and the San Francisco Bay (Barnard et al., 2006). Figure 1.2 shows measurements of sand waves in the San Francisco Bay.

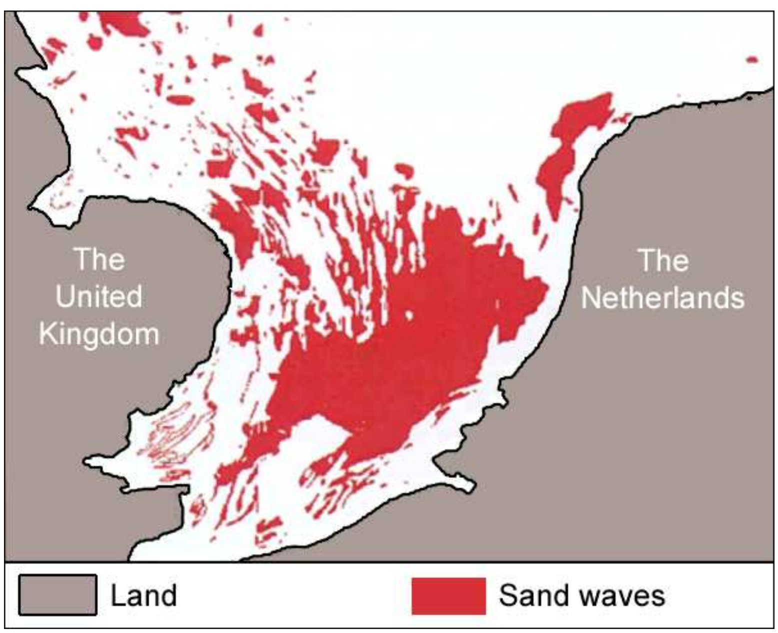

Figure 1.1: Observed sand waves in the North Sea (Hulscher and Van de Brink, 2001).

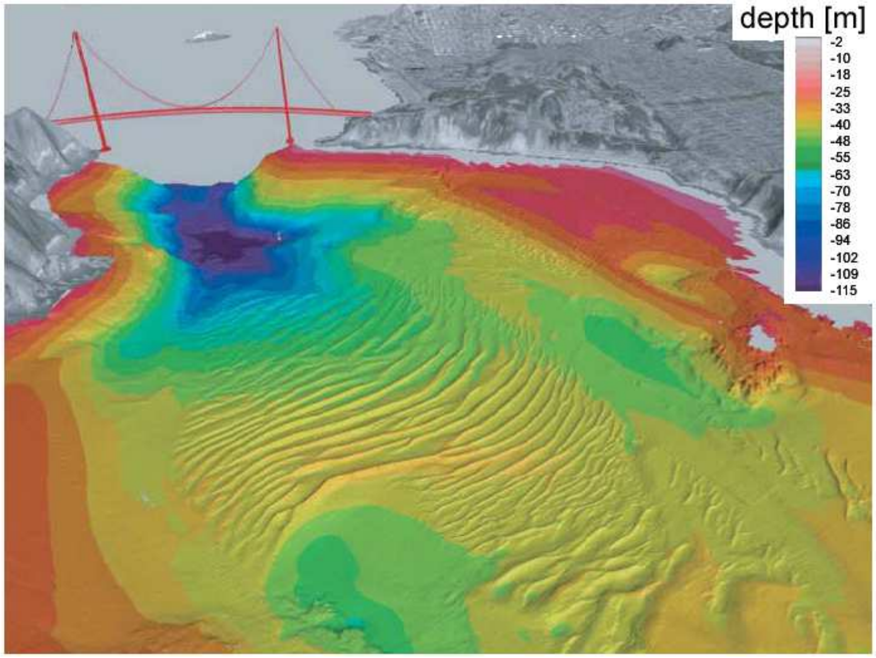

Figure 1.2: Oblique view of measured sand waves and other bed forms at the mouth of San Francisco Bay (Barnard et al., 2006).

The generation of sand waves in shallow seas has been studied by various researchers. Hulscher (1996) modelled the interaction between a tidal flow and the seabed. Sand waves are described as free instabilities in a system of a sandy bed and a tidal flow. Vertical vortices play a crucial role in the generation of sand waves. Averaged over the tidal cycle, small vertical net circulation flow occurs (Figure 1.3). A net transport to the crests may occur, which causes the perturbation to grow. This process can be described using a linear stability analysis. Small perturbations of the sea floor cause small perturbations in the flow field and vice versa. The system is called unstable if the perturbations grow, and the system is called stable if disturbances disappear in time.

Hulscher and Van de Brink (2001) tested observations of sand banks and sand waves against the morphologic model. The model is able to predict contours of sand wave fields, but within

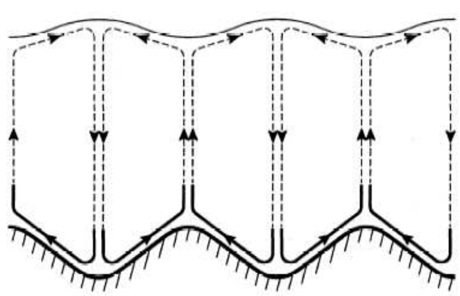

Figure 1.3: Strong near bed circulation which supports the growth of the bottom perturbation. The backward circulation in the upper flow part uses a larger part of the water column and is weaker (Hulscher, 1996).

these fields the sand waves could not be predicted correctly. The type of bed deposit turned out to be important in the occurrence of sand waves. From the observations in the North Sea and the model it has appeared that fractions of gravel or mud in the bed lead to the absence of sand waves. Van der Veen et al. (2006) state that, due to the presence of gravel, only small patches of sand waves are found at locations where a large sand wave area is expected.

Sand waves in the Bisanseto Channel in Japan, studied by Knaapen and Hulscher (2002), reduce the navigation depth considerably and as a result they need to be dredged. After dredging these sand waves tend to regenerate. The costs of repeated dredging are significant and more knowledge about regeneration is needed to reduce these costs. In the North Sea only individual large sand waves have been topped off by dredging (Knaapen and Hulscher, 2002) or the sand is only moved from the top of a sand wave to a lower area, which is called hydraulic dredging (Stolk, 2006). In navigation channels sand waves tend to regenerate, but are dredged away before they do (Stolk, 2007). In navigation channels dredging activities take place quite frequently (Hoogewoning and Boers, 2001; Wüst, 2007).

It is generally accepted that sand waves are subject to seasonal changes in sand wave height (Tobias, 1989). This change in sand wave height is due to an increase in surface wave activities in the winter. The increased wave activity leads to erosion of the sand wave crests. Heavy storms result in a reduced sand wave height (Van Maren, 1998).

1.1.2 Migration

Migration of sand waves is hard to measure, since the migration rates are small compared to the measurement errors. Publications on observed migration are scarce (Knaapen, 2005). Sand waves are assumed to migrate in the direction of the residual current. Németh et al. (2002) modelled the physical mechanisms that may cause migration. They split the tidal current in a steady residual current and a sinusoidal tidal motion. It appears that the tidal currents are the main mechanism responsible for the formation of sand waves, whereas the steady current causes sand wave migration. Németh et al. (2002) found that asymmetry in the bed shear stress has a larger effect on the migration than the flow velocity. Rates of migration and wave lengths found by Németh et al. (2002) agree with theoretical and empirical values reported in the literature.

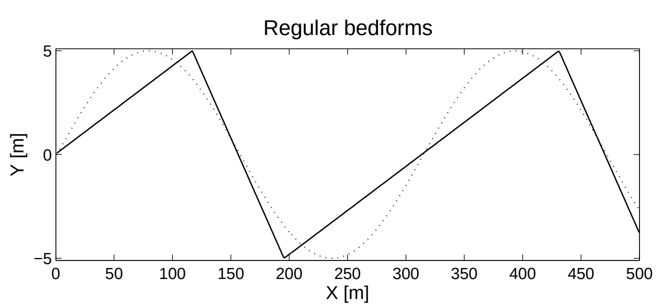

Figure 1.4: Longitudinal profile of simplified shaped bedforms. The flow is to the right.

Knaapen (2005) developed a mean sand wave migration predictor based on median shape characteristics. The difference in the migration rate between a group of sand waves at one location and a group of sand waves at another location is larger than the difference between sand waves within one migrating group. Therefore Knaapen (2005) assumes that sand waves migrate as a group. Knaapen (2005) determines sand wave migration rates from the change in the crest position deduced from long time series of echo-sound data on bathymetry. The crests are defined as the extremes in a profile, in which ripples and megaripples are filtered out. Knaapen (2005) finds a consistent migration rate of several metres per year.

A strong correlation between the median sand wave shape and the mean migration rate is translated into a migration predictor. The predictor assumes that the sand waves migrate in the direction of the steepest slope, following a quadratic relation with the asymmetry. Furthermore, it is concluded that sand waves with a longer wave length travel faster, while higher sand waves travel slower (Knaapen, 2005).

1.2 Irregularity of sand waves

Sand waves are morphodynamic features and have a significant effect on the human activities taking place in the North Sea. In order to be able to predict bedform dynamics and other processes influenced by sand waves, it is important to get insight in the behaviour, geometric properties and spatial distribution of the bed patterns. Bedforms show irregularity in height, length and shape. Irregularity of sand waves is discussed in this section.

1.2.1 Shape and symmetry

Sand waves are often schematised as a sine wave or sawtooth function (Figure 1.4). According to Morelissen et al. (2003) and Van Dijk and Kleinhans (2005), in the North Sea the crests of sand waves are not always in the middle of the sand wave length, but sand waves may also look like the sawtooth function in Figure 1.4. The lee and stoss side do not have the same length. The lee side is steeper and shorter than the stoss side.

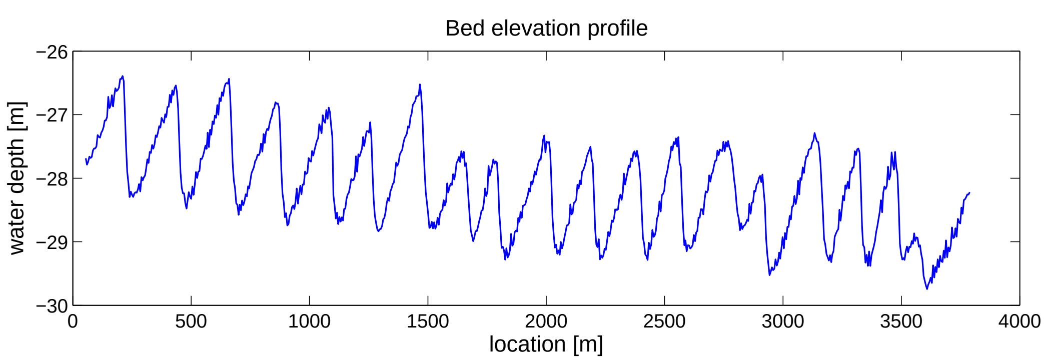

Figure 1.5: Longitudinal bed elevation profile of a sand wave field in the North Sea (Ecomorf 3 area).

In reality bedforms are not as regular as shown in Figure 1.4, but look more like Figure 1.5. This figure shows a longitudinal bed elevation profile that is taken from a sand wave field in the North Sea. Figure 1.6(a) shows this sand wave field in plan view. Although this plan view looks regular, Figure 1.5 shows that in this sand wave field the sand waves are asymmetric and irregular in size.

1.2.2 Short crested sand waves and long crested sand waves

Besides irregularity in size and shape, sand wave fields also show irregularity in plan view. Figure 1.6(a) shows sand waves at the Ecomorf 3 location and Figure 1.6(b) shows sand waves from a selected location (R0302D) from the Noordhinder area. The total Noordhinder area is 19×17 km and the Ecomorf area is 2.4×5.2 km. Figure 1.7 shows where the locations are found in the North Sea. Sand waves at the Noordhinder location are more irregular in plan view and show more bifurcations in the sand wave crests than the Ecomorf 3 sand wave field.

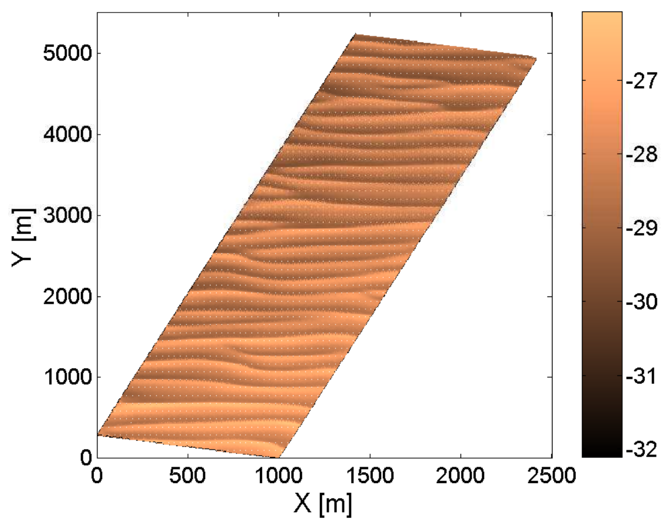

(a)

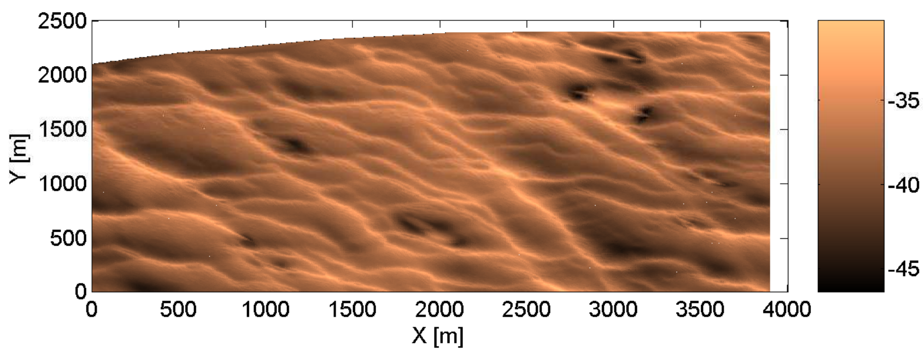

(b)

Figure 1.6: The difference between short crested and long crested sand waves. (a) A plan view of the long crested sand waves at the area Ecomorf 3 in 2002. And (b) a plan view of irregular short crested sand waves in a selected area in Noordhinder in 2003.

Sand waves can be classified as long crested or short crested (Bijker, 2006). Short crested sand waves can be compared to wind generated surface waves. Long crested sand waves are more comparable to sea swell waves at the water surface. Sea swell waves are not influenced by the wind and their length and amplitude are stretched and their height is declined compared to the wind waves (Bijker, 2006). Figure 1.6(a) gives an example of long crested sand waves and Figure 1.6(b) shows an example of short crested sand waves.

In a long crested sand wave field, sand waves have crests more or less parallel to the other crests in the sand wave field. In plan view (Figure 1.6) the bifurcations of the crest lines are visible. A bifurcation is a location where the sand wave crest line splits into two or more crest lines. Long crested sand wave fields show less bifurcations than short crested sand wave fields. This makes the extraction of longitudinal bed elevation profiles more justified than in extracting profiles from a short crested sand wave field. The field can be considered 1D when the crests are parallel to each other (Bijker, 2006).

To determine whether a sand wave field may be short crested or long crested we count the number of bifurcations in the area. The number of bifurcations is divided by the surface of the area. This variable is called the bifurcation number B and gives the number of bifurcations per square kilometre. The different areas can now be compared in their irregularity in plan view. The bifurcation number is calculated for the study areas in the next chapter. The

Figure 1.7: Locations of bathymetry data sets in the southern North Sea.

bifurcation number gives an indication whether an area is short crested or long crested. The sand wave length is different in the various study areas. We have to keep this in mind when interpreting the bifurcation number. The sand wave length influences the number of bifurcations per square kilometre.

1.2.3 Stochastics of bedforms in rivers en flumes

Various studies into stochastic characteristics of bedforms in rivers and laboratory flumes will be discussed in this section (see Table 1.2). There will be attention towards definitions and relationships of different stochastic characteristics. Based on visual judgement of density functions, researchers state that some geometric properties of bedforms are distributed according to a known probability distribution function. The results of these studies are compared to the probability distributions that correspond with the distribution of the geometric properties in this study.

In most studies the so-called zero-crossing method is used to determine crest and trough locations in a longitudinal profile of measured bed elevations. Figure 1.8 shows how the crossings of the bed elevation profile with the mean bed level are identified. The local maxima or minima between individual pairs of crossings are used to determine bedform definitions. The statistical distribution of bedform wavelength, positive and negative wave amplitudes and dune height are determined (Yang and Sayre, 1971).

Nordin and Algert (1966) were the first to analyse the longitudinal profiles statistically. They used autocorrelation techniques and spectral density functions to analyse and describe the characteristics of bed patterns in a laboratory flume. They considered bed elevation as a function of the distance along a laboratory flume. The variance of the process appeared to be related to the average height of the highest crests. Ashida and Tanaka (1967) also used spectral density functions for bed elevation of a laboratory flume both in time and in space in order to determine the probability distributions of the sand waves characteristics. The sand wave lengths and amplitudes were visually considered to follow the Rayleigh distribution.

After analysing an extensive amount of data from flume experiments Squarer (1970) concludes that bedform processes are nondeterministic and need to be measured and analysed as

Table 1.2: Studies into stochastic characteristics of bedforms

		Probability density distribution of:	
Study	**Data**	**wave length**	**wave height**
Nordin and Algert (1966)	Laboratory flume	-	-
Ashida and Tanaka (1967)	Laboratory flume	Rayleigh	Rayleigh
Yang and Sayre (1971)	Laboratory flume	-	-
Nordin (1971)	Field & laboratory	Exponential	Rayleigh
Annambhotla et al. (1972)	Missouri River	Exponential	Exponential
Mahmood and Ahmadi-Karvigh (1976)	Canals Pakistan	Normal	-
Cheong and Shen (1976)	Field & laboratory	Gamma	-
Shen and Cheong (1977)	Field & laboratory	-	-
Wang and Shen (1980)	Laboratory flume	Weibull	Gamma
Leclair et al. (1997)	Laboratory flumes	-	Gamma
Van der Mark et al. (2005)	Laboratory flumes	-	-

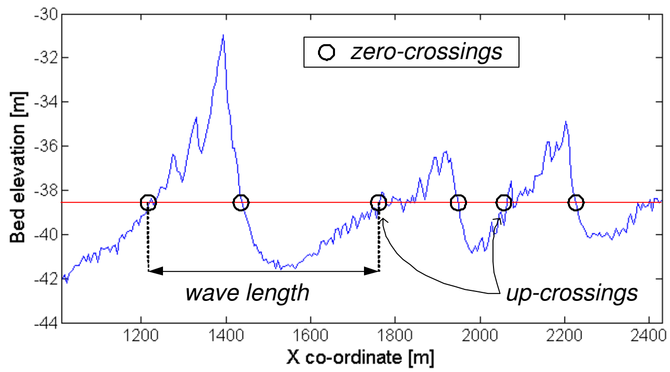

Figure 1.8: Definition sketch of bedform definitions, based on zero crossings (Yang and Sayre, 1971). The flow is directed to the right.

stochastic data. Four main types of statistical functions have been used to describe the bed elevation in space and in time: mean-square value; probability density functions; autocorrelation functions; and power spectral density functions. The mean-square value is a statistical measure of the magnitude of a varying quantity. It is especially useful when variates are positive and negative. Reliable measures of characteristic bedform height and length can be obtained from the spectral density and the autocorrelation functions.

Yang and Sayre (1971) analysed laboratory flume experiments in one dimension, as the movement of sediment in an alluvial channel is irregular and random. Figure 1.8 shows in what way the mean bed level and sand wave length were defined. Series of laboratory flume experiments were conducted to investigate the movement and longitudinal dispersion of particles along the flume, and the penetration of particles into the bed. Statistical analyses of bed configuration data were made to find the mean rest period of tracer particles. Yang and Sayre (1971) found that the distribution of bed elevation in space and time closely follows the normal distribution.

Nordin (1971) used the same definitions as shown in Figure 1.8. Data was collected in laboratory flumes and bed elevations in space and time were analysed statistically. The analyses show that bed elevation can be approximately represented as a Gaussian process, as was found by Yang and Sayre (1971). Nordin (1971) found that dune lengths were exponentially distributed and dune heights followed the Rayleigh distribution.

Annambhotla et al. (1972) determined definitions in the same way as in Figure 1.8. Field data from the Missouri River were used to study longitudinal bed elevation profiles. This data was obtained using an echo sounder mounted on a boat. The longitudinal measuring density was nonuniform as the boat was unable to keep a constant speed. This may have affected the results. Methods used were the autocorrelation and probability density functions. They also analysed the distance between zero-crossings and the amplitude. Bed elevations were found to be distributed approximately according to the normal distribution. Wave lengths and amplitudes were all found to be distributed in accordance with the exponential distribution.

Mahmood and Ahmadi-Karvigh (1976) used definitions as shown in Figure 1.8. Bedform characteristics of field data from channels in Pakistan were analysed through autocorrelation and spectral density functions. Using the spectral density functions of the bed elevation data, the dominant wave characteristics were determined. Wave lengths appeared to be normally distributed. This differs from the earlier studies where the wave lengths were found to follow the exponential distribution or the Rayleigh distribution. Mahmood and Ahmadi-Karvigh (1976) did compare their results with various frequency distributions and tested their results using the Kolmogorov-Smirnov test (KS test). The KS test is used to determine whether two probability distributions differ, or whether a data set follows a hypothesised distribution. Mahmood and Ahmadi-Karvigh (1976) concluded that the normal distribution corresponded with distribution of the sand wave length.

Cheong and Shen (1976) defined the crossings of the bed profile the same way as the previous studies. Comparing this study with the studies described above is however hard to do, since the analysed geometric properties differ from the previous studies. Successive zero-crossings were analysed, rather than the wavelengths in data sets from the Missouri River and laboratory data. They were analysed using spectral density functions and frequency histograms were created. The intervals between successive zero crossings of filtered sand bed profiles were found to be well represented by the gamma distribution. Table 1.2 shows that the wavelengths follow a gamma distribution, but the actual geometric property is the distance between successive zero crossings. This means that the Cheong and Shen (1976) analysed approximately half of the dune length instead of a full dune length.

Shen and Cheong (1977) examined spectral similarity among bed form data collected in the field and laboratory over a broad range of hydraulic conditions. Frequency analyses of bed elevations in time and space showed that the bed elevations may be approximately represented by a Gaussian (or normal) distribution. Wang and Shen (1980) conducted a series of flume experiments and found that the variation in dune height could be described by a Weibull distribution. The variations of both dune length and upstream angle is described by the gamma distribution.

Leclair et al. (1997) studied cross strata data sets in laboratory flumes. Leclair et al. (1997) plotted histograms of dune height, trough elevation and the mean bed-height. Smaller superimposed dunes were filtered out of the data by determining a minimal value for the sand wave length. Sand wave length is defined as the distance between two troughs. Dune height is determined as the distance between a trough and the downstream crest. The trough elevation is defined as the lowest values below a down-crossing and an up-crossing of the mean bed level. Leclair et al. (1997) fitted gamma distributions over the histograms based on least squares minimisation techniques for fitting. The dune height and trough elevation were considered to be well represented by the Gamma distribution.

Van der Mark et al. (2005) analysed the variability of geometric properties of bedforms for three sets of flume experiments, considering probability density functions of bedform height, trough elevation and crest elevation divided by mean values for these parameters. Their definition of geometric properties of bedforms is given in Figure 1.9. Van der Mark et al. (2007) analysed the stochastics of river dunes using a larger quantity of data from flume experiments and field data. It appears that the ratio of standard deviation to mean value (coefficient of variation) of the bedform height is within a narrow range for nearly all experiments. This appears to be valid for trough elevation and crest elevation as well. Van der Mark et al. (2005)

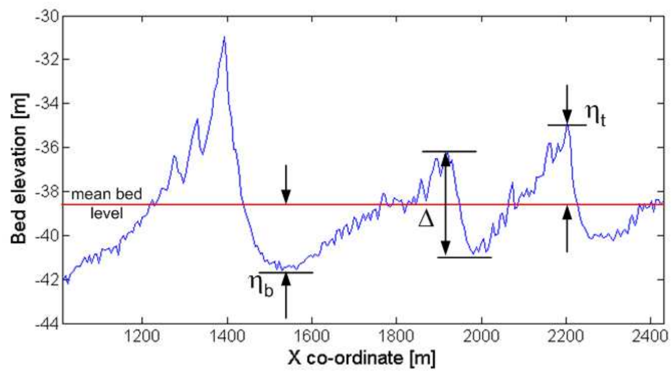

Figure 1.9: Definition of geometric properties of the bedform (Van der Mark et al., 2005). The flow is directed to the right.

state that for some modeling purposes, it seems sufficient to assume that the coefficient of variation as a constant, so that the variation in the geometric properties of the bedform is known when the mean geometric properties of the bedform are known. However, in other cases more detailed information may be needed about the variability in geometric properties of the bedforms.

1.3 Relevance

The North Sea is enclosed by densely populated industrialised countries. As much as 80 million people live in a radius of 150 km around the North Sea coast. A lot of activities take place in the North Sea: navigation, fishery, tourism, industry, oil and gas mining, sand and gravel mining and monitoring. Other user functions in the North Sea are windmill parks, pipelines and cables (Stolk, 2000). Human interventions in the North Seabed influence the morphology. In the current section the activities will be outlined in order to get more insight in the activities that take place on the North Sea. For several economic activities, information only on mean geometric properties of bedforms is not sufficient. Often also knowledge is needed on the more extreme values of, for example, the bedform height or the crest and trough elevations.

In navigational charts the minimum water depth is used. This means that the shallowest point in a channel or area is determined as the water depth available for navigation. The amplitude of sand waves can reach 5 m and they are subject to migration. As a result sand waves may interfere with navigation channels and entrances to ports. Therefore the seabed is monitored by the Directorate North Sea of the Dutch Ministry of Transport, Public Works and Water Management *(Rijkswaterstaat)* and the Hydrographic Service of the Royal Netherlands Navy. If sand waves reach an unacceptable level due to migration or growth, they hinder the navigation and are dredged.

Knowledge about the migrating sand waves and their extreme values of sand wave height is important. The highest sand waves interfere with navigation most. Therefore knowledge about only the mean value is not sufficient. The Port of Rotterdam in the Netherlands is the largest port connected to the North Sea and one of the biggest seaports in the world,

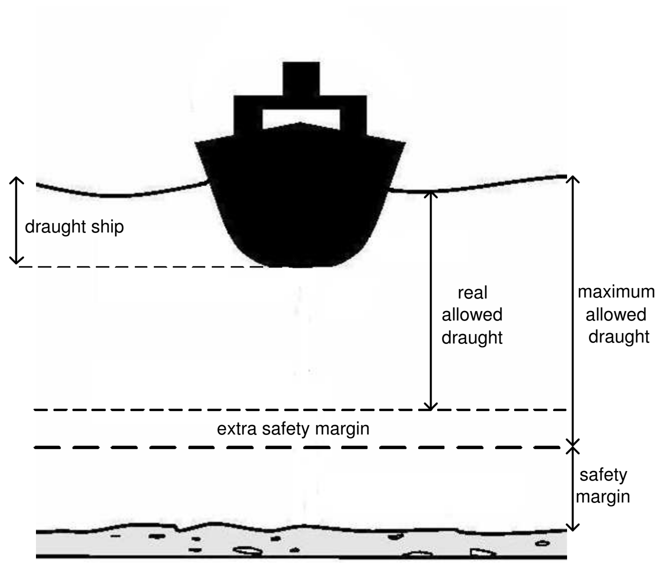

Figure 1.10: Allowed draught of ships and the safety margin (Wüst, 2007).

with a transhipment of 370 million tons of goods in 2005 (Havenbedrijf Rotterdam, 2006). So running aground of a ship in a navigation channel brings along high costs. Knowledge on the variability in bedform height helps in making a more efficient dredging program. A better understanding of the stochastic properties of sand wave geometric properties may reduce the measurement frequency and reduce costs.
Draughts of ships in navigation channels depend on different variables, among them are the navigation speed, wind, currents and weather. The higher the navigation speed of a ship, the deeper the draught. Calculating the draught of a ship is a complex statistical process. Based on this calculation a maximum allowed draught is defined as Figure 1.10 shows. An extra safety margin is introduced which may not be crossed by the draught of a ship. The biggest ships are only able to visit the Port of Rotterdam during high tide. The time gap in which they can enter the port is quite short. When a ship has to wait for another tide this brings extra costs. So, more knowledge about what takes place below the safety margin could lead to lowering the safety margin. The result of this is a longer time gap for the biggest bulk ships to enter the Port of Rotterdam and therefore the costs will reduce (Wüst, 2007).

Hundreds of kilometres of pipelines and cables for transport of fossil fuels and electricity are buried in the North Sea. As burying pipelines and cables is expensive, it is preferred not to bury them too deep. The mean trough level of sand waves alone is not sufficient to determine at which elevation of the bed pipelines have to be buried. A migrating deep trough may expose the pipeline and this may increase the chance of damage to the pipeline. Free spans may develop, causing stresses due to gravity or turbulence of the flow. Damaged pipelines may harm the environment. Pipelines with certain smaller diameters are able to follow the sand waves on the seabed, as long as the sand waves are not too steep (Bijker, 2006).

In the North Sea, regions are indicated where wind farms are being built. Wind farms consist of free-standing wind mills. At these locations sand waves occur. These sand waves can erode or deposit sediment at the windmill foot, causing resonance of the windmills. The extreme values for crest elevation and trough elevation determine the dimensions of the foundation of the windmills.

Little is known about the irregularities in the geometric properties of sand waves. Examples of stochastic characteristics of the geometric properties of river dunes are the mean value, the standard deviation and the probability distribution. In the different studies different stochastic characteristics were found to be distributed according to probability distributions. For river dunes, Van der Mark et al. (2005) found a relationship between stochastic characterise of the geometric properties. For sand waves, not much is known about the stochastic characteristics of the geometric properties. It is unknown if these stochastic characteristics are distributed according to a known probability distribution. For the stochastic characteristics of sand waves, a relationship like was found by Van der Mark et al. (2005) may exist as well. Knowledge about extreme values for the stochastic characteristics of sand waves is unavailable. Knowledge about these extreme values is very important as described in the section above.

Knaapen (2006) studied sand wave height, sand wave length and sand wave asymmetry in the North Sea. The definitions used are different from definitions that will be used in this study, but his definition of asymmetry is applied in this study. Knaapen (2006) plotted probability distributions of these geometric properties for thirteen areas. However, he did no attempt to determine whether his data corresponded with a probability distribution.

1.4 Problem statement

Based on the above, the problem is formulated as follows:

Little knowledge exists on the stochastic characteristics of geometric properties of sand waves in the North Sea. Furthermore not much is known about the extreme values of geometric properties of sand waves.

1.5 Research objectives

The objectives of this study are the following:

i. to get more insight in the stochastic characteristics of geometric properties of sand waves in the North Sea.

ii. to determine whether geometric properties of sand waves are distributed according to known probability distributions, focussing on geometric properties of sand waves such as wave height, wave length, trough elevation, crest elevation and asymmetry.

iii. to determine whether a relation exists among mean values and standard deviations of the geometric properties of sand waves.

iv. to create more insight in the extreme values of geometric properties of sand waves.

1.6 Research questions

The research questions of this study are the following:

1. What do the different actors within the North Sea area need to know about the stochastic characteristics of sand waves and their extreme values?
2. How do we analyse the North Sea data?
   a. How do we define geometric properties of sand waves?
   b. How do we define longitudinal profiles in an area?
   c. How do we define the trend line in the longitudinal profiles?
   d. How do we filter the measured data?
   e. How can available software tools be altered in order to be used in this study?
3. What are the stochastic characteristics (mean value, standard deviation, shape of probability distribution) of geometric properties of sand waves?
4. Are the different geometric properties in the available data sets from the North Sea distributed according to a known probability distribution?
5. Is there a relation between the standard deviation and the mean value for different geometric properties of sand waves, like was found for river dunes?
6. Is there a relationship between the above stochastic characteristics and the extreme values of geometric properties of sand waves?

1.7 Methodology

The methodology for this study is described in this section. The research questions of the previous section serve as a guidance.

RQ1. Actors

Interviews are a suitable way to find out what different actors within the North Sea area need to know about the stochastic characteristics of sand waves and their extreme values. It was chosen to restrict the amount of people contacted, as interviews with actors have already been performed in the past by members of the Water Engineering & Management (WEM) department at the University of Twente (Németh et al., 2002; Németh and Hulscher, 2003).

RQ2. Analysis of bathymetry data

In this study we analyse multi-beam data obtained in the North Sea. Figure 1.7 shows the locations from where available data originates. As Figure 1.1 shows, sand waves cover a large area of the North Sea, but are not found everywhere. In this study, locations are selected where sand waves are found and are suitable for the extraction of longitudinal profiles. Both short crested and long crested sand waves are analysed. Long crested sand waves used in this study are found in the Ecomorf 3 area and short crested sand waves used in this study are found in the Noordhinder area. Figure 1.6 shows plan views of both areas. Another area that is included in this study is the so-called TWIN area.

RQ2a. Definition of geometric properties of sand waves
Within this study it is important to make a choice how to define the geometric properties of sand waves. For this purpose, previous studies into sand wave probability distributions and previous studies into sand waves in the North Sea are considered with respect to their definitions. Continuity with previous work is desirable, under the condition that the choices are suitable for this study.

RQ2b. Longitudinal profiles
Longitudinal profiles are needed in order to define crests, troughs, wave height and length. We need to determine where and how many longitudinal profiles have to be taken from the field data. Crests of long crested sand waves are oriented perpendicular to the direction of the residual tidal current. In order to determine the orientation of the troughs and crests in the sand wave field, the lowest gradient in vertical displacement of the sand wave field has to be determined. A small part of the interpolation method *Digipol*, which was developed by the National Institute for Coastal and Marine Management (RWS RIKZ) enables us to determine the lowest gradient for a sand wave field (RIKZ, 1997).

RQ2c. Determination of trend line
The seabed slope or the mean bed level over space needs to be accounted for. The bed slope or mean bed level may be a linear line. Figure 1.11 shows a longitudinal profile of field data in the North Sea with an added linear trend line. When the seabed slope is not linear the trend line should be considered as a non linear trend line.

RQ2d. Filtering
Since various bedform patterns occur in the North Sea, it is likely that the field measurements contain bedform patterns other than the sand waves. Since our focus is on sand waves, other patterns are filtered out of the raw data. Knaapen (2005) and Morelissen et al. (2003) filtered data below certain values to remove megaripples and ripples. The available tool by Van der Mark and Blom (2007) is used to filter the smaller bedforms.

RQ2e. Available tool
Van der Mark and Blom (2007) developed a tool which analyses longitudinal bed elevation

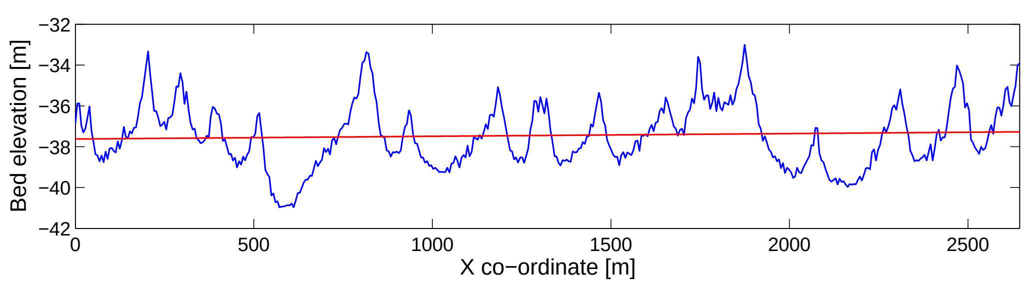

Figure 1.11: Bed elevation along a longitudinal bed elevation profile with a linear trend line.

profiles for their geometric properties and stochastics. This tool is called the bedform tracking tool *(BTT)*. Longitudinal bed elevation profiles serve as input for this tool. The tool was analysed in order to become clear what parts have to be altered and what has to be added. The code is altered with respect to the choices made for the definitions of geometric properties of sand waves.

RQ3. Stochastic characteristics

The next step in the process is to analyse the output of the BTT code. The output consists of geometric properties of individual sand waves, such as sand wave height, crest elevation, trough elevation, wave length and asymmetry. The output for all these properties for each individual sand wave is put together. Every data set will have a certain number (n) of sand wave heights, wave lengths, crest elevations, trough elevations and asymmetries. These stochastic characteristics are then plotted in probability density functions. The mean value μ and the standard deviation σ for each geometric property are determined.

RQ4. Probability density functions

With the probability density functions (PDFs), it is possible to determine whether the different geometric properties of the field data are distributed in conformity with a known probability distribution. The Kolmogorov-Smirnov goodness-of-fit test is used in order to determine whether a data set is distributed according to a known probability distribution or to determine whether two data sets are distributed in the same way. As the Kolmogorov-Smirnov test cannot compare probability distribution, a method is found to determine which probability distribution is the best fit.

RQ5. Existence of relationships

We determine whether different stochastic characteristics are related to each other. For flume experiments, which represent fluvial conditions under unidirectional flow, it appeared that the coefficient of variation C defined by dividing the standard deviation σ by the mean value μ of dune height is more or less a constant (Van der Mark et al., 2005). This means that when the mean dune height is known, we can determine the variation around the mean value. It will be examined whether a relationship between stochastic characteristics, such as the mean value μ and the standard deviation σ, for geometric properties of sand waves can also be found, analogous to geometric properties of river dunes.

RQ6. Extreme values

Finally we study the tails of the probability distributions. The tails represent the extreme values of the geometric properties of sand waves. We determine whether there is a relationship between the stochastic characteristics and the extreme values of the various geometric properties of sand waves. The values of the highest extreme values (Δ_{95}) and the lowest extreme values (Δ_5) and the relationship between them are analysed.

Chapter 2

Data processing

In this chapter we explain how bathymetric data from the North Sea is analysed. First, we explain about the way bathymetric data is obtained from the North Sea. More will be outlined about the data sets used. We describe how the definitions of geometric properties of sand waves, such as sand wave height and length, used in this study are chosen. Furthermore the process of data analysis is explained. In this chapter is explained how the process of determining the orientation of the sand wave field works. When this orientation is found, longitudinal bed elevation profiles are taken from the bathymetric data. The longitudinal bed elevation profiles serve as input for the bedform tracking tool (BTT). The output of the tool is used to analyse the stochastic characteristics of the sand waves.

2.1 Measurements

Bathymetric data is mostly obtained using single-beam or multi-beam echo sounders. Using single-beam echo sounders, the depth directly below the survey vessel is measured. Using the multi-beam echo sounders it is possible to measure an area with a width of several times the water depth. When gathering data, survey vessels with a single-beam echo sounder tend to follow the direction perpendicular to the troughs of the sand waves in order to include all the passing sand waves (Dorst, 2006). This direction is known from previous measurements. When multi-beam echo sounders are used, it is no longer necessary to follow this direction.

In this study multi-beam data sets are used, so single-beam is not further discussed. Using the multi-beam method full bottom coverage is obtained. In this method grid cells on the seabed are created. For each grid cell the water depth is measured and the minimum depth is assigned to that grid cell. In reality the depth within a grid cell may differ, so the data does not really cover the whole measured seabed. Often a grid size of several metres is chosen.

Figure 2.1 shows that lobes of sound are sent from the echo sounder underneath a vessel. Usually the echo sounder does not hang underneath a ship, but is mounted in the hull of a ship. In the figure one lobe is fully drawn. This lobe of sound is reflected by obstacles. The depth belonging to the first signal returning from a grid cell is the minimal depth in the grid cell. The water depth at this location is assigned to the grid. Note that there may be deeper locations within the grid cell, but these are neglected. As a result, an obstacle such as the rock in the figure influences the measurements. The North Sea bed is sandy and obstacles like rocks are hardly found (Dorst, 2006). The influence of surface waves on the vessel and therefore on the measurements are corrected by the use of inertial measurement units (IHB, 2005).

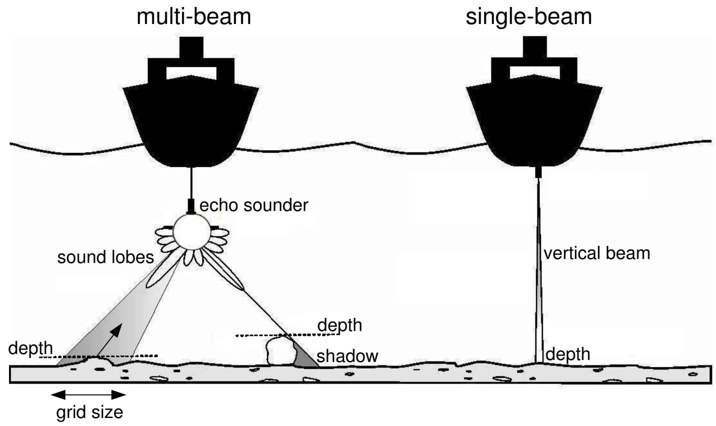

Figure 2.1: The multi-beam and single-beam echo sounders.

2.2 Data sets

Figure 1.7 shows locations where bathymetry data was obtained. It was already mentioned that data sets from the Ecomorf 3 area, Noordhinder area and the TWIN area are used in this study. The data sets from these three areas consist of multi-beam data with a resolution $\Delta y \times \Delta x$ of $5\,\mathrm{m} \times 5\,\mathrm{m}$. Multi-beam echo-sounders are used to obtain bathymetry data. The data sets were obtained in 2003 by the Dutch Directorate for Public Works and Water Management *(Rijkswaterstaat)*. In Section 1.1.1 is stated that storms and seasons have an

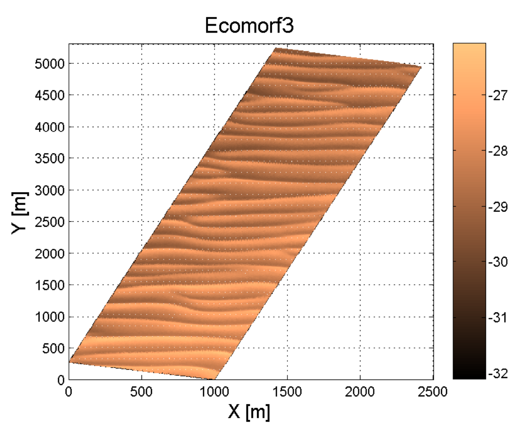

(a)

Figure 2.2: Plan view of the Ecomorf 3 area (2003). The water depth [m] is indicated with the color bar on the right.

Table 2.1: Characteristics of the study areas (www.noordzeeatlas.nl).

Area	Short or long crested?	Average depth [m]	Grain size [μm]	Tidal difference [m]	Tidal current [knots]
Ecomorf 3	long crested	-28.3	250-500	0.5-1.0	1.1-1.5
R0302C	short crested	-39.9	250-500	1.0-1.5	2.6-3.0
R0302D	short crested	-38.3	250-500	1.0-1.5	2.6-3.0
R0303C	short crested	-37.9	250-500	1.0-1.5	2.6-3.0
R0304D	short crested	-40.0	250-500	1.0-1.5	2.6-3.0
R0305A	short crested	-38.4	250-500	1.0-1.5	2.6-3.0
R0305B	short crested	-38.4	250-500	1.0-1.5	2.6-3.0
TWIN 01	short crested	-36.9	250-500	1.5-2.0	2.6-3.0
TWIN 02	short crested	-36.2	250-500	1.5-2.0	2.6-3.0

influence on the sand wave height. It is unknown in which season the data sets used in this study were obtained. The Ecomorf 3 area is measured for research objectives and the other two areas are measured in order to monitor the navigation channels. The data files consist of three columns with coordinates (eastward x and northward y) in metres and the water depth in metres.

The plan view of the Ecomorf 3 area can be found in Figure 2.2. The Ecomorf 3 area is considered as a long crested sand wave area and the Noordhinder and TWIN areas as short crested. The Ecomorf 3 area is $2.4 \times 5.2\,\mathrm{km}^2$. The total TWIN area is $7.1 \times 8.4\,\mathrm{km}^2$ and the total Noordhinder area is $19 \times 17\,\mathrm{km}^2$. From the TWIN area two areas of about $2.25 \times 4.2\,\mathrm{km}^2$ are analysed. Figure 2.3 shows these two areas, which are found next to each other. From the Noordhinder six areas are selected from the available data sets. These areas are about $2.5 \times 4\,\mathrm{km}^2$ and are shown in Figure 2.4. The areas are still named in the way they were initially named: R0302C, R0302D, R0303C, R0304D, R0305A, and R0305B. The areas are all situated next to each other within the Noordhinder area. More about the data sets can be found in Table 2.1.

The water depth influences the sand wave height (Van Maren, 1998) and therefore also values of the crest elevation and trough elevation. Table 2.1 shows that the long crested Ecomorf 3 area has an average water depth of 28.3 m and the short crested areas have an average depth of almost 40 m. Figure 2.2 shows the total difference (about 5 m) in bed elevation in the Ecomorf 3 area. The other areas (Figure 2.3 and Figure 2.4) show a larger difference in bed elevation of over 10 m. The difference in water depth may explain the difference in bed elevation, which means higher sand wave heights in the short crested areas.

The water depth may be a reason for the difference in irregularity. The grain size of the bed material may not be causing this difference, since this is the same for the study areas (Table 2.1). Other possible characteristics causing irregularity may be the differences in the tidal currents and tidal differences. Table 2.1 shows that the tidal currents and the tidal differences are higher for the short crested areas than for the long crested area. This difference may be a reason for the differences in the irregularity in plan view. In the Ecomorf 3 area no dredging takes place (Hoogewoning and Boers, 2001). In the TWIN areas frequent dredging takes place (Wüst, 2004, 2007) and of the Noordhinder area no information is found on dredging.

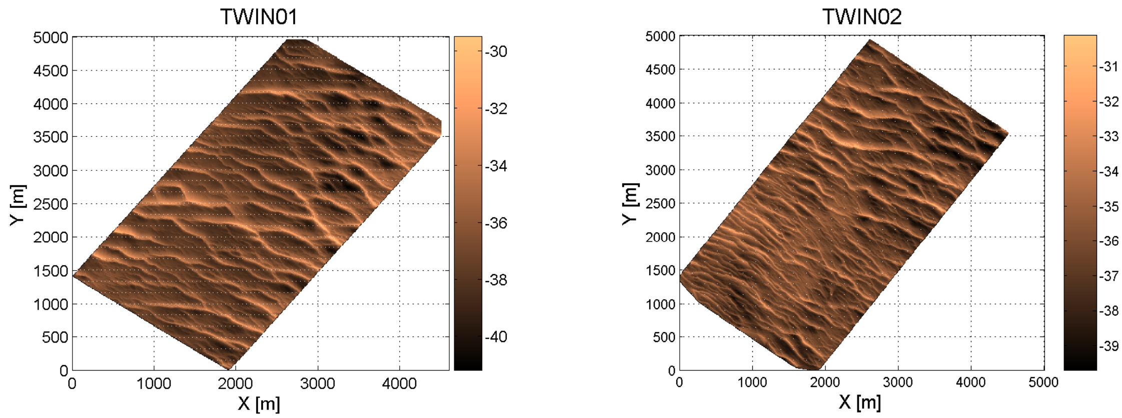

(a) (b)

Figure 2.3: Plan view of the TWIN areas (2003). The water depth [m] is indicated with the color bar on the right.

Irregularity in plan view shows crest lines that are not perpendicular to each other and many bifurcations can be seen. An area with a high number of bifurcations is defined as a short crested area. A lower bifurcation number B means a long crested area. We choose a critical value of the bifurcation number of 3. Areas with bifurcation numbers below 3 are defined as long crested and values above 3 as short crested areas. Table 2.2 shows for each of the study areas the amount of bifurcations and the number of bifurcations per square kilometre. The number of bifurcations in the TWIN areas were hard to count, but in those areas more than 100 bifurcations can be seen. The bifurcation number already exceeds a value of 4.

Knaapen (2006) also determined the amount of bifurcations in his study areas. It is not clear if Knaapen (2006) counts the bifurcations in the same way as is done in this study. The bifurcation number B for all areas is found around a value of 10, except for one area. This area has a value of 2.2 which is in a different order and very close to the number of the long crested area in this study.

Table 2.2: The number of bifurcations in an area, the total surface of the area and the number of bifurcations per square kilometre.

Area	**Bifurcations**	**Surface**	B
-	-	[km^2]	[km^{-2}]
Ecomorf 3	9	5.24	1.91
R0302C	36	9.30	7.31
R0302D	68	4.19	8.60
R0303C	54	7.36	7.34
R0304D	44	5.15	8.54
R0305A	66	8.68	7.61
R0305B	61	9.30	6.56
TWIN 01	>100	22.00	>4.55
TWIN 01	>100	22.00	>4.55

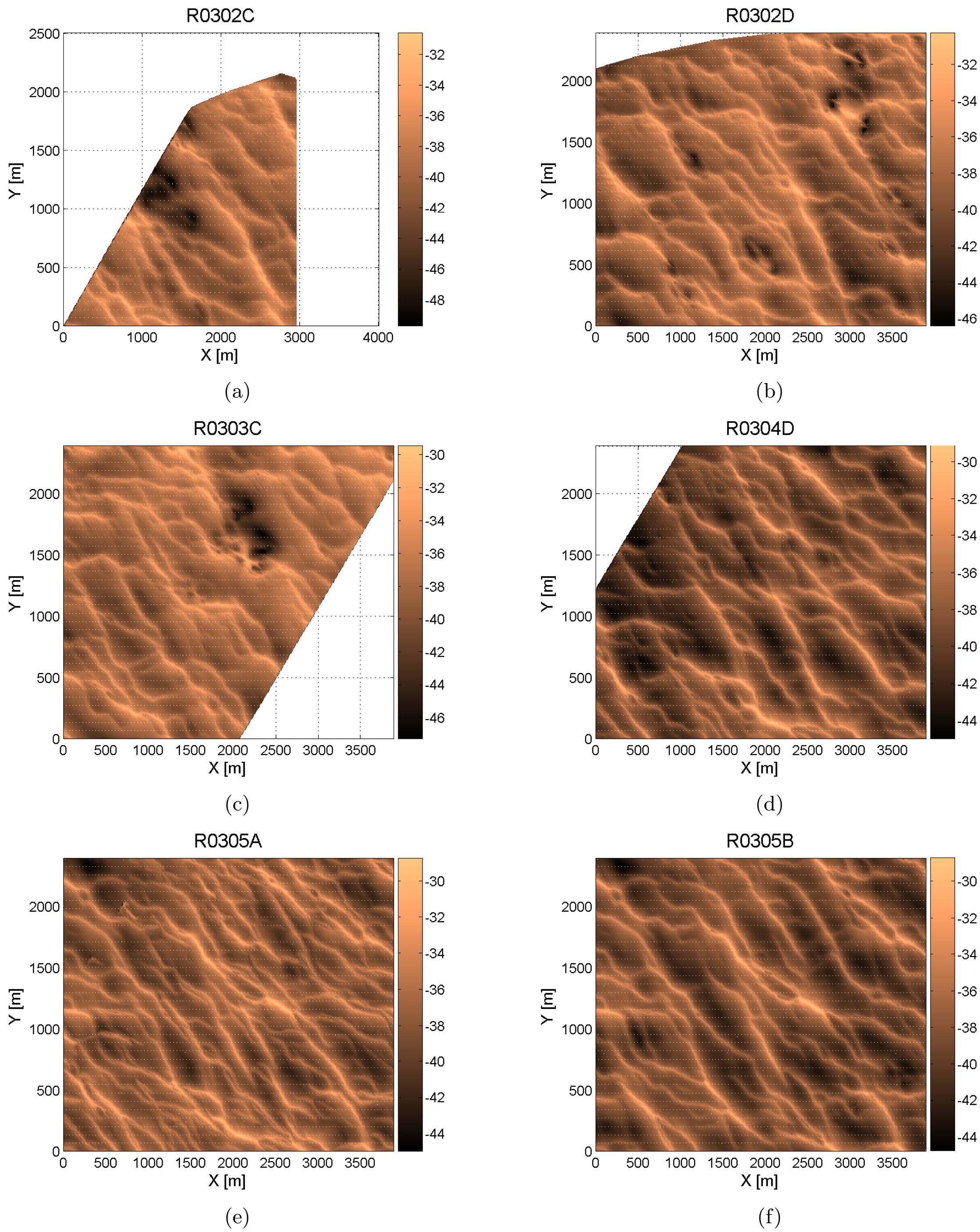

Figure 2.4: Plan view of the Noordhinder areas (2003). The water depth [m] is indicated with the color bar on the right.

2.3 Definition of geometric properties of sand waves

In the 1960s and 1970s different studies were carried out into stochastic characteristics of river dunes, but it is hard to compare the results of different researchers. Crickmore (1970) states that different researchers use different definitions for geometric properties of bedforms and use different preprocessing methods. So these studies cannot be compared because different definitions may affect the results (Crickmore, 1970).

The problem described by Crickmore (1970) is also encountered for sand waves (Van Maren, 1998). Tobias (1989) analysed currents, wave data, echo soundings and sediment for marine environments in the North Sea. His definition of geometric properties of sand waves is the same as in the study by Knaapen (2005). Knaapen (2005) also characterised asymmetry of the sand waves. Figure 2.5 shows their definitions for sand wave height and sand wave length. Both the authors do not explain why they made their choices.

The bedform tracking tool of Van der Mark and Blom (2007) is used in this study. Figure 2.6 shows geometric properties of sand waves that are determined from detrended bed elevation profiles and stored in the BTT. The slope of the lee side is also determined by Van der Mark and Blom (2007), but is not included in this study. The slope of the sand waves is left out, because at first it was not available and afterwards the choice was made, because of the time span, to focus on five geometric properties. The method used by to determine the slope Van der Mark and Blom (2007) is also applicable for sand waves.

The geometric properties that are analysed in this study are outlined in Table 2.3 and are shown in Figure 2.6 with the bold symbols. The sand wave height Δ_l is the distance between a crest and its subsequent trough. The analysed sand wave length L_c is the distance between two crests. The sand wave is not defined between two troughs as troughs are often quite flattened and defining the lowest point is harder than defining the highest point of a crest (Stolk, 2007). The crest elevation η_c and trough elevation η_t are also analysed. The elevation of the crests η_c and the elevation of the troughs η_t are determined relative to the mean bed level.

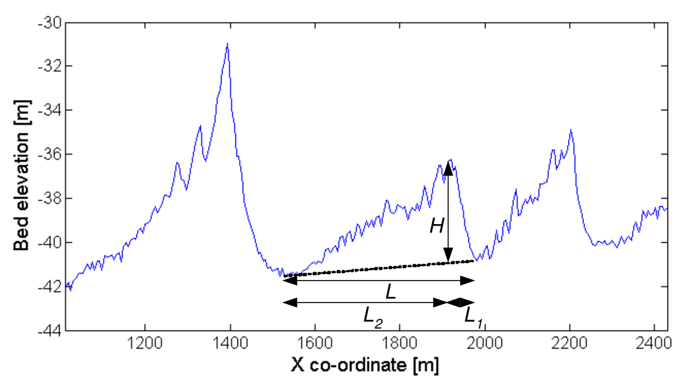

Figure 2.5: Definition of geometric properties of bedforms (Tobias, 1989; Knaapen, 2005).

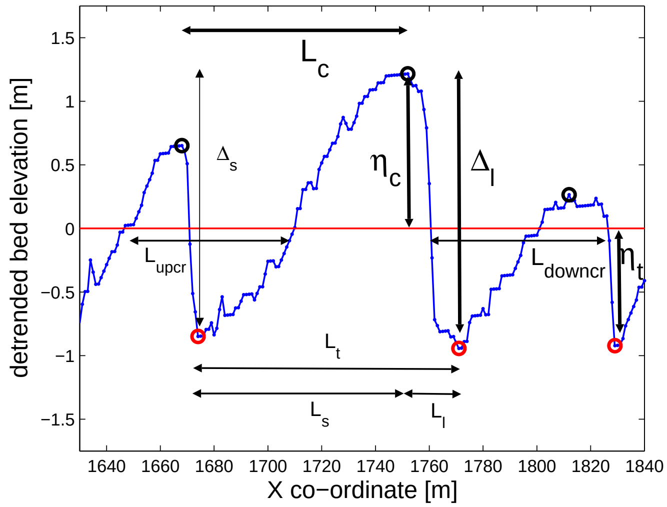

Figure 2.6: Definitions of the calculated geometric properties of the bedform in BTT (Van der Mark and Blom, 2007). The flow is to the right.

Another analysed geometric property of sand waves is the asymmetry. Asymmetry is not defined by Van der Mark et al. (2005). Knaapen (2005) defined asymmetry as a dimensionless variable and his method is applied here. Asymmetry A is defined as the difference between the length of the stoss side of a sand wave and the length of the lee side of a sand wave divided by the sand wave length, defined as the distance between two troughs. Equation 2.1 shows this for the definitions used in this study (Figure 2.6):

$$A = \frac{L_s - L_l}{L_t} \tag{2.1}$$

2.4 Orientation of sand wave field

The orientation of the sand wave field is needed to obtain longitudinal profiles directed perpendicular to the crests. Figure 2.7 shows a plan view of a sand wave field and in this sand

Table 2.3: Explanation of the symbols of geometric properties used in this study in the bedform tracking tool (BTT)

Symbol	Explanation
η_c	Crest elevation: vertical distance from crest to equilibrium trend line
η_t	Trough elevation: vertical distance from trough to equilibrium trend line
Δ_l	Height of lee side: vertical distance between crest and downstream trough
L_s	Length of stoss side: horizontal distance between crest and upstream trough
L_l	Length of lee side: horizontal distance between crest and downstream trough
L_c	Bedform length between crests: horizontal distance between two subsequent crests

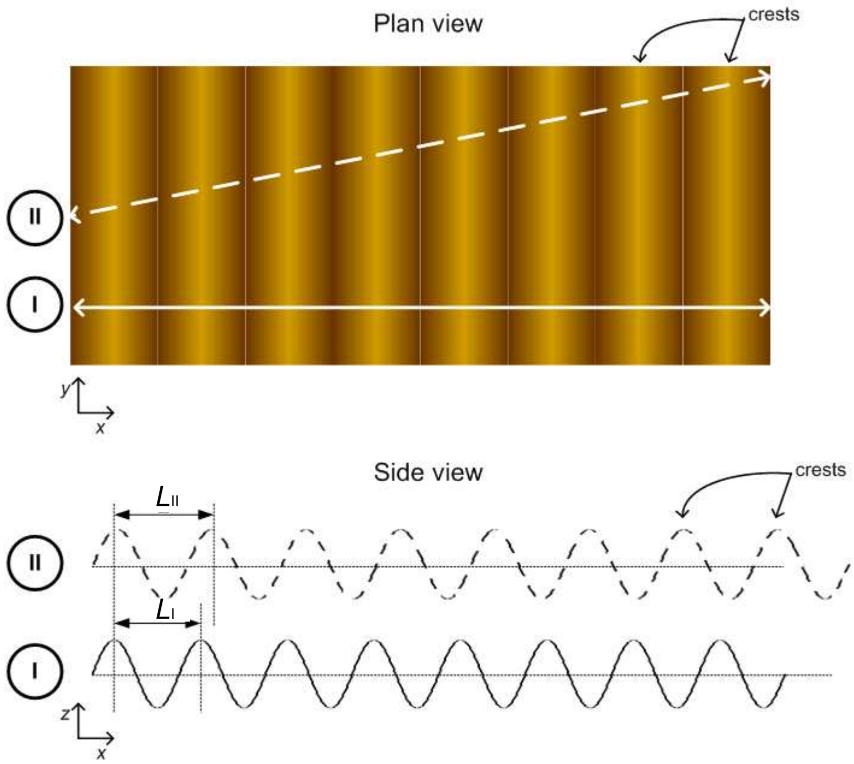

Figure 2.7: Plan view of a sand wave field in which longitudinal bed elevation profiles are drawn (I en II). The two longitudinal bed elevation profiles are shown in side view below the plan view. The first (I) is the longitudinal bed elevation profile perpendicular to the crest lines. The other (II) is not perpendicular to the crest lines. The difference in sand wave length L_I and L_{II} can be seen in the side view.

wave field two longitudinal bed elevation profiles are taken. One is perpendicular to the crests (I) and the other is not perpendicular to the crests (II). Figure 2.7 shows that longitudinal bed elevation profiles have to be taken perpendiuclar to the crest lines in order to obtain the correct sand wave lengths.

In the Ecomorf 3 area, as shown in Figure 1.6(a), the crests are almost parallel to each other, but this situation is exceptional. In most cases the crests of sand waves are not parallel to each other but look more like the sand waves in Figure 1.6(b). A mean orientation for the whole sand wave field has to be determined. It may occur that a determined orientation for a sand wave field does not represent all parts of the area. To determine whether the orientation represents the whole sand wave field, the area is subdivided and the orientation of the subareas is determined. The outcome for each subarea is compared and should correspond with each other and with the orientation of the whole area. The subareas are determined by selecting subareas in x direction over the full length of y. Subareas are also determined by selecting areas in y direction over the full length of x.

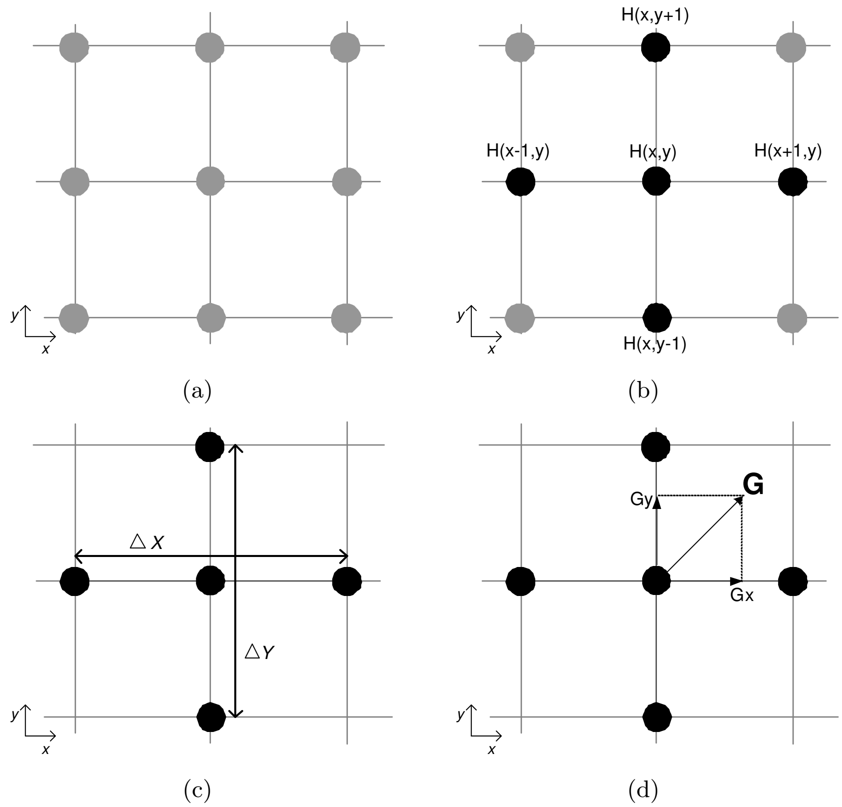

Figure 2.8: (a) Points on a grid with random values for the bed elevation, wherein the grid point in the middle (b) has bed elevation level $H_{x,y}$ at location *x,y*. (c) The differences in bed elevation over Δx and Δy around the grid point $H_{x,y}$ determine the gradients in *x* and *y* direction of the grid point under consideration. (d) G_x and G_y determine the gradient vector *G* at $H_{x,y}$.

2.4.1 Method

In order to estimate the orientation of the sand wave field, a small part of the *Digipol* interpolation method is used (RIKZ, 1997). A bathymetry data set contains grid points with x and y coordinates and a bed elevation *H*. Figure 2.8(a) shows points on a grid with a certain random value for the bed elevation. Figure 2.8(b) shows that the grid point in the middle at location *(x,y)* has a certain bed elevation $H_{x,y}$. The grid point at location *(x+1,y)* has a certain bed elevation $H_{x+1,y}$. In Figure 2.8(c) the changes in x and y direction are determined as the differences in bed elevation between the four surrounding grid points. In order to determine the gradient in grid point $H_{x,y}$ the differences in bed elevation over Δx and Δy have to be determined. So the gradients G_x and G_y are determined by dividing the difference in bed elevation by the difference in distance in x or y direction:

$$G_x = \frac{H_{(x+1,y)} - H_{(x-1,y)}}{(x+1) - (x-1)} = \frac{\Delta H_x}{\Delta x} \tag{2.2}$$

$$G_y = \frac{H_{(x,y+1)} - H_{(x,y-1)}}{(y+1) - (y-1)} = \frac{\Delta H_y}{\Delta y} \tag{2.3}$$

The length of the gradient vector $|\overrightarrow{G}|$ for grid point $H_{x,y}$ in Figure 2.8(d) is now determined using the gradients G_x and G_y:

$$|\overrightarrow{G}| = \sqrt{G_x^2 + G_y^2} \tag{2.4}$$

Figure 2.9 shows an example of data points on a grid with random values for the bed elevation in a data set. For each point the gradient vector $|\overrightarrow{G}|$ is determined. Figure 2.9 shows a line with orientation α on which the absolute value of the gradient vectors are projected as L. Figure 2.9 and Equation 2.5 show how L is determined for one grid point. The angle β depends on the rotation of the line. The total gradient has to be determined so the projected values L are positive. The total sum of all the values for L is the total gradient L_i for this angle α_i of the line. The angle α of the line in the figure is arbitrary and the total gradient is calculated for every angle. Figure 2.10 shows how the orientation of the sand wave field is defined (Dorst, 2006).

$$L = |cos(\beta) \cdot |\overrightarrow{G}|| \tag{2.5}$$

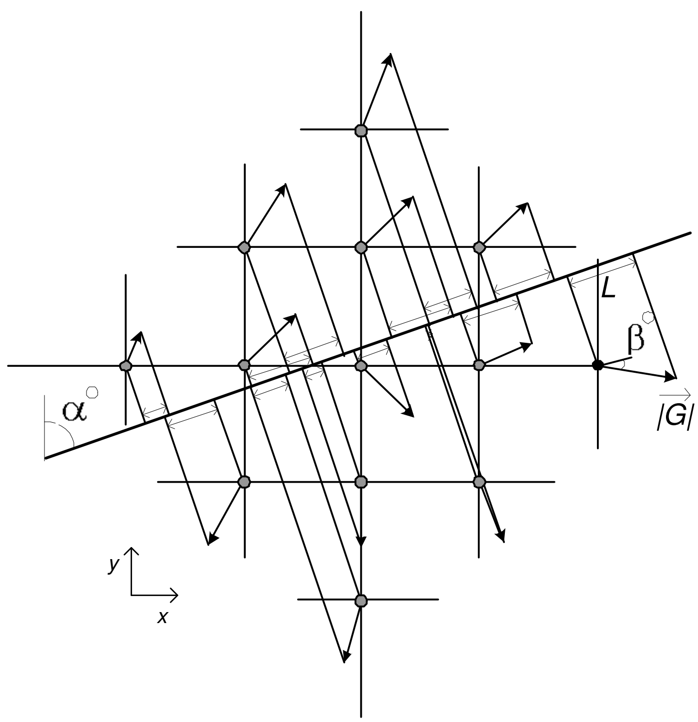

Figure 2.9: Projection of the gradient vectors in order to determine the orientation of the field. A line is drawn oriented to the y axis by angle α. On this line the gradients are projected as L. For one grid point (black) is shown how L is determined based on the angle β and gradient vector $|\overrightarrow{G}|$.

By rotating the line, the total gradient for each angle can be determined. The angle α (Figure 2.9) with the highest value for the total gradient is the direction that corresponds best with the dominant orientation of the individual gradients. This angle (α_{max}) is the orientation with the highest gradient and therefore equals the direction perpendicular to the crest lines. The angles for which the total gradient is calculated, is increased in steps of one degree from 0° to 179°. These steps of one degree are implemented in order to limit the amount of calculation time. The *Digipol* method was implemented in Matlab by Dorst (2006). This Matlab code is used in this study. Some adjustments were made, since the bathymetry data used by Dorst (2006) is single-beam data and in this study multi-beam data is used.

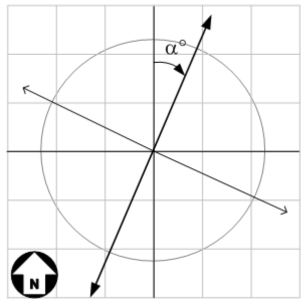

Figure 2.10: The way α is defined in the output of *digipol*.

2.4.2 Results

The angle α_{max} is the angle for which the total calculated gradient $L_{tot,i}$ has the highest value. For the Ecomorf 3 area the calculated angle α_{max} of the sand wave field for the whole area is 3°. Figure 2.11 shows the plan view of the total area. The Ecomorf 3 area is divided into smaller areas to define whether the calculated α_{max} represents the area as a whole. The α_{max} calculated for subareas of the Ecomorf 3 area and the α for each area is plotted with the belonging gradient $L_{tot,i}$ in Figure 2.11(b). The total gradient $L_{tot,i}$ for each angle of the plot of the total area and the subareas is made dimensionless in order to compare the results with other areas. This is done by subtracting the average value of the gradients from the $L_{tot,i}$ for a certain angle and divide the outcome by the average value:

$$L^*_{tot,i} = \frac{L_{tot,i} - L_{tot,avg}}{L_{tot,avg}} \tag{2.6}$$

The bold line is the plot of the dimensionless gradients for the total area. The dashed and dotted lines are plots of the subareas. Figure 2.11(b) shows that in this case the α_{max} of 3° represents the whole area.

The bathymetry data from the larger Noordhinder area consists of multiple areas. Six of them are analysed in this study. In this chapter one area is outlined. Figure 2.12 shows the plan view of area R0302D and the plot of the dimensionless gradient. Figure 2.12(b) shows that in this case the α_{max} of 28° represents the whole area. Plan views of the other areas are outlined in Appendix A. It is clear that the orientation of the sand waves in these areas differs from the Ecomorf 3 area. Dividing these areas leads to the conclusion that the angle for the whole area and the subareas have approximately the same value for α_{max}.

Also the TWIN 01 area is analysed. This area consists of two subareas in which is dredged regularly (Wüst, 2004, 2007). For the TWIN 01 area the calculated angle α_{max} of the sand

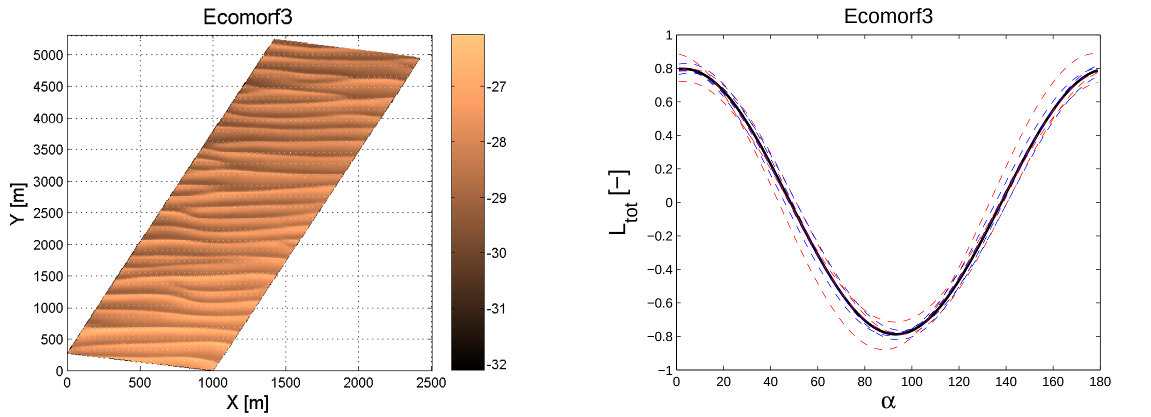

(a) (b)

Figure 2.11: The Ecomorf 3 area and a plot of the dimensionless gradient $L_{tot,i}$ for each angle α. (α_{max} is 3°). The bold line is the plot of the dimensionless gradients for the total area. The dashed and dotted lines are plots of the subareas.

wave field for the whole area is 30°. It appears that both in the long crested area and in the short crested areas the *digipol* method is able to find a distinct α_{max}. Because of the distinct α_{max} the method is applicable to short crested sand wave fields.

2.5 Longitudinal profiles

The next step in the process is the creation of longitudinal bed elevation profiles. When α_{max} is determined, the longitudinal bed elevation profiles can be derived from the bathymetry grid data. Figure 2.14 shows possible longitudinal profiles in the data as arrows. A method is needed to assign values to the drawn line. The bathymetry data actually consists of grid cells,

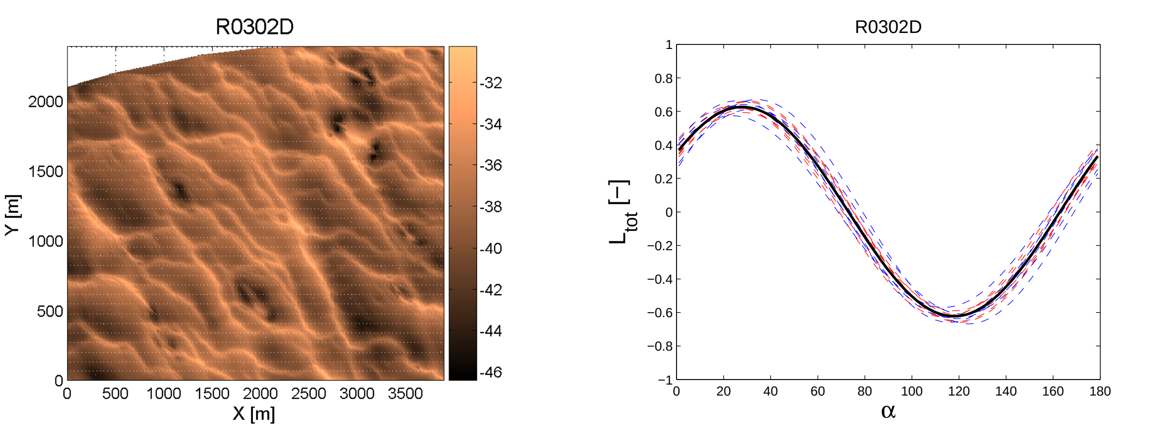

(a) (b)

Figure 2.12: Area R0302D in the Noordhinder area and a plot of the dimensionless gradient for each angle α. (α_{max} is 28°). The bold line is the plot of the dimensionless gradients for the total area. The dashed and dotted lines are plots of the subareas.

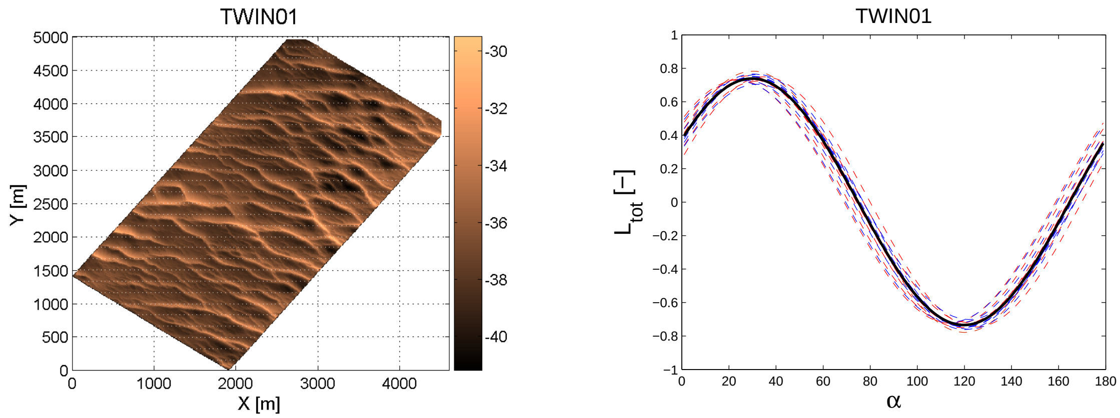

(a) (b)

Figure 2.13: Area TWIN01 and a plot of the dimensionless gradient for each angle α. (α_{max} is 30°). The bold line is the plot of the dimensionless gradients for the total area. The dashed and dotted lines are plots of the subareas.

but the data can be seen as points. In the bathymetry data obtained by the Dutch Ministry for Transport, Public Works and Water Management, North Sea Directorate the grid size is $5\,\mathrm{m} \times 5\,\mathrm{m}$. Figure 2.14 shows the grid points and the cells around them.

The longitudinal bed elevation profiles can be realised by assigning every distance $\Delta y'$ the value of the grid cell to the arrows in Figure 2.14. $\Delta y'$ is determined by:

$$\Delta y' = \frac{\Delta y}{\sin \alpha} \tag{2.7}$$

Figure 2.14 shows that longitudinal bed elevation profiles are taken from the data set every 25 metres. This distance is 5 times the grid size Δx. The choice for a distance of 25 m between two subsequent longitudinal bed elevation profiles was made subjectively. A very short distance between two subsequent profiles will lead to more or less similar longitudinal bed elevation profiles. Choosing a long distance may lead to too few longitudinal bed elevation profiles to analyse.

2.6 Procedure of the bedform tracking tool

The input of the bedform tracking tool (Van der Mark and Blom, 2007) are the longitudinal bed elevation profiles. The procedure of the BTT is shortly listed below in steps:

1. For each longitudinal bed elevation profile (BEP) outliers are found and replaced.

2. For each BEP the trend line is determined.

3. The BEP is detrended using the first order polynomial trend line. The new BEP fluctuates around the zero line.

4. A weighted moving average filter is applied. This yields a filtered BEP which is used for determining the zero up-crossings and down-crossings.

5. The zero up-crossings and down-crossings are determined.
6. Crests and troughs are determined. A crest is the highest point between an up-crossing and a down-crossing. A trough is the lowest point between an up-crossing and a down-crossing.
7. Bedform characteristics are determined and saved (sand wave heights, sand wave lengths, crest elevations, trough elevation and sand wave asymmetry)

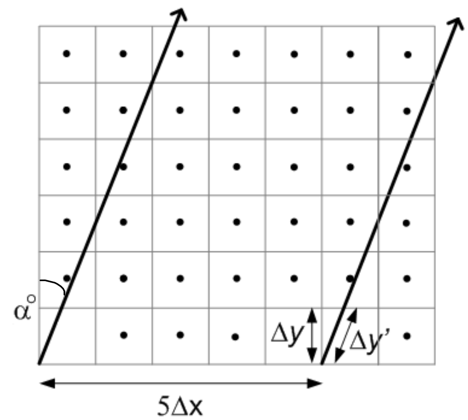

Figure 2.14: Longitudinal bed elevation profiles trough the data with the orientation α of the sand wave field.

2.6.1 Trend line

The choice of trend line is the same for all analysed data. In the bedform tracking tool (BTT), the used trend line in the longitudinal bed elevation profiles is a linear line as is shown in Figure 2.15(a). A moving average trend line can also be used. A moving average trend line uses data before and after a certain location to calculate the average for this location along the longitudinal bed elevation profile. When this type of trend line is used, the edges of the longitudinal bed elevation profiles cannot be used. It turns out that half of the profiles will be lost when the moving average method is used in the BTT. In this study we want to include all the sand waves in the BEPs. No large differences in average water depth are found and therefore we use a linear trend line. The straight trend line is defined as a first order polynomial:

$$F_1(x) = ax + b \tag{2.8}$$

The values for a and b are based on the BEP and determined in Matlab with the *polyfit* function, which fits a polynomial trough data.

Knaapen (2006) used a fourth order polynomial as trend line. After analysing higher order polynomials as trend line it turns out that in this study the higher order polynomials are not suitable to describe the small differences in average bed elevation.

A cause of large differences in the average water depth are sand banks. Sand banks are not found in the Ecomorf 3 area (DelftCluster, 2003). Also the Noordhinder area is not located near any sand bank (Van de Meene and Van Rijn, 2000). The TWIN area is located close to the Hinder banks (Van de Meene and Van Rijn, 2000) and may be influenced by it. However the average depth in the area does not show many differences.

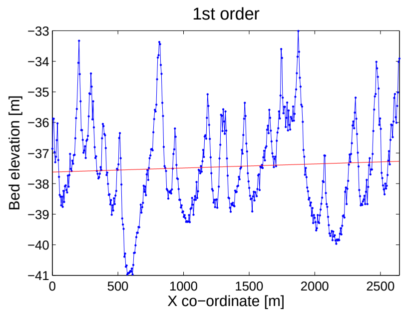

(a)

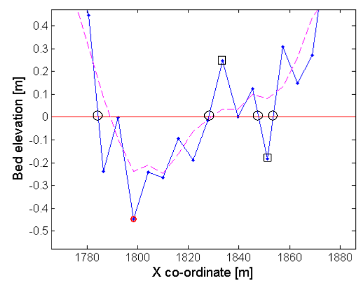

(b)

Figure 2.15: (a) Longitudinal bed elevation profile 100 (Noordhinder R0302D) with a first order polynomial trend line. (b) Longitudinal bed elevation profile with the filter line (dashed). Filtered crossings are indicated with a circle.

2.6.2 Filtering and defining crossings, troughs and crests

The chosen trend line is subtracted from the longitudinal bed elevation profile. In this way a detrended longitudinal bed elevation profile is determined. The values of the BEP now fluctuate around the zero level. In this study only the geometric properties of sand waves are of interest. A filter is applied that smoothes the BEP so that the smaller scale bedforms, megaripples, fluctuating around the zero level are not included in the analysis.

Figure 2.15(b) shows the up-crossings and down-crossings of the megaripples marked with a circle. The square markers indicate a crest or trough caused by a fluctuating megaripple. The filter is shown as the dashed line in Figure 2.15(b) and the crossings of this line are used as the zero up-crossings and the zero down-crossings of sand waves in this study. The lowest point between these crossings is determined as the trough. The filter line is based on a moving average. The next step in the BTT is determining the crests and troughs and then the bedform characteristics can be determined. For each data set a certain number n of sand wave heights, sand wave lengths, crest elevations, trough elevations and sand wave asymmetry values are saved.

Chapter 3

Distribution of geometric properties of sand waves

In this chapter we will describe the results of the analysis of the longitudinal bed elevation profiles taken from the bathymetry data. With the longitudinal bed elevation profiles as input we used the bedform tracking tool to determine the geometric properties of sand waves for every sand wave in the study. The geometric properties analysed are the sand wave height, sand wave length, crest elevation, trough elevation and asymmetry of the sand waves. We analysed the stochastic characteristics of the sand waves by plotting probability density functions. It is also determined if the stochastic characteristics are distributed according to known probability distributions. A goodness-of-fit test is used to determine if a data set can be represented by a certain probability distribution. We also determined the total vertical difference between the cumulative density of the data and the cumulative density of different probability distributions. A low value for this difference means more resemblance between a certain probability distribution and the distribution of the data.

3.1 Goodness-of-fit tests

To determine whether the different geometric properties of sand waves follow a certain probability distribution, a goodness-of-fit test, the Kolmogorov-Smirnov test (KS test), is used. The KS test uses cumulative probability distributions (CDFs). The CDF describes the probability that the sand wave height has a value less than or equal to a value on the x axis. Figure 3.1 shows the CDF of the sand wave length in the Ecomorf 3 area. When a vertical line is drawn from the x axis at 250 to the probability distributions, this figure shows that almost 80% of the total sand wave lengths is below 250 metres.

Consider a data set with an unknown distribution $\mathbb{P}$ and we would like to test the hypothesis that the distribution of this data is equal to a particular probability distribution $\mathbb{P}_0$. We define the following hypotheses:

$$H_0 : \mathbb{P} = \mathbb{P}_0, \qquad H_1 : \mathbb{P} \neq \mathbb{P}_0 \tag{3.1}$$

So when H_0 is accepted the distributions may be equal and the hypothesis is rejected when the distributions are not equal. The hypothesis is rejected if the test is significant at the 5% level. This means that when the difference between the data and the probability distribution

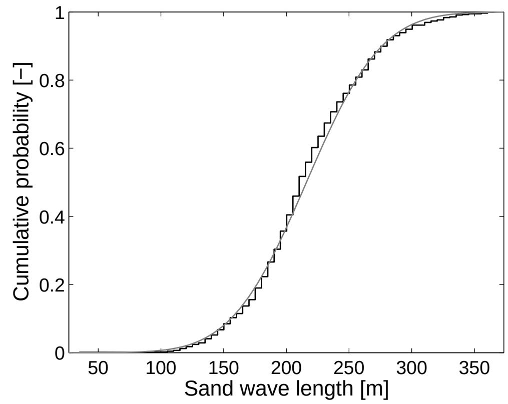

Figure 3.1: The cumulative distribution function of the sand wave length with the data (black) and the continuous normal distributed plot (grey).

is less than 5% it is assumed that the small difference is unlikely to have occurred by chance.

In the KS test the cumulative distribution functions (CDFs) of $\mathbb{P}$ and $\mathbb{P}_0$ are compared for each x value. This x value is used in the Matlab tool and is different form the x coordinate described earlier. The use of cumulative distribution functions means that the data set tested needs to be a continuous distribution (NIST/SEMATECH, 2006). In this study field data is used which is not continuous. In the Kolmogorov-Smirnov test the cumulative distribution function of the tested data set has to be determined by the user in advance and can then be tested (Mathworks, 2001).

The *ksstat* in Matlab returns the maximum difference found between the CDF of the data and the CDF of the distribution at a certain x value. When the *ksstat* has a value below a, by the significance defined, critical value then the hypothesis is accepted. The *ksstat* is defined by:

$$ksstat = max(|P(x) - P_0(x)|) \tag{3.2}$$

In this equation $P(x)$ is the proportion of values in $\mathbb{P}_0$ less than or equal to x. $P_0(x)$ is, for instance, the standard normal cumulative distribution function.

The Matlab function *kstest* is based on the maximum difference between the cumulative distribution function of the data $\mathbb{P}$ and the CDF of estimated data $\mathbb{P}_0$. As a result a distribution may represent a data set well, but the hypothesis $H_0 : \mathbb{P} = \mathbb{P}_0$ may still be rejected based on just one x value in which the two CDFs differ too much from each other. In order to know more about how well the CDF of the data and of the CDF of the probability distributions correspond with each other, we determine the total vertical difference between the CDFs.

This is done by subtracting the CDF of the data in $\mathbb{P}$ from the CDF of $\mathbb{P}_0$. For every determined geometric property in a data set the CDF value is subtracted from the estimated CDF value of the $\mathbb{P}_0$. We calculate the difference S_i for a certain data point. At some locations the value of the distribution of the data exceeds the particular probability distribution. Part of the values for S_i returned by this subtraction may be negative and by adding these up the total difference may become very close to the value of 0. The different outcomes are then hard to compare, so we determine the sum of the squares and take the square root of the total sum as the total dimensionless positive difference S:

$$S = \sum \sqrt{S_i^2} \tag{3.3}$$

A value for the total difference S closer to 0 indicates a better fit. We express the S value of a PDF fit as a percentage of the total error of all the eight PDF fits. The data sets of each geometric property are tested for different probability distributions:

Normal distribution (N)	Exponential distribution (E)
Gamma distribution (G)	Beta distribution (B)
Rayleigh distribution (R)	Lognormal distribution (L)
Weibull distribution (W)	Extreme value distribution (Ev)

Figure 3.2 shows an example of a CDF of a data set $\mathbb{P}$ with all the different probability distributions $\mathbb{P}_{0,n}$ fitted in it. The CDF is defined as the cumulative probability of the number n of sand wave heights. So the cumulative probability of this example equals 0 at $n_{min} = 0$ and equals 1 when all the sand wave heights are considered at $n_{max} = 555$. The CDF of the data is now a straight line and in this way the different CDFs can easily be compared.

3.2 Probability Density Functions

After calculating the total differences S and determining which probability distributions may correspond best with the data, we plot probability density functions. The probability density functions are plotted in the distribution fitting toolbox *dfittool* in Matlab. Figure 3.3 shows an example of a PDF of the sand wave length for a certain area. A fit of the normal distribution is plotted over the data. The location of mean value μ and the standard deviation σ are indicated. Figure 3.3 shows that the distribution of the sand wave length in this area seems

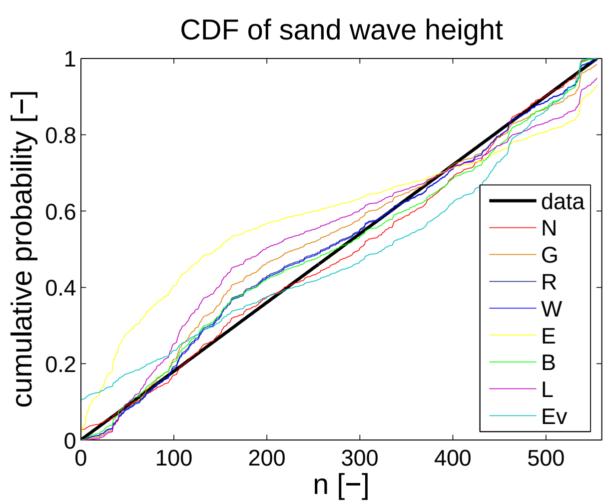

Figure 3.2: CDF for sand wave length with plots of different probability distributions. The normal distribution is the best fit.

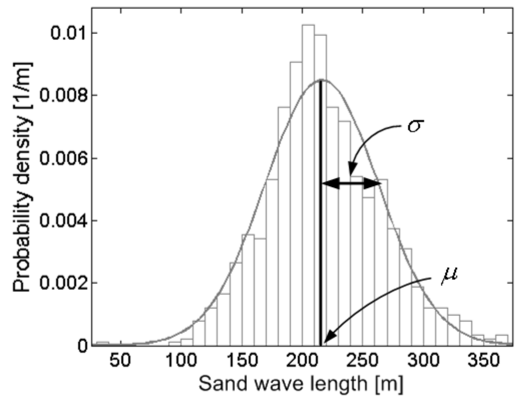

Figure 3.3: Probability density function for sand wave length with a plot of a fitted normal distribution with a mean value μ of 216 m and a standard deviation σ of 47 m.

visually to be well represented by the normal distribution.

Table 3.2 shows that the hypothesis that the sand wave length in the Ecomorf 3 area is normally distributed is rejected by the KS test. This is shown by the 1 in the table. It can also be seen that the Gamma distribution has a low value for the total difference S and is also rejected by the KS test. Visual judgement alone turns out to be insufficient to determine which probability distribution corresponds with the data. The KS test is also considered not sufficient to determine how a data set is distributed and not able to show difference between different probability distributions. In the next tables it is shown that there is no correlation between the results of the KS test and the values for S.

Skewness s is a measure of the asymmetry of the probability distribution function and can be determined in Matlab. We define a positive skew when the PDF is skewed to the right and a negative skew when the PDF is skewed to the left. A positive skew means that the right tail is the longest and the mass of the distribution is concentrated on the left of the figure. For a negative skew the left tail is the longest and the mass of the distribution is concentrated on the right of the figure.

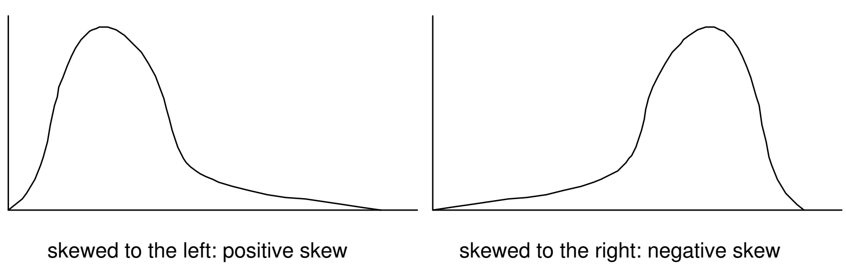

Figure 3.4: Skewness to the left (positive) and to the right (negative).

The skewness is defined in Matlab as:

$$s = \frac{E(x-\mu)^3}{\sigma^3} \tag{3.4}$$

Herein is μ the mean of x and σ is the standard deviation of x, and $E(n)$ represents the expected value of the quantity n. A value of 0 means that no skewness is observed (Mathworks, 2001).

A probability distribution is considered to correspond well with a data set when the value for the the total vertical difference S is low. When the symmetric normal distribution has a low value for S the skewness is also calculated in order to determine whether a nonsymmetric distribution, with a low value for S, corresponds with the data as well. The bulk of the data distribution is then probably best described by the normal distribution and its tail by the nonsymmetric probability distribution.

3.2.1 Sand wave height

In Table 3.1 the lowest values found for the differences S between the CDF of the data and of the probability distribution are bold. Table 3.1 shows that the total difference S is often lower for probability distributions that fail the KS test than for probability distributions for which the hypothesis is accepted. The Noordhinder areas have the smallest differences between the CDF of the data and the CDF of the Weibull distribution, while other probability distributions (normal, Gamma, Rayleigh) are accepted by the KS test. The KS test results are shown in the tables to show the lack of correlation between the KS test and the S values.

Table 3.1: Cumulative probability distribution of the sand wave height compared with cumulative probability distribution of distribution functions.

	Value of S [%] for each probability distribution								KS test							
Area	**N**	**G**	**R**	**W**	**E**	**B**	**L**	**Ev**	**N**	**G**	**R**	**W**	**E**	**B**	**L**	**Ev**
Ecomorf 3	**3.50**	7.31	27.6	3.90	36.0	5.02	10.0	6.60	1	1	1	1	1	1	1	1
R0302C	**5.13**	11.1	6.91	6.48	31.0	7.71	17.1	14.5	0	1	1	1	1	1	1	1
R0302D	7.10	8.16	7.56	**5.17**	34.4	6.70	14.1	16.8	1	1	1	1	1	1	1	1
R0303C	4.94	8.42	8.95	**4.76**	35.0	6.07	14.3	17.6	1	1	1	1	1	1	1	1
R0304D	8.63	7.49	5.10	**4.51**	32.8	8.31	13.5	19.7	0	0	1	1	1	1	1	1
R0305A	6.00	5.07	11.1	**3.25**	40.2	7.64	10.3	16.5	0	1	0	1	1	1	1	1
R0305B	7.42	4.57	9.68	**3.31**	40.8	6.91	10.5	16.8	0	0	1	1	1	1	1	1
TWIN 01	7.36	12.4	9.35	9.13	32.3	**4.28**	16.4	8.81	0	1	1	1	1	1	1	1
TWIN 02	12.5	7.56	15.9	7.23	23.1	**5.92**	11.13	16.6	1	1	1	1	1	1	1	1

Figure 3.5 shows the PDFs of three different areas: the long crested Ecomorf 3 area, the R0302D area from the short crested Noordhinder area and the short crested TWIN 01 area. Figure 3.5(a) shows the probability density functions of 966 (n) relative sand wave heights from the Ecomorf 3 area. The relative sand wave height $\Delta^*_{l,i}$ is determined by dividing the sand wave height $\Delta_{l,i}$ by the highest value for the sand wave height $\Delta_{l,max}$:

$$\Delta^*_{l,i} = \frac{\Delta_{l,i}}{\Delta_{l,max}} \tag{3.5}$$

The probability density function for the relative sand wave height is now plotted for values between 0 and 1. All PDFs can now be compared to each other and it can be seen whether a distribution is skewed to the left or the right.

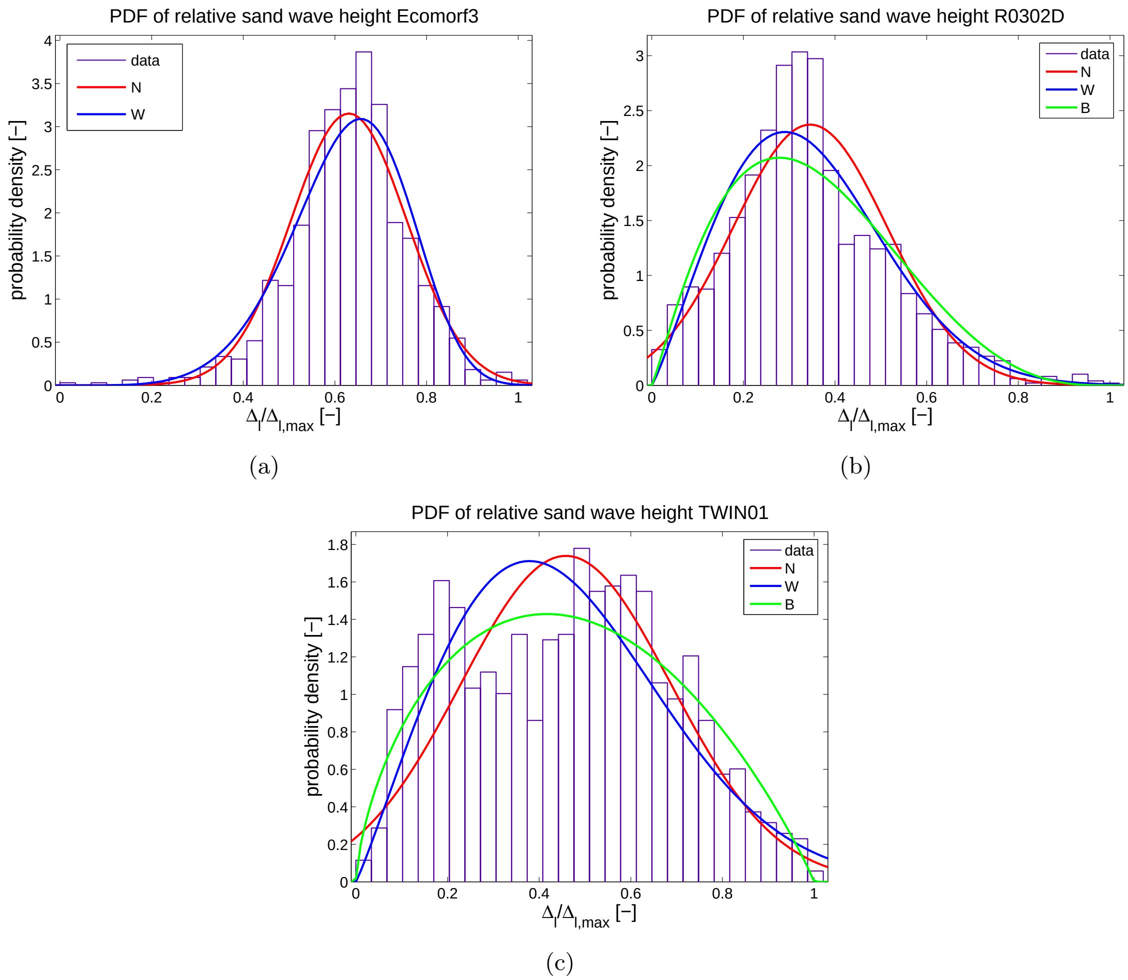

Figure 3.5: Stochastics of sand wave height in the (a) Ecomorf 3 area ($n = 966$), (b) the R0302D area ($n = 1444$) and (c) TWIN 01 area ($n = 1025$). PDFs of the relative sand wave height Δ_l^* with different distributions fitted over them.

Table 3.1 shows that the total difference S is the lowest for the normal distribution and the Weibull distribution for the Ecomorf 3 data. So we plot the PDF of the sand wave height in the Ecomorf 3 area and fit these two probability distributions over it. We observe that the two fits of the distributions are not very different from each other. Even though the normal distribution has a slightly lower value for S, the Weibull distribution is a better fit for the tail of the data. The PDF shows that the mass of the distribution is skewed to the right and the tail of the distribution is longer on the left. In Matlab the skewness is determined and this confirms the visual observed negative skewness. The calculated skewness s equals -0.50. The Weibull fit is able to describe the asymmetry of the distribution and a normal distribution is not. We consider both distributions to correspond well with the data.

Figure 3.5(b) shows a plot of the distribution of the 1444 relative sand wave heights in R0302D area from the Noordhinder area. The PDFs of the sand wave heights in the other Noordhinder areas can be found in Appendix B. When looked at the PDF in Figure 3.5(b) and in

Appendix B it can be seen that the PDFs are skewed to the left ($s = 0.98$) and have a longer tail towards the higher values. Table 3.1 shows that for five of the six Noordhinder areas the difference S is the smallest for the Weibull distribution. The Weibull is therefore plotted in every PDF of the Noordhinder areas together with other probability distributions with small differences S with a value close or below 5%.

Figure 3.5(b) shows three fits plotted over the distribution of the R0302D data. The Beta distribution can only be used for values between 0 and 1 (NIST/SEMATECH, 2006). The Weibull distribution is the best fit based on the differences S in Table 3.1.

The R0302C area (Appendix B) shows the same situation as was the case for the PDF of the Ecomorf 3 area in Figure 3.5(a). According to Table 3.1, the distribution of the 555 sand wave heights in R0302C are best described by a normal fit. Due to a skewness s of 0.90 the normal distribution is unable to describe the tail of the data sufficiently. The tail is better described by other probability distributions with low values for the difference S: the Weibull distribution. The Weibull distribution has the lowest S value and is chosen as best fit for the R0302C data and especially the tail of the distribution.

Table 3.1 and the figures in Appendix B show that the distribution of the sand wave heights in the other four Noordhinder areas (R0303C, R0304D, R0305A and R0305B) are best described by the Weibull distribution. The Weibull fit is the closest to the CDF of the data and has the lowest value for the difference S for all data sets. The Weibull distribution is chosen as best fit for the Noordhinder areaa.

Figure 3.5(c) shows a plot of the distribution of the 1025 relative sand wave heights in the TWIN 01 area. The plot of the distribution of the 1282 sand wave heights in TWIN 02 area is shown in Figure B.2(b). We notice that the shape of the PDFs of the sand wave heights in the TWIN areas are different from the areas discussed above. Figure 3.5(c) shows that two peaks can be noticed situated at a value for the relative sand wave height Δ_l^* of 0.2 and 0.5. The PDFs of the other short crested areas show one peak around the relative sand wave height of 0.3. The PDF of the sand wave height distribution of the TWIN 02 area in Figure B.2(b) also shows a different kind of distribution. These differences may be the result of the dredging that takes place in the TWIN area.

Table 3.1 shows that the lowest values of the differences S between the CDFs of the TWIN data and the different probability distributions are found for the Beta distribution. Other probability distributions have values above the value of 5%. Figure 3.5(c) shows the plot of the fit of the Beta distribution, which is very different from the plots of the Normal fit and the Weibull fit. For the TWIN areas we choose the Beta distribution as best fit, since the value S is much lower. The other probability distributions are better able to describe the tail of the PDFs of the TWIN areas. So the distribution with the the second lowest value for S is also determined. For the TWIN 01 area this is the normal distribution and for the TWIN 02 area this is the Weibull distribution.

In Knaapen (2006) probability distributions of geometric properties of sand waves of different areas are plotted. Among these distributions also sand wave height is shown. One of these areas studied show similarity with the Ecomorf 3. In this area Knaapen (2006) counted 2.2

bifurcations per square kilometre, while in the other areas the bifurcation number B is higher than 10. This area may be considered long crested and the other areas short crested. Some of the distributions of these short crested areas show similarity with the TWIN areas, but most are shaped like the PDFs of the sand wave height in the Noordhinder areas. The crests of the distribution of Knaapen (2006) are also shifted to the left with a longer tail towards the higher values for sand wave height.

3.2.2 Sand wave length

Table 3.2 shows the total differences S between the data and the probability distribution. Again the value for S is often lower for probability distributions that fail the KS test than for probability distributions for which the hypothesis is accepted. The lowest values found for the differences S between the CDF of the data and of the probability distribution are bold. Figure 3.6 shows the PDFs of the relative sand wave lengths L_c^* for the three different study areas. We observe that several probability distributions correspond well with the data and have low values for S.

Figure 3.6(a) shows the probability distributions with the lowest values for S fitted over the PDF of the sand wave lengths in the Ecomorf 3 area. The three distributions are the normal distribution, Gamma distribution and the Lognormal distribution. The PDF is skewed to the right ($s = 0.28$) and therefore the Normal distribution corresponds less with the tail of the distribution than the other probability distribution. The Gamma distribution has a lower value for S than the Lognormal distribution and the Normal distribution and is therefore the best choice.

Figure 3.6(b) and Appendix C show that the PDFs of the Noordhinder areas are all skewed to the left. The Normal distribution is therefore probably not a good fit. The low values for S indicate that the nonsymmetric probability distributions seem to correspond quite well with the PDFs of the Noordhinder areas. Figure 3.6(b) shows three probability distributions that seem to be good fits for the data. The lowest value for S is found for the Gamma distribution and is therefore the choice as best fit for the PDF of the sand wave length in R0302D.

Besides the R0302D area also the R0302C and R0304D areas correspond best with the Gamma distirbution, based on the value for the total vertical difference S. For the other three areas

Table 3.2: Cumulative probability distribution of the sand wave length compared with cumulative probability distribution of distribution functions.

	Value of S [%] for each distribution								KS test							
Area	**N**	**G**	**R**	**W**	**E**	**B**	**L**	**Ev**	**N**	**G**	**R**	**W**	**E**	**B**	**L**	**Ev**
Ecomorf 3	3.95	**2.93**	28.1	5.97	39.0	6.30	3.73	10.0	1	1	1	1	1	1	1	1
R0302C	12.5	**5.66**	9.17	6.62	28.5	7.95	10.2	19.4	0	0	1	1	1	1	1	1
R0302D	12.2	**2.93**	5.60	5.15	37.4	6.27	7.08	23.4	0	1	1	1	1	1	1	1
R0303C	14.0	5.77	11.8	8.33	25.1	9.31	**3.34**	22.4	1	1	1	1	1	1	1	1
R0304D	13.3	**3.83**	10.9	6.14	28.5	9.58	5.57	22.3	0	1	0	1	1	1	1	1
R0305A	13.1	4.88	7.00	8.03	33.3	10.7	**2.96**	20.0	1	1	1	1	1	1	1	1
R0305B	13.4	4.79	8.10	7.59	31.4	9.75	**2.89**	22.1	0	1	1	1	1	1	1	1
TWIN 01	11.2	4.21	**3.38**	4.03	41.4	4.01	9.16	22.7	0	0	0	0	1	1	1	1
TWIN 02	13.1	**2.99**	13.4	3.14	29.6	3.87	8.61	25.3	0	0	0	1	1	1	1	1

(R0303C, R0305A and R0305B) the Lognormal distribution has a lower S value and is the better fit of the two. We plotted the Gamma distribution and the Lognormal distribution over every Noordhinder data distribution to show the small difference between the two distributions.

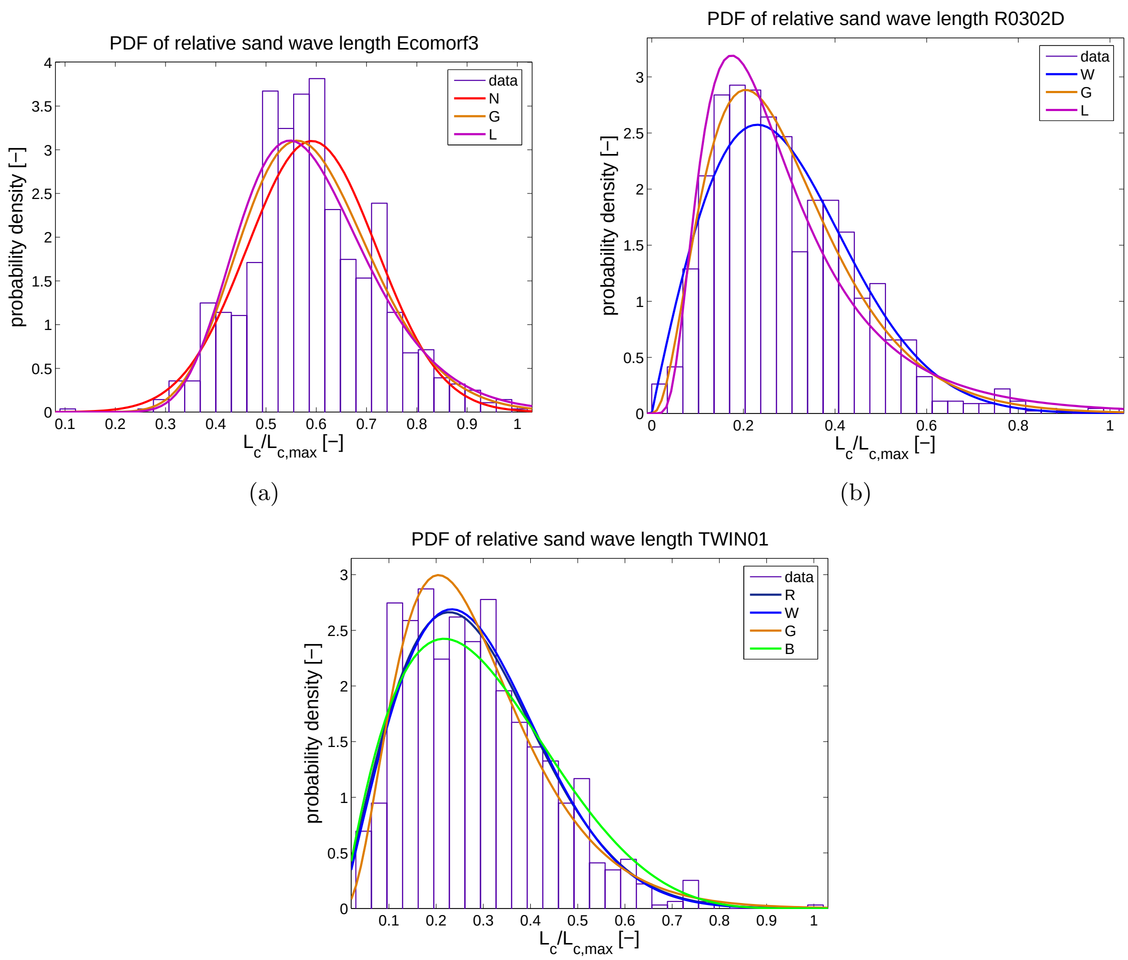

Figure 3.6: Stochastics of sand wave length in the Ecomorf 3 area ($n = 905$), the R0302D area ($n = 1347$) and TWIN 01 ($n = 960$) area. PDFs of the relative sand wave length L_c^* with different distributions fitted over them.

The difference between the CDF of the data and the CDF of the Lognormal distribution is much higher for the TWIN areas. We plotted the probability distributions with the lowest values for the TWIN 01 area in Figure 3.6(c) and for TWIN 02 in Appendix C. The Beta distribution, Weibull distribution, Gamma distribution and Rayleigh distribution are among these lowest values for S and their values are quite close to each other. The Beta fit seems to underestimate the PDF of the data. The Weibull fit and Rayleigh fit are almost alike and the Gamma seems to correspond well for the TWIN 02 area but overestimates the PDF of the TWIN 01 area.

Making a distinct choice of distribution for the total TWIN areas is quite hard, because of the many low values for S. For the TWIN 01 area the Rayleigh and Weibull are the best options, but the Rayleigh is not suitable for the TWIN 02 area. The TWIN 02 area corresponds best with the Gamma distribution and the Weibull distribution.

3.2.3 Crest elevation

Table 3.3 shows that for the short crested areas the lowest values are found for the differences S between CDFs of the data and the CDFs of the Beta distribution. All the PDFs of the short crested areas are skewed to the left. We observe in Table 3.3 that values for the difference S for other distributions are not as low as for the Beta distribution.

Figure 3.7 shows that the Ecomorf 3 area differs from the other areas in shape. The median value of the PDF (Figure 3.7(a)) is almost in the middle of the distribution almost leading to a normal distribution. The value for the difference between the CDF of the data and the CDF of a Weibull ditribution is a little lower, so there probably is a small skewness in the PDF. The difference S between the CDF of the crest elevation in the Ecomorf area and the CDF of the Beta distribution is also quite small, but the Beta fit does not correspond with the PDF as well as the other two plotted fits.

Figure 3.7(b) and Figure 3.7(c) show that the PDFs of the short crested areas are best fitted by the Beta distribution, because of the higher density for the smallest and the higher values of the crest elevation. In Appendix D this can be seen for the Noordhinder areas and in Appendix D for the TWIN 02 area. We notice that the shape of the PDFs of the crest elevation in the TWIN areas are different from the Noordhinder areas as was already seen for the sand wave height. Again two crests can be seen in Figure 3.7(c). Also this difference in shape may be the result of dredging in the areas. The PDF of the R0304D area in Appendix D also shows two crests, so dredging may also take place in this area.

In the plotted PDFs for the crest elevation the Beta distribution shows less correspondence with the tails of the data distribution than the Weibull or Rayleigh distribution. The Beta distribution shows a round tail, but the data shows a flattened out tail. So the Beta distribution is considered to correspond well with the mass of the PDF and the Weibull or Rayleigh

Table 3.3: Cumulative probability distribution of the crest elevation compared with cumulative probability distribution of distribution functions.

	Value of S [%] for each probability distribution								KS test							
Area	**N**	**G**	**R**	**W**	**E**	**B**	**L**	**Ev**	**N**	**G**	**R**	**W**	**E**	**B**	**L**	**Ev**
Ecomorf 3	2.16	7.17	22.0	**2.01**	42.5	3.16	11.9	9.07	0	0	0	1	1	1	1	1
R0302C	7.80	10.7	11.5	6.48	25.8	**3.60**	18.9	15.2	0	0	1	1	1	1	1	1
R0302D	5.91	11.5	7.45	6.48	28.5	**5.29**	19.8	15.1	1	1	1	1	1	1	1	1
R0303C	6.87	11.8	6.61	6.78	30.9	**4.31**	19.4	13.4	1	1	1	1	1	1	1	1
R0304D	7.37	12.3	13.0	9.84	22.1	**5.94**	17.4	12.0	1	1	1	1	1	1	1	1
R0305A	9.02	8.76	5.28	4.45	36.6	**3.16**	16.5	16.1	0	0	0	1	1	1	1	1
R0305B	8.95	9.06	7.88	4.29	32.9	**2.46**	17.3	17.2	0	0	1	1	1	1	1	1
TWIN 01	8.94	12.0	15.5	10.1	20.3	**4.54**	16.9	11.7	1	1	1	1	1	1	1	1
TWIN 02	13.3	8.55	26.5	8.56	9.93	**5.46**	12.0	15.7	1	1	1	1	1	1	1	1

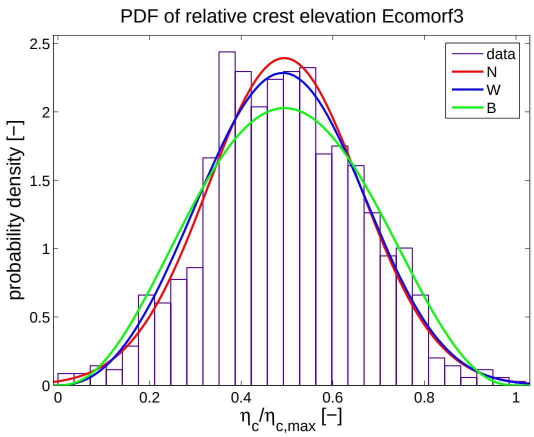

(a)

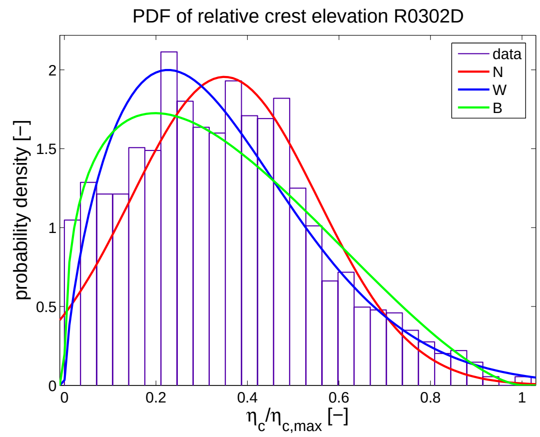

(b)

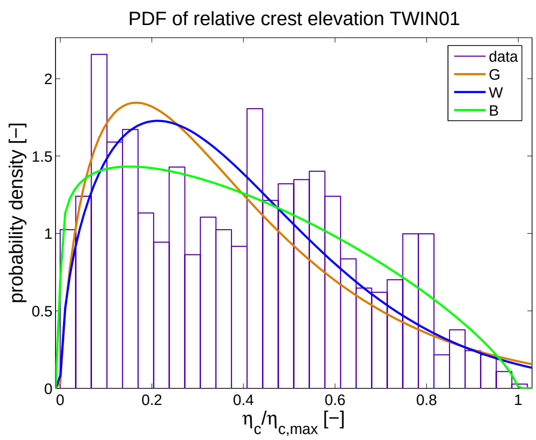

(c)

Figure 3.7: Stochastics of crest elevation in the Ecomorf 3 area ($n = 991$), the R0302D area ($n = 1547$) and TWIN 01 ($n = 1091$) area. PDFs of the relative crest elevation η_c^* with different distributions fitted over them.

correspond well with the tail.

3.2.4 Trough elevation

Table 3.4 shows the total differences S between the data and the probability distribution. Figure 3.8 shows the PDFs of the relative trough elevation η_t^* for the three different study areas. Figure 3.8(a) shows that the PDF of the trough elevation in the Ecomorf 3 area is skewed to the right and shows that the Extreme value fit corresponds well with the PDF. Table 3.4 shows that only the Extreme value distribution has a low value for S.

The PDFs of the Noordhinder areas are skewed to the right as can be seen in Figure 3.8(b) and Appendix E. A distinct difference in S values as is found for the crest elevation in the Noordhinder areas is not the case for the trough elevation. However three distribution have the lowest values for the difference between the CDF of the data and the CDF of the probability distribution: the Gamma distribution, the Weibull distribution and the Beta distribution.

Table 3.4: Cumulative probability distribution of the trough elevation compared with cumulative probability distribution of distribution functions.

	Value of S [%] for each probability distribution								KS test							
Area	**N**	**G**	**R**	**W**	**E**	**B**	**L**	**Ev**	**N**	**G**	**R**	**W**	**E**	**B**	**L**	**Ev**
Ecomorf 3	6.48	10.8	25.2	4.14	32.3	5.88	13.4	**1.75**	0	1	1	1	1	1	1	1
R0302C	10.9	6.92	14.8	**5.82**	17.1	9.44	12.7	22.3	1	1	1	1	1	1	1	1
R0302D	14.1	3.00	21.1	**1.55**	21.8	3.20	10.9	24.4	0	0	0	1	1	1	1	1
R0303C	12.5	**2.88**	16.0	3.79	21.5	7.03	8.92	27.4	0	0	1	1	1	1	1	1
R0304D	15.3	**3.10**	22.6	4.32	17.6	8.19	7.18	21.8	0	0	1	1	1	1	1	1
R0305A	14.2	**3.06**	17.1	4.08	24.5	7.50	8.34	21.3	0	0	1	1	1	1	1	1
R0305B	12.0	7.13	12.0	6.62	27.8	**6.32**	11.5	16.7	1	1	1	1	1	1	1	1
TWIN 01	**4.31**	11.5	6.29	6.82	32.8	6.66	17.3	14.4	0	1	1	1	1	1	1	1
TWIN 02	8.73	10.6	12.3	7.66	26.2	**3.97**	16.9	13.6	0	1	1	1	1	1	1	1

Figure 3.8(b) shows a plot of the PDF of the R0302D area with fits of these three probability distributions. This plot shows similarity with the PDFs for the other areas in Appendix E. Visually the Weibull fit and the Gamma fit are not very different, but based on their values for the difference S a choice can be made. The probability distribution with the lowest value for S is chosen. Except for the R0305B area in which the difference in S between the Beta and the Weibull is less than 1%.

The TWIN 01 area plotted in Figure 3.8(c) shows a PDF that is slightly different from the PDFs of the Noordhinder areas. The PDF of the TWIN 01 area is skewed to the right as well, but the tail in the PDFs of the Noordhinder areas are longer. The same is observed for the TWIN 02 area plotted in Appendix E. This results in different values for the total vertical difference S between CDFs. The lowest values for the difference S for the TWIN 01 area are found for the Rayleigh and the Beta distribution. The lowest value for the TWIN 02 area is found for the the Beta distribution.

3.2.5 Sand wave asymmetry

PDfs of three different study areas are plotted in Figure 3.9. For the Ecomorf 3 area the lowest values for the difference S between the CDFs is found for the Extreme value distribution and the Weibull distribution (Table 3.5). Figure 3.9(b) shows the PDF of the data with these probability distributions fitted over it. The Extreme value distribution corresponds the best with the PDF of the sand wave asymmetry in the Ecomorf 3 area.

For the Noordhinder area the distributions with the lowest values for S found show some scatter. Figure 3.9 shows the PDF of the R0302D area as an example. The lowest value is found for the Beta distribution. The Beta distribution is fitted in the PDF together with the Extreme value distribution. In Appendix F the PDFs of the other Noordhinder areas can be found. The Beta distribution or the Extreme value distribution correspond best with the Noordhinder areas.

The PDFs of sand wave asymmetry in the TWIN areas are shown in Figure 3.9(c) and in Appendix F. The PDFs are skewed to the right. Table 3.5 shows that the Beta distribution and the Extreme value distribution correspond best with PDFs of the sand wave asymmetry.

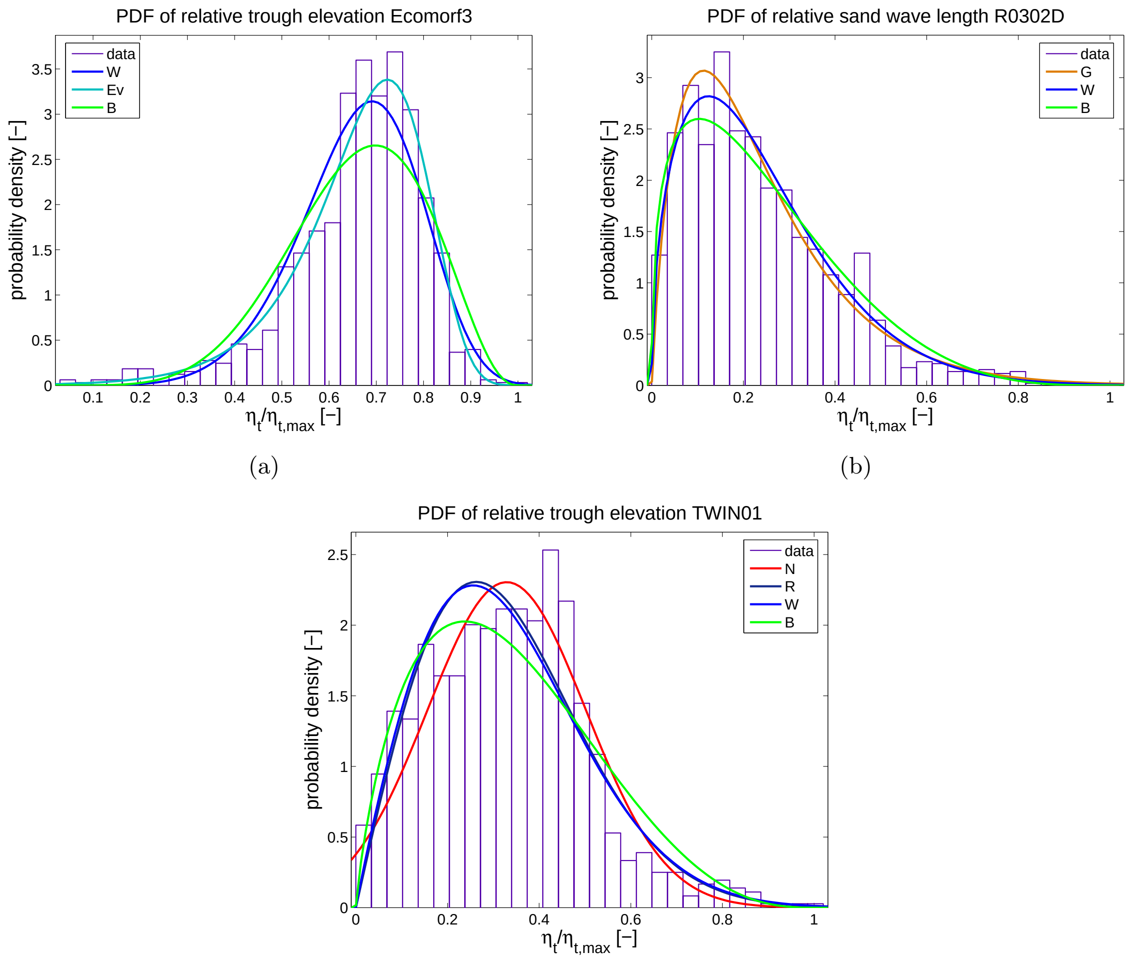

(a) (b)

(c)

Figure 3.8: Stochastics of trough elevation in the Ecomorf 3 area ($n = 994$). The (a) PDF of the trough elevation η_t and the (b) PDF of the relative trough elevation η_t^*. The Weibull distribution (W), the Extreme value distribution (Ev) and the Beta distribution (B) are fitted over the PDFs.

Table 3.5: Cumulative probability distribution of the sand wave asymmetry compared with cumulative probability distribution of distribution functions.

	Value of S [%] for each probability distribution								KS test							
Area	**N**	**G**	**R**	**W**	**E**	**B**	**L**	**Ev**	**N**	**G**	**R**	**W**	**E**	**B**	**L**	**Ev**
Ecomorf 3	6.28	11.0	25.7	4.08	32.8	4.28	15.2	**0.77**	0	1	1	1	1	1	1	1
R0302C	5.51	9.88	17.8	5.66	37.4	**2.95**	14.7	6.09	0	1	1	1	1	1	1	1
R0302D	5.62	11.2	18.3	6.25	35.5	4.43	15.26	**3.42**	0	0	0	1	1	1	1	1
R0303C	5.73	11.6	19.2	6.26	34.7	4.65	15.4	**2.53**	0	0	1	1	1	1	1	1
R0304D	6.06	10.2	17.6	6.15	33.9	**3.36**	16.6	6.08	0	1	1	1	1	1	1	1
R0305A	4.73	11.9	15.7	6.41	35.4	4.64	16.9	**4.32**	1	1	1	1	1	1	1	1
R0305B	6.03	8.85	14.2	5.35	40.3	**2.82**	13.4	9.09	0	1	1	1	1	1	1	1
TWIN 01	6.67	11.4	20.0	6.66	34.0	3.79	14.6	**2.92**	0	1	1	1	1	1	1	1
TWIN 02	6.04	11.5	19.0	6.54	35.0	**2.67**	2.99	3.80	0	1	1	1	1	1	1	1

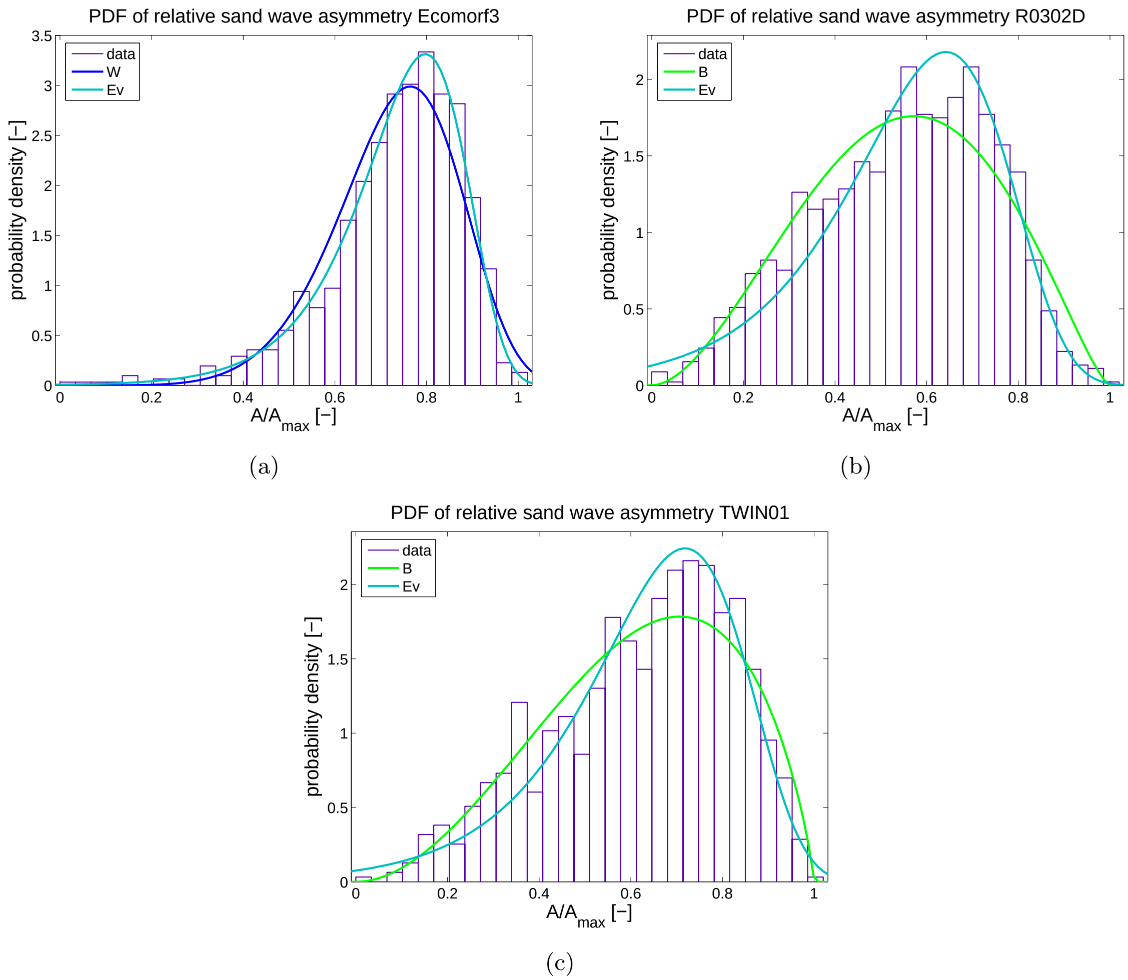

Figure 3.9: Stochastics of sand wave asymmetry in (a) the Ecomorf 3 area ($n = 908$), (b) the Noordhinder area ($n = 1329$) and (c) the TWIN 01 area ($n = 926$). The PDFs of the sand wave asymmetry A and fits of different distributions. The normal distribution (N), Weibull distribution (W), Beta distribution (B) and the Extreme value distribution (Ev) are fitted over the PDFs.

The PDFs of the asymmetry show that the sand waves in the Ecomorf 3 area look more like each other in asymmetry than the short crested areas. We observe the smaller shape of the PDF and the high amount of values above 0.5, which means an asymmetry as in Figure 2.5. We also observe the small amount of values below 0.5, which are sand waves with an asymmetry in which the crest of the sand wave is situated to the left of the middle.

3.3 Overview

We showed that the KS test in some situations accepts probability distributions while it is not expected. In other situations the KS test rejects probability distributions in which it is not expected. The KS test cannot be used to determine the difference between the fits of probability distributions and cannot determine accurately if the geometric properties in the field data are distributed according to a known probability distribution. This may be the result of the fact that field data is more irregular than the ideal CDFs the CDF of the data is compared with. This leads to maximum differences found by the KS test that exceeds the critical value, while actually the CDFs are quite similar and the value for S is low.

Table 3.6 gives an overview of all the probability distributions found that correspond with the distribution of the geometric properties of each study area. For some areas the difference between two or more probability distributions is very small and can therefore all be found in the table. We observe the differences and resemblances between the long crested Ecomorf 3 area and the short crested areas. Some geometric properties seem to be well represented by one probability distribution, like the sand wave height and the crest elevation. The Weibull distribution corresponds best with the sand wave height in the Ecomorf and Noordhinder area. Possibly to the dredging the Weibull fits the TWIN areas less well and the Beta distribution turns out the best option.

The division between the Noordhinder area and the TWIN area can also be seen for the sand wave length. The Gamma distribution and the Lognormal distribution show the best fits for the Ecomorf 3 and Nooordhinder areas. The best fit for the Noordhinder area is harder to determine and three distributions are selected. Due to the high porbability density for low values, the crest elevation corresponds best with the Beta distribution. The Ecomorf area however, shows another almost normally distributed PDF. The Weibull distribution describes the PDF a little better due to the small skewness.

As explained before, the Ecomorf 3 sand waves are long crested and show less bifurcations. The Noordhinder sand wave fields are short crested and many bifurcations can be counted in the plan views (Table 2.2). The bifurcations may be the reason that these sand wave fields are less well described by the normal distribution than the Ecomorf 3 sand wave field. Large sand waves are found in the data, but also new sand waves originate at bifurcations. In this way an amount of sand waves with lower values are formed and are visual in the longitudinal bed elevation profile. These sand waves are quite small near the bifurcation. Therefore Figure 3.10 shows this difference in shape between the PDFs of the sand wave height of the long crested area and short crested areas.

The PDFs of the trough elevation show the same difference between the long crested area and the short crested areas. The trough elevation in the Ecomorf 3 area is best described by

Table 3.6: Corresponding distributions of the geometric properties of sand waves in the study areas.

Area	**Height** Δ_l	**Length** L_l	**Crest** η_c	**Trough** η_t	**Asymmetry** A
Ecomorf 3	N/W	G/L/N	W/N	Ev/W	Ev/B/W
R0302C	N/W	G/W	B/W	W/G	B/N/W
R0302D	W	G/W	B/W	W/G	Ev/B
R0303C	W	L/G	B/R/W	G/W	Ev/B
R0304D	W	G/L	B/W	G/W	B/N/Ev
R0305A	W	L/G	B/W	G/W	Ev/B/N
R0305B	W	L/G	B/W	B/W/G	B/W/N
TWIN 01	B/N	R/W	B/W	N/R	Ev/B
TWIN 02	B/W	G/W	B/R/W	B/W	B/Ev

the Extreme value distirbution. For the short crested areas more probability distributions are found with low values for the difference S between the CDFs. This leads to different probability distributions that correspond best with different study areas as can be seen in Table 3.6. For the sand wave asymmetry we observe two probability distributions (Extreme value and Beta) that correspond best with the different areas.

In the literature in Table 1.2 (Section 1.2.3) the probability distributions found describing the river dune height are the Rayleigh distribution, the Exponential distribution and the Gamma distribution. We found the Weibull distribution and the Beta distribution as best fits. So the distribution of sand wave height and river dune height can probably not be compared. The Rayleigh and the Weibull functions are however related and also in our study the differences between the two turned out to be small. So based on this there may be some resemblance between the distribution of sand wave height and the distribution of river dune height found by Ashida and Tanaka (1967) and Nordin (1971).

The river dune length is found by Ashida and Tanaka (1967) to correspond with the Rayleigh distribution. Nordin (1971) and Annambhotla et al. (1972) found the Exponential distribution and Mahmood and Ahmadi-Karvigh (1976) found the the normal distribution. Also the Gamma distribution (Cheong and Shen, 1976) and the Weibull distribution (Wang and Shen, 1980) are found. So not much resemblance is found between different studies into the river dune length. In this study the Gamma distribution seems to correspond the best with sand wave length. So again some resemblance with the river dune length (Cheong and Shen, 1976) is found. The reasons for the differences in the determined probability distribution may be influenced by the way the data was processed in the studies.

It is hard to compare the results of Knaapen (2006) to our results as it has to be done visually. A resemblance is seen in the skewness of the probability distribution for sand wave height, sand wave length and asymmetry. More cannot be determined from the plots of the distribution of the geometric properties.

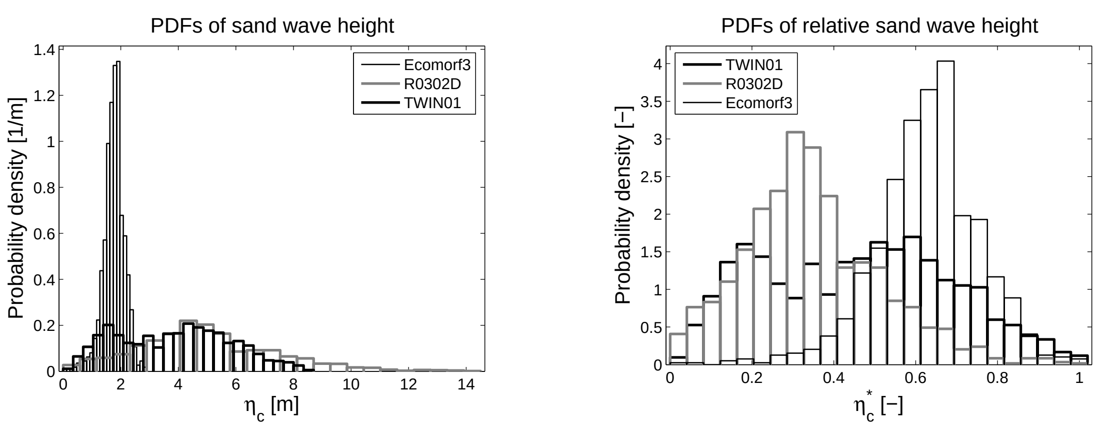

(a) (b)

Figure 3.10: The PDFs of (a) sand wave height and (b) relative sand wave height of the Ecomorf 3 area, the Noordhinder area and TWIN area.

We also compare the distributions of the crest elevation and the trough elevation. These geometric properties are often referred to as the amplitude of the sand waves after detrending the longitudinal bed elevation profile. In the ideal sinus-like BEP the crest elevation and the trough elevation are the same and can be referred to as amplitude. In reality the shape of the sand waves is not sinus-like and the values found for crest elevation and trough elevation in the short crested sand wave fields are not the same. Also the distribution of the trough elevation and crest elevation is different. So referring to both the crest elevation and trough elevation is not correct when analysing short crested sand waves. The sum of the mean crest elevation and the mean trough elevation does equal the mean sand wave height. For long crested sand waves the crest elevation and trough elevation show more similarity.

Chapter 4

Relation between geometric properties

In this chapter we will determine whether there is a relationship between the mean value and standard deviation of the field data in the different study areas. We determine the coefficient of variation, which is calculated by dividing the standard deviation by the mean value. This is done for every geometric property of the sand waves for every data set. The outcomes are visualised by plotting the mean values to the standard deviations. We compare the study areas and determine if the coefficient of variation is a constant. When the coefficient is a constant we may be able to estimate the standard deviation, which is a measure for the spread of a geometric property, based on the mean value. The results are compared to results found for river dunes by various researchers. We also look into the relation between the mean values of sand wave height and sand wave length. Also the relation between mean crest elevation and mean trough elevation is shortly discussed.

4.1 Coefficient of variation

It is determined whether the mean value and the standard deviation are related to each other for every analysed geometric property. The ratio of standard deviation to mean value is the coefficient of variation C and can be determined in Matlab as the standard deviation of the relative data distribution. The coefficient of variation C can also be calculated by dividing the standard deviation σ by the mean value μ:

$$C = |\frac{\sigma}{\mu}| \tag{4.1}$$

For all the areas the outcomes are listed in the tables below. The coefficients of variation of the Noordhinder area, TWIN area and the Ecomorf 3 area are averaged up separately. In the figures we plot markers with the mean value of a data set for a certain geometric property against the standard deviation. Then we plot a linear fit trough the data through the origin and a slope equalling the average coefficient of variation. The deviation of the markers around the fit determines whether the coefficient of variation is a constant for a geometric property.

Table 4.1: Standard deviation, mean and coefficient of variation of sand wave height and sand wave length.

Sand wave height					**Sand wave length**				
Area	n	σ	μ	C_Δ	**Area**	n	σ	μ	C_L
-	-	[m]	[m]	[-]	-	-	[m]	[m]	[-]
R0302C	555	2.88	5.70	0.51	R0302C	489	179.9	316.2	0.57
R0302D	1444	2.40	4.95	0.48	R0302D	1347	136.5	254.6	0.54
R0303C	1170	2.28	4.84	0.47	R0303C	1101	157.1	260.7	0.60
R0304D	589	3.21	5.83	0.55	R0304D	522	201.9	341.2	0.59
R0305A	1215	2.50	5.67	0.44	R0305A	1199	147.7	291.6	0.51
R0305B	1265	2.55	5.64	0.45	R0305B	1168	163.5	300.7	0.54
Average of C_Δ				0.48	Average of C_L				0.56
TWIN01	1025	1.94	3.88	0.50	TWIN01	960	155.8	300.5	0.52
TWIN02	1282	1.74	2.82	0.62	TWIN02	1201	151.6	245.3	0.62
Average of C_Δ				0.56	Average of C_L				0.57
Ecomorf 3	966	0.36	1.75	0.20	Ecomorf 3	905	47.0	216.1	0.22
Total average of C_Δ				0.47	Total average of C_L				0.52

4.2 Sand wave height

The mean values, standard deviations and coefficients of variation of sand wave height and sand wave length for each study area are shown in Table 4.1. The variables shown are the amount of data points n, the standard deviation σ, the mean value μ and the relative coefficient of variation C. The average values for each study area are calculated and can be found in the table.

The Ecomorf 3 area is the study area with long crested sand waves and the other study areas consist of short crested sand waves. The outcomes of the coefficient of variation C_Δ for the sand wave height in Noordhinder vary between 0.44 and 0.55 with a mean value of 0.48. The TWIN areas have an average coefficient of variation for the sand wave height of 0.56. The Ecomorf 3 area outcome differs from the outcome of the Noordhinder and TWIN areas. The Ecomorf 3 area has a value for the coefficient of variation C_Δ of 0.20.

The different coefficients of variation for the long crested and short crested sand waves can be concluded from the shape of the PDFs of the data sets. The PDF of sand wave height in the Ecomorf 3 area is much smaller and has a higher probability density than the Noordhinder and TWIN areas (Figure 3.10). This means that a smaller range of sand wave heights is found and that relatively more sand waves are observed with a value close to the mean value. This lead to a smaller standard deviation for the Ecomorf 3 area and therefore a smaller value for the coefficient of variation C_Δ.

Figure 4.1 confirms the difference between the short crested and long crested areas. The distance between the markers of the long crested Ecomorf 3 data and the short crested areas is distinct. The slope of the fit representing the coefficient of variation in the Ecomorf 3 area is about half of the other slope of the other fits.

More or less the same values are found for the values of C_Δ in the two short crested areas (Noordhinder and TWIN). Figure 4.1 shows that the data point lie more or less on a straight

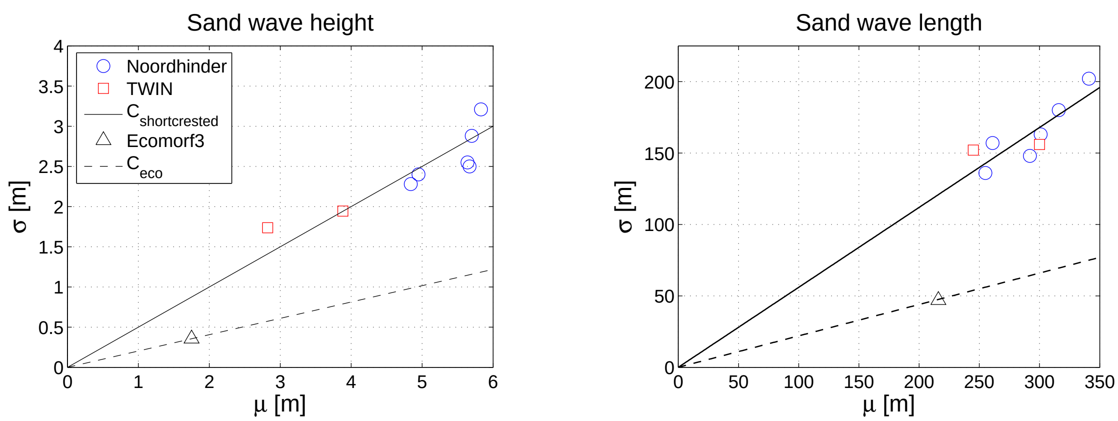

(a) (b)

Figure 4.1: (a) The mean μ of the sand wave heights in each study area plotted against the standard deviation σ. (b) The mean μ of the sand wave lengths in each study area plotted against the standard deviation. The slope in the fits equal the coefficients of variation C for the different areas.

line and this indicates the linear relationship between the mean and the standard deviation for each area. We observe that the fits of the two short crested areas are close to each other for the sand wave height. We also plotted a fit with the average value of C_Δ for the short crested areas. The short crested areas show a linear relationship for the fit with the value $C_{\Delta_{avg}}$ as slope. We can determine this average:

$$C_\Delta = |\frac{\sigma}{\mu}| = 0.50$$

We are now able to give a rough estimation the standard deviation when the mean value of sand wave height is known. We must keep in mind that this is based on two areas in the North Sea and are the data is obtained at one moment in time.

4.3 Sand wave length

The same is done for the sand wave length. The average of the coefficient of variation C_L for the sand wave length in Noordhinder equals 0.56. The coefficient of variation of the sand wave length in the TWIN areas has an average value of 0.57. The short crested areas have values very close to each other. The long crested Ecomorf 3 area outcome differs from the outcome of the short crested areas. The Ecomorf 3 area has a value for the coefficient of variation of sand wave height of 0.22.

We observe a linear relation between the mean values and the standard deviation for the short crested areas. The Ecomorf 3 area has a value for the coefficient of variation of sand wave length of 0.22. So the long crested area is also different from the short crested areas for the sand wave length. By comparing the PDFs of the relative sand wave length this difference is already observed. The PDF of the Ecomorf 3 area is smaller and has a higher probability density. So we calculate the relationship between the mean and the standard deviation only

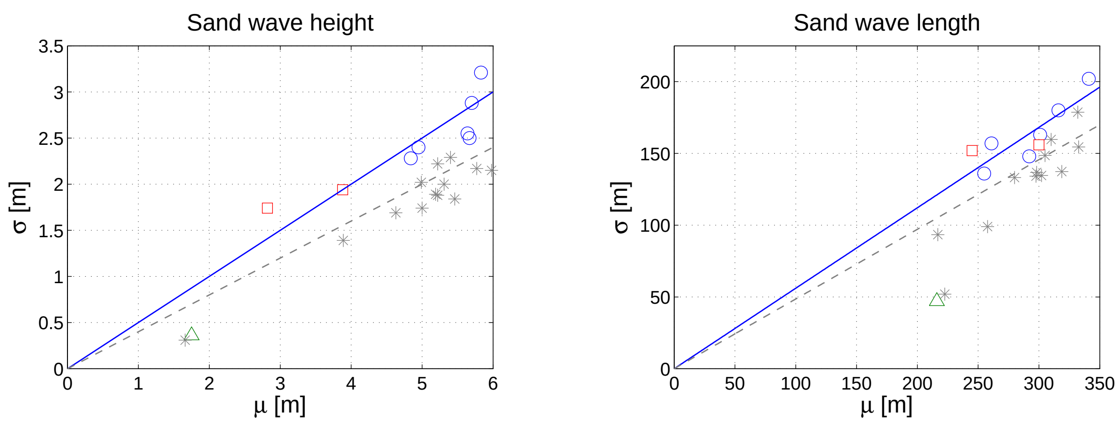

(a) (b)

Figure 4.2: (a) The mean μ of the sand wave heights in each study area plotted against the standard deviation σ. (b) The mean μ of the sand wave lengths in each study area plotted against the standard deviation. Results of Knaapen (2006) are also included. The slope in the solid fit equals the average coefficient of variation the short crested areas in this study. The dashed fit represents the data of Knaapen (2006) $\bigcirc$ = Noordhinder $\square$ = TWIN $\triangle$ = Ecomorf 3 $*$ = Knaapen (2006)

for the short crested areas and we exclude the Ecomorf 3 area.

The average coefficient of variation C_L of the short crested areas is 0.56. The standard deviation of a sand wave length distribution in a short crested data set can be estimated by the product of the mean value and the average coefficient of variation with the value 0.56. The relation between the mean and the standard deviation for short crested areas is:

$$C_L = |\frac{\sigma}{\mu}| = 0.56$$

4.4 Crest elevation

The mean values, standard deviations and the coefficients of variation of the crest elevation and the trough elevation are shown in Table 4.2. The calculated coefficient of variation C_{η_c} in the short crested areas for the crest elevation varies within a narrow range of 0.53 and 0.76 with a mean of 0.61. It appears that the coefficient of variation C_{η_c} defined as $|\sigma/\mu|$ is more or less a constant for the crest elevation in the short crested areas.

The Ecomorf 3 area has a value for the coefficient of crest elevation C_{η_c} of 0.34. So the coefficient of variation in the long crested Ecomorf 3 area is again lower than those of the other data sets. Figure 4.3 shows that the marker of the Ecomorf 3 area is closer to the plots of the fits trough the short crested data sets than for the sand wave height and sand wave length. The fit trough the data sets and the lower value for the coefficient C_{η_c} show that the long crested and short crested areas should be considered differently. This is the result of the

Table 4.2: Standard deviation, mean and coefficient of variation of crest elevation and trough elevation.

Crest elevation					Trough elevation				
Area	n	σ	μ	C_{η_c}	**Area**	n	σ	μ	C_{η_t}
-	-	[m]	[m]	[-]	-	-	[m]	[m]	[-]
R0302C	605	2.15	3.53	0.61	R0302C	601	1.56	2.15	0.73
R0302D	1547	1.81	3.10	0.58	R0302D	1529	1.28	1.85	0.69
R0303C	1261	1.70	3.09	0.55	R0303C	1238	1.27	1.82	0.70
R0304D	647	2.28	3.69	0.62	R0304D	645	1.57	2.18	0.72
R0305A	1380	2.00	3.75	0.53	R0305A	1199	1.24	1.95	0.64
R0305B	1350	2.05	3.62	0.57	R0305B	1363	1.17	2.03	0.58
Average of C_{η_c}				0.58	Average of C_{η_t}				0.67
TWIN01	1091	1.57	2.50	0.63	TWIN01	1057	0.73	1.39	0.53
TWIN02	1336	1.33	1.74	0.76	TWIN02	1341	0.66	1.11	0.60
Average of C_{η_c}				0.70	Average of C_{η_t}				0.56
Ecomorf 3	991	0.31	0.92	0.34	Ecomorf 3	994	0.18	0.85	0.21
Total average of C_{η_c}				0.58	Total average of C_{η_t}				0.60

smaller shaped PDF found for the crest elevation of the long crested area.

The plotted fits with the average coefficient of variation as slope for the Noordhinder areas and the TWIN areas are again close to each other as was observed for the sand wave height and the sand wave length, but the average coefficients of variation C are not as close to each other as is found for the sand wave height and sand wave length. However based on the small scatter around the fit of the average coefficient of variation we consider the plot of the fit with slope 0.61 as a good fit for the short crested area. This means for the crest elevation in a short crested data area:

$$C_{\eta_c} = |\frac{\sigma}{\mu}| = 0.61$$

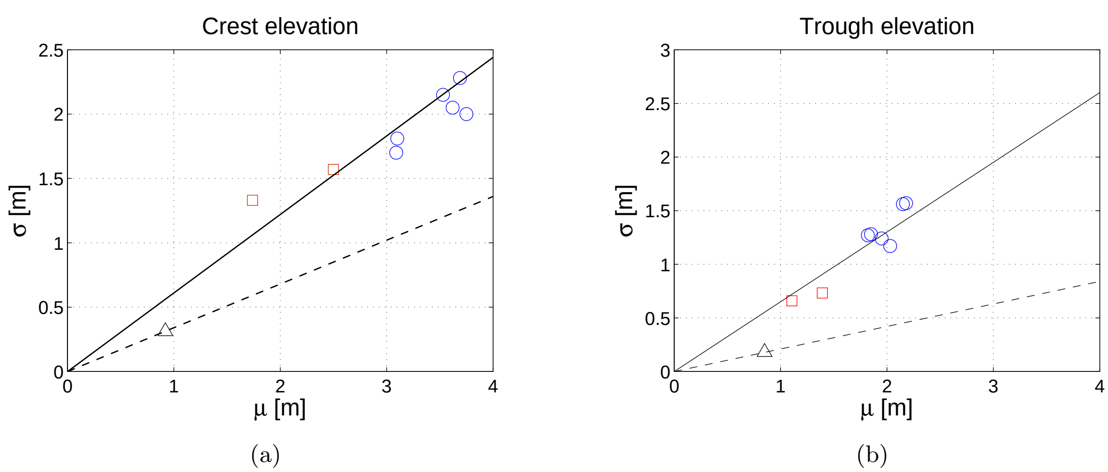

Figure 4.3: The mean μ of the crest elevations in each study area plotted against the standard deviation σ (a). The mean μ of the trough elevations in each study area plotted against the standard deviation (b). The slopes of the fits are equal to the coefficient of variation. The bold solid fit represents the total average of the coefficient of variation. ◯ = Noordhinder □ = TWIN △ = Ecomorf 3

4.5 Trough elevation

Table 4.2 shows that the outcome of the coefficient of variation $C_{\eta t}$ in the short crested areas for the trough elevation varies within a range of 0.53 and 0.73, with a mean of 0.65. It appears that the coefficient of variation $C_{\eta t}$ defined as $|\sigma/\mu|$ is also more or less a constant for the trough elevation in the short crested areas. The Ecomorf 3 area has a coefficient of variation $C_{\eta t}$ of 0.18 and is considered separately. This is the result of the smaller PDF found for the trough elevation of the long crested area.

The average of the coefficient of variation $C_{\eta t,avg}$ for the trough elevation in the short crested data sets is 0.65, within a range of 0.53 and 0.73. This means for the trough elevation in a short crested data area:

$$C_{\eta t} = |\frac{\sigma}{\mu}| = 0.65$$

4.6 Sand wave asymmetry

The coefficient of variation does not seem to be a constant for any data set for the sand wave asymmetry, based on Table 4.3. Figure 4.4 and Table 4.3 show this wider range of values. In Table 4.3 and Figure 4.4 we observe that the standard deviations in each data set do not differ so much from each other, but dividing these values by a number close to zero leads to a high variation in the results. The outcome of the coefficient of variation for the sand wave asymmetry varies within a much wider range of 1.69 and 6.19, with a mean of 3.60. The TWIN areas have an average value for the coefficient of variation for the asymmetry of 1.52. The Ecomorf 3 area has a much lower value for the coefficient of variation of sand wave asymmetry of 0.32. In the PDFs of the asymmetry we already observed that the shape of the sand waves in the Ecomorf 3 area show more resemblance to each other than the sand waves in the short crested area. In the short crested areas a wider range of A values for asymmetry are found than in the long crested area. The coefficient of variation in the long crested area

Table 4.3: Standard deviation, mean and coefficient of variation of sand wave asymmetry.

Area	n	σ	μ	C_A
-	-	[m]	[m]	[-]
R0302C	485	0.36	0.12	3.06
R0302D	1329	0.35	0.15	2.36
R0303C	1078	0.36	0.16	2.21
R0304D	520	0.37	0.22	1.69
R0305A	1155	0.41	0.07	6.10
R0305B	1180	0.34	0.05	6.19
Average of C_A				3.60
TWIN01	926	0.35	0.31	1.15
TWIN02	1206	0.40	0.21	1.88
Average of C_A				1.52
Ecomorf 3	908	0.15	0.48	0.32
Total average of C_A				2.77

is therefore lower than in the short crested areas.

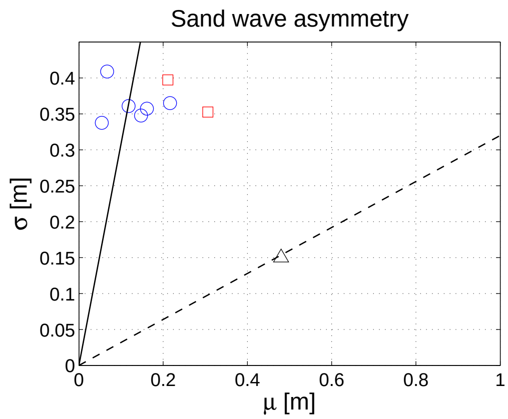

(a)

Figure 4.4: The mean μ of the sand wave asymmetry in each study area plotted against the standard deviation σ. The slopes of the fits are equal to the coefficient of variation. The bold solid fit represents the total average of the coefficient of variation. $\bigcirc$ = Noordhinder $\square$ = TWIN $\triangle$ = Ecomorf 3.

4.7 Overview

We compare our results with values for the coefficient of variation found for river dune height, river dune length, crest elevation and trough elevation by Gabel (1993), Leclair et al. (1997) and Van der Mark et al. (2007). Van der Mark et al. (2005) also found values for the coefficient of variation for bedforms, but Van der Mark et al. (2007) used more data than Van der Mark et al. (2005).

Van der Mark et al. (2007) found a value for the average coefficient of variation for the bedform height of 0.40. This value is the average of the values found for data from flume experiments (C_Δ = 0.41) and from field measurements (C_Δ = 0.39). Gabel (1993) found values of C_Δ varying between 0.36 and 0.53 and Leclair et al. (1997) reports values between 0.39 and 0.48 for the coefficient of variation for the dune height C_Δ. Table 4.1 shows that in this study the coefficient of variation C_Δ for the short crested areas varies between 0.44 and 0.62 for the sand wave height. The values for the coefficient of variation C_Δ reported in literature have slightly lower values than found in this study and the variation is in the same order.

Since the study of Gabel (1993), Leclair et al. (1997), Van der Mark et al. (2005) and Van der Mark et al. (2007) are based on river dunes it may be better to compare the values for the coefficient of variation C_Δ with data from a marine environment. Figure 4.2 shows the plots of the mean values and the standard deviations for sand wave height and sand wave length provided by Knaapen (2006). We observe a linear relation between the mean values and standard deviations determined by Knaapen (2006). A small deviation occurs between the plots of this study and the plots of data from the study of Knaapen (2006). A reason for the small deviation in Figure 4.2(a) may be the difference in data processing used and the definition used for sand wave height. One of the areas of Knaapen may be long crested since there are only a few bifurcations. This data set is also plotted and its location is distant from the other areas, but very close to the long crested Ecomorf 3 area.

We conclude that for the bedform height the coefficient of variation C_Δ is a constant for both the river dunes and the sand waves. The ranges and values found for the bedform height vary in this study. Based on the small range of the coefficients of variation C_Δ in this study, the average value for C_Δ is considered relatively accurate in estimating the standard deviation based on the mean bedform height.

For dune length Gabel (1993) reports values of C_L between 0.30 and 0.55. Leclair et al. (1997) reports values between 0.32 and 0.36 for the coefficient of variation. The value of the average coefficient of variation for dune length reported by Van der Mark et al. (2007) is 0.50. In Table 4.1 we observe that the coefficient of variation C_L for the short crested areas in this study varies between 0.51 and 0.62 for the sand wave length. This narrow range allows us to use the average coefficient of variation C_L as an estimator for the standard deviation based on the mean value.

Figure 4.2(b) shows a small deviation between our study and Knaapen (2006) for the sand wave length. This study has an average coefficient of variation of 0.52 for the sand wave length and the average coefficient of variation in the study of Knaapen (2006) is 0.47 with a range between 0.38 and 0.54. The lowest value, which is the result of the long crested area, is not considered in the range. The deviation between the average coefficients of variation in Knaapen (2006) and in this study is less than for the sand wave height. In Figure 4.2 the area with just a few bifurcations is again located near the Ecomorf 3 data.

Van der Mark et al. (2007) found an average value for the average coefficient of variation for the crest elevation C_{η_c} of 0.52. In this study the values are found within a range 0.53 and 0.76 with an average coefficient of variation for crest elevation equalling 0.61. The C_{η_c} may serve as an estimator for the standard deviation based on the mean value, but probably less accurate than for the sand wave height and sand wave length.

Van der Mark et al. (2007) found an average value for the average coefficient of variation for the trough elevation C_{η_t} of 0.55. The coefficient of variation for trough elevation C_{η_t} found in this study has a value of 0.65 with a range between 0.53 and 0.73. The value of C_{η_t} may serve as an estimator for the standard deviation. The coefficient is, as was seen for the crest elevation, probably less accurate than for the sand wave height and sand wave length.

We also look into the relation between different geometric properties. In the tables above the mean values of these different geometric properties are given. Table 4.4 shows the relation between the mean values of sand wave length and the sand wave height. We observe that for the Noordhinder study areas the values are more or less the same. The other study areas however show a different relation. The mean values for the sand wave lengths in TWIN areas have the same values as found for the Noordhinder areas, but the mean sand wave heights are quite lower. This may be the result of the the dredging that takes place in the TWIN areas. As we do not have information about the period in which the measurements were done, the seasonal influence may also be the cause of this difference. The sand wave length in the Noordhidner areas can be estimated by multiplying the sand wave height by 54.

The long crested sand waves in the Ecomorf 3 area show a completely different result. The value for $L_{c,avg}/\Delta_{l,avg}$ is much higher. The water depth in this area is very different from the short crested areas and water depth probably influences the sand wave height and sand wave length. So it is not possible to compare the long and short crested areas.

In Chapter 3 is already shown that stochastics of the crest elevation and the trough elevation are not equal and cannot be referred to as amplitude. The difference between the values of the crest elevation and the trough elevation is due to the fact that the crests and the troughs have different shapes. The shape of the crests looks like a small peak and the shape of the troughs is flatter.

Table 4.4 shows the relation between the mean values of crest elevation and trough elevation. The closer the value $\eta_{c,avg}/\eta_{t,avg}$ is to 1, the more resemblance is seen between the crest elevation and trough elevation. In the long crested area this is the case, but for the short crested areas the values for crest elevation are about 1.72 times larger than the mean values of the trough elevations.

Table 4.4: Relation between mean sand wave height and mean sand wave length and the relation between the mean crest elevation and mean trough elevation.

Area	$L_{c,avg}/\Delta_{l,avg}$ [-]	$\eta_{c,avg}/\eta_{t,avg}$ [-]
R0302C	55.5	1.64
R0302D	51.4	1.68
R0303C	53.7	1.70
R0304D	58.5	1.69
R0305A	51.4	1.92
R0305B	53.3	1.78
TWIN01	77.4	1.79
TWIN02	86.9	1.58
Ecomorf 3	123	1.08

Chapter 5

Extreme values

In this chapter we analyse the extreme values of the data sets. The value Δ_5 for which 5% of the field data is smaller is determined. This is also done for the Δ_{95} value. A relation between the two tells us more about the asymmetry of the extreme values and shows different values for long crested sand waves and short crested areas. For the users in the North Sea the high extreme values are of importance. Besides the value of which 5% of all the values is higher we also determine the largest 1% from the field data. We determine how distant these values are from the mean and when this distance is a constant we may be able to estimate the extreme values.

5.1 Method

The tails of the PDFs represent the extreme values of the geometric properties of sand waves. It is determined whether there is a relationship between the stochastic characteristics and the extreme values of the data set. The process is described using the sand wave length L as an example. Figure 5.1(a) shows the CDF of the sand wave lengths in the Ecomorf 3 area.

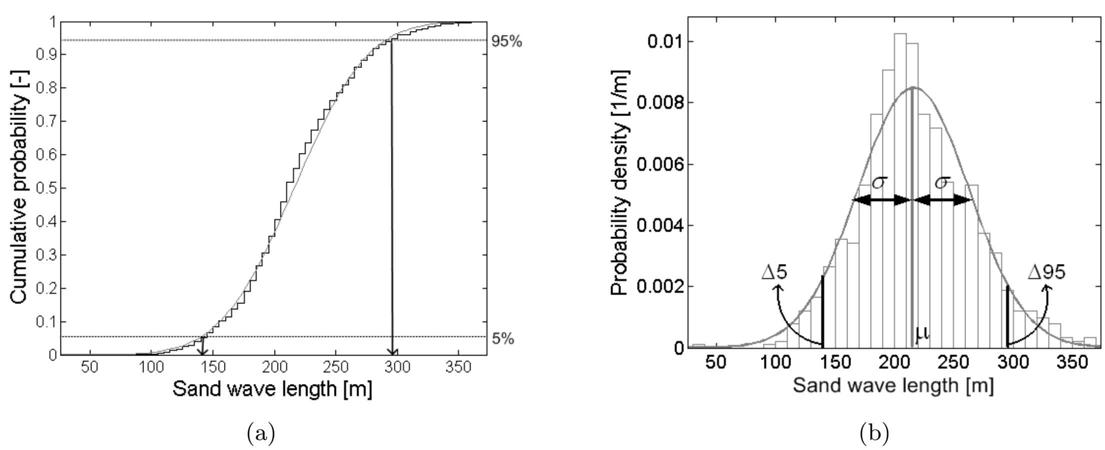

Figure 5.1: The CDF (a) and PDF (b) of the sand wave length. The way Δ_5, Δ_{95}, δ_5 and δ_{95} are defined.

Two levels are highlighted in the CDF. The values larger than ~300 m and smaller than ~150 m are considered as the extreme values. Figure 5.1(b) shows the PDF of the sand wave length and shows how the defined extreme values are related to the probability density plot. At 95% the value for the sand wave length (Δ_{95}) is determined. This means that 95% of the sand wave lengths are shorter than the Δ_{95} value. At 5% the value for the sand wave length (Δ_5) is determined. This means that 5% of the sand wave lengths are shorter than the Δ_5 value.

Since the users in the North Sea are also interested in the highest extreme values values, we also determine the Δ_{99}. So the highest 1% of the values found for the geometric properties of the sand waves. The relationship between the high extremes, the low extreme values and the mean and standard deviation is determined. First two variables for distances are introduced as shown in Figure 5.1(b).

$$\delta_5 = \mu - \Delta_5 \tag{5.1}$$

$$\delta_{95} = \Delta_{95} - \mu \tag{5.2}$$

$$\delta_{99} = \Delta_{99} - \mu \tag{5.3}$$

Also three variables (a, b and c) are introduced to determine the relation between the extreme values and the standard deviation σ. These introduced variables are defined as the distance between the extreme value and the mean value divided by the standard deviation. So for the sand wave length this means:

$$a_L = \frac{\delta_5}{\sigma} \tag{5.4}$$

$$b_L = \frac{\delta_{95}}{\sigma} \tag{5.5}$$

$$c_L = \frac{\delta_{99}}{\sigma} \tag{5.6}$$

When the value c_L turns out to be a constant, then the Δ_{99} value can be estimated when the standard deviation σ is known:

$$\delta_{99} = \frac{c_L}{\sigma} \tag{5.7}$$

A relationship between the high and the low extreme values can now be defined:

$$E_L = \frac{a_L}{b_L} \tag{5.8}$$

The variable E_L is a measure of asymmetry of the extreme values for sand wave length. A value of 1 for E_L means that the Δ_{95} value and the Δ_5 are at situated the same distance from the mean. A value above 1 means that the Δ_{95} is situated further away from the mean than the Δ_5.

For sand wave height these variables are defined as a_Δ, b_Δ, c_Δ and E_Δ. For crest elevation these variables are defined as a_{η_c}, b_{η_c}, c_{η_c} and E_{η_c}. Trough elevation is defined as a_{η_t}, b_{η_t}, b_{η_t} and E_{η_t} and asymmetry as a_A, b_A, b_A and E_A.

The extreme values are analysed for the geometric properties of sand waves discussed before and for each study area. It is determined whether there is an asymmetry in the extreme values Δ_5 and Δ_{95} using the introduced variable E.

For each study area the a, b and c can be determined and their averages can be calculated. The Δ_5 value and Δ_{95} value can be estimated when the a_{avg}, b_{avg} and c_{avg} are constants and the mean μ and the standard deviation σ are known for the sand waves in a data set. Determined from Equation 5.1 to Equation 5.5:

$$a = \frac{\mu - \Delta_5}{\sigma} \qquad b = \frac{\Delta_{95} - \mu}{\sigma} \qquad c = \frac{\Delta_{99} - \mu}{\sigma} \tag{5.9}$$

When the coefficient of variation C in Equation 4.1 is a known constant we can determine the standard deviation σ and the mean value is the only variable needed to determine the values of Δ_5, Δ_{95} and Δ_{99}.

5.2 Sand wave height

First we analyse the extreme values and their relationship for the sand wave height in order to determine if a, b and c are constants. Table 5.1 shows the areas analysed, the Δ_5, Δ_{95} and Δ_{99} values, the standard deviation σ and mean value μ, the δ_5, δ_{95} and δ_{99} values, the a, b and c values and finally the E value. In the table the average values for the a, b, c and E of the Noordhinder area and the TWIN areas are given. The b and c are the most interesting values as the tell more about the highest values found for sand waves heights.

For the Noordhinder areas the a_Δ values are lower than b_Δ values, this leads to an average E_Δ smaller than one. Only the a_Δ value in the R0302C area is higher than the b_Δ, resulting in a value for E_Δ above 1. The PDF of the sand wave height in Appendix B shows that there are a lot of sand wave heights found with low values and therefore the δ_5 has a distance further away from the mean value. The value for E does not determine if the PDF is skewed to the left or right.

Figure 5.2 shows the values of δ_5, δ_{95}, δ_{99} plotted against their corresponding standard deviation σ. The plotted fits have the slope of the average value for δ/σ, which means the average

Table 5.1: Extreme values of the sand wave height

Area	Δ_5	Δ_{95}	Δ_{99}	σ	μ	δ_5	δ_{95}	δ_{99}	a_Δ	b_Δ	c_Δ	E_Δ
	[m]	[m]	[m]	[m]	[m]	[m]	[m]	[m]	[-]	[-]	[-]	[-]
R0302C	1.05	10.3	13.8	2.88	5.70	4.65	4.60	8.11	1.61	1.60	2.82	1.01
R0302D	1.22	9.34	11.6	2.40	4.95	3.73	4.39	6.65	1.55	1.83	2.77	0.85
R0303C	1.37	8.59	12.1	2.28	4.84	3.47	3.75	7.30	1.52	1.64	3.20	0.93
R0304D	1.44	12.8	14.1	3.21	5.83	4.39	6.97	8.27	1.37	2.17	2.58	0.63
R0305A	2.09	10.7	12.5	2.50	5.67	3.58	5.03	6.80	1.43	2.01	2.72	0.71
R0305B	1.88	10.5	12.2	2.55	5.64	3.76	4.86	6.56	1.47	1.91	2.57	0.77
Average									1.49	1.86	2.78	0.82
TWIN01	0.89	7.09	8.04	1.94	3.88	2.99	3.21	4.16	1.54	1.65	2.14	0.93
TWIN02	0.48	5.84	6.71	1.74	2.82	2.34	3.02	3.89	1.35	1.74	2.24	0.78
Average									1.44	1.69	2.19	0.85
Ecomorf 3	1.18	2.33	2.55	0.36	1.75	0.57	0.58	0.80	1.60	1.63	2.25	0.84
Total averages									1.50	1.80	2.59	0.84

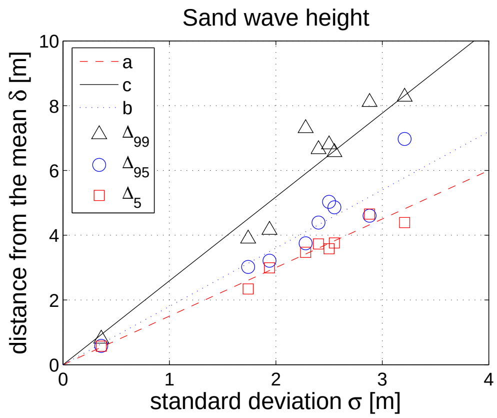

(a)

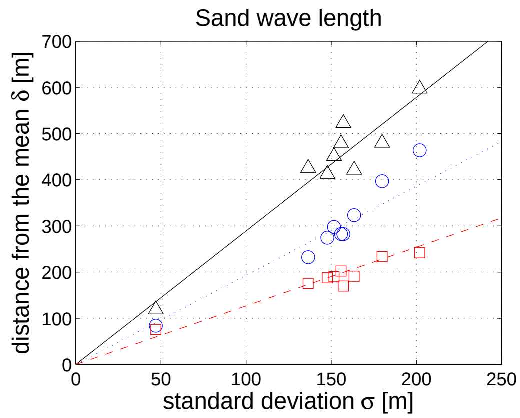

(b)

Figure 5.2: The Δ_5, Δ_{95} and the Δ_{99} of the sand wave height and sand wave length for each study area plotted against the standard deviation. $\square = \Delta_5$ $\bigcirc = \Delta_{95}$ $\triangle = \Delta_{99}$ The linear fits are the average values of *a*, *b* and *c*.

values for the a, b and c. Table 5.1 shows these values for a, b and c and shows that they are close to each other except for the value for c. Figure 5.2(a) shows this scatter of the values of δ_{99} around the fit with the slope of the average c. The lower the value of δ on the y axis, the smaller the distance between the extreme value and the mean value. The δ_5 and δ_{95} values are close to each other indicating that the extreme values are situated quite symmetrical around the mean value. This can also be concluded when looked at the fits in Figure 5.2(a). The closer the value for E in Table 5.1 is to a value of 1, the more symmetric the relation between the highest and lowest 5% of the values.

Figure 5.2(a) shows that a linear relationship exists between the δ values of the different extreme values and the standard deviation σ. Even for the Δ_{99} values a fit can be plotted for which the data points do not deviate significantly. The average value of a is 1.50 with a range between 1.35 and 1.61. The average value of b is 1.80 with a range between 1.60 and 2.17. So the values for b show more variation. The values of c vary between 2.14 and 3.20 with an average value of 2.59. The values for the largest 99% show the largest variation in values. This is not surprising since the quantity of sand wave heights is quite small for the largest percent and this leads to higher differences compared to the 5% extreme values.

5.3 Sand wave length

Figure 5.2(b) and Table 5.2 show that the distribution of the extreme values for the sand wave length is less symmetric than was seen for the sand wave height. The total average of E_L has a value of 0.67. So the extreme values above the Δ_{95} value are further away from the mean value μ than the Δ_5. A difference can be seen between the short crested areas and the long crested Ecomorf 3 area. The average of E_L for the Noordhinder area equals 0.62 and the average for the TWIN area equals 0.68. The relation between the high an low extreme values in the Ecomorf 3 area is more symmetric with a value for E of 0.90. This can also be seen in the PDF of the sand wave length (Figure 3.6(a)) of the Ecomorf 3 area. Figure 3.6(b) shows that the tail on the right in the PDF of the R0302D area is much longer. The same is seen for the other short crested data sets.

Again it is determined if a linear relationship can be found for the δ values of the extreme values and the corresponding standard deviation. The Δ_5 values are close to the fitted line in Figure 5.2(b) and the Δ_{95} values show a little more variation than the Δ_5 values. The value of the slope of the fits equals the average values for a and b, which are respectively 1.27 and 1.93. The variation in a values is indeed smaller than for b with values between 0.93 and 1.61. The b values vary between 1.70 and 2.30. The variation in the plots of the Δ_{99} values is even wider between 2.53 and 3.58, but in Figure 5.2(b) can be seen that the markers are still more or less situated on a straight line.

Table 5.2: Extreme values of the sand wave length

Area	Δ_5	Δ_{95}	Δ_{99}	σ	μ	δ_5	δ_{95}	δ_{99}	a_L	b_L	c_L	E_L
	[m]	[m]	[m]	[m]	[m]	[m]	[m]	[m]	[-]	[-]	[-]	[-]
R0302C	82.5	713	796	180	316	234	397	479	1.30	2.21	2.67	0.59
R0302D	79.2	487	680	136	255	175	232	425	1.12	1.70	3.12	0.75
R0303C	91.0	543	783	157	261	170	282	522	0.93	1.80	3.32	0.52
R0304D	99.3	805	938	202	341	242	464	597	1.20	2.30	2.96	0.52
R0305A	104	566	704	148	292	188	274	412	1.11	2.30	2.79	0.68
R0305B	110	624	722	163	301	191	323	421	1.28	1.86	2.58	0.59
Average									1.22	1.97	2.91	0.62
TWIN01	98.2	583	779	156	300	202	283	479	1.30	1.81	3.07	0.72
TWIN02	54.9	543	696	152	245	190	298	451	1.26	1.96	2.97	0.64
Average									1.28	1.89	3.02	0.68
Ecomorf 3	140	300	335	47	216	75.9	83.9	119	1.61	1.79	2.53	0.90
Total averages									1.27	1.93	2.89	0.67

5.4 Crest elevation

In Table 5.3 we present the results for the extreme values for the crest elevation. The values in Table 5.3 for the symmetry E_{η_c} of the data sets show that the distribution of the crest elevations are asymmetric towards the high values. The Ecomorf 3 area is different from the other data sets, because the relation between the low and high extreme values E_{η_c} is different with a value close to 1. So the long crested area shows a more symmetrical distribution of the extreme values than the short crested areas.

Figure 5.3(a) shows that a linear relationship exists between the δ values of the different extreme values and the standard deviation σ. The Δ_{99} values show a reasonable good linear fit for which the data points do not deviate significantly. The values of a vary between 1.12 and 1.71 with an average value of 1.47. The average value of b is 1.65 with the same range of variation as a between 1.28 and 1.81. The average value of c is 2.39 with a range between 2.17 and 2.61. So the values for c show a smaller range of variation than a and b. This is surprising since the quantity of sand wave heights is quite small for the largest percent. We

Table 5.3: Extreme values of the crest elevation

Area	Δ_5	Δ_{95}	Δ_{99}	σ	μ	δ_5	δ_{95}	δ_{99}	a_{η_c}	b_{η_c}	c_{η_c}	E_{η_c}
	[m]	[m]	[m]	[m]	[m]	[m]	[m]	[m]	[-]	[-]	[-]	[-]
R0302C	0.40	7.33	8.56	2.15	3.53	3.13	3.80	5.03	1.46	1.77	2.34	0.82
R0302D	0.40	5.42	7.74	1.81	3.10	2.70	2.32	4.64	1.49	1.28	2.56	1.16
R0303C	0.42	6.01	6.78	1.70	3.09	2.67	2.92	3.69	1.57	1.72	2.17	0.91
R0304D	0.43	7.83	9.65	2.28	3.69	3.26	4.14	5.96	1.43	1.82	2.61	0.79
R0305A	0.80	7.19	8.52	2.00	3.75	2.95	3.44	4.77	1.48	1.72	2.39	0.86
R0305B	0.62	7.33	8.70	2.05	3.62	3.00	3.71	5.08	1.46	1.81	2.48	0.81
Average									1.48	1.69	2.43	0.89
TWIN01	0.29	5.12	5.88	1.57	2.50	2.01	2.31	3.38	1.28	1.47	2.15	0.84
TWIN02	0.15	4.01	5.21	1.33	1.74	1.48	1.89	3.47	1.12	1.42	2.61	0.70
Average									1.30	1.69	2.38	0.77
Ecomorf 3	0.39	1.42	1.61	0.31	0.92	0.53	0.50	0.69	1.71	1.61	2.23	1.06
Total averages									1.47	1.65	2.39	0.88

observe a wider variation for the highest 99% values of the sand wave height and sand wave length.

5.5 Trough elevation

In Table 5.4 we present the results for the extreme values for the trough elevation. Figure 5.3(b) shows that the data points shows more deviation from the linear fit than was seen before. The E_{η_t} values are now for almost all data sets below the value of 1, so the asymmetry is headed towards the Δ_{95} value. The long crested Ecomorf 3 area shows a different relation between the high and low extreme values then the short crested areas with a value of 1.50 for E_{η_t}.

The difference between the long crested and short crested area is not seen, when determining

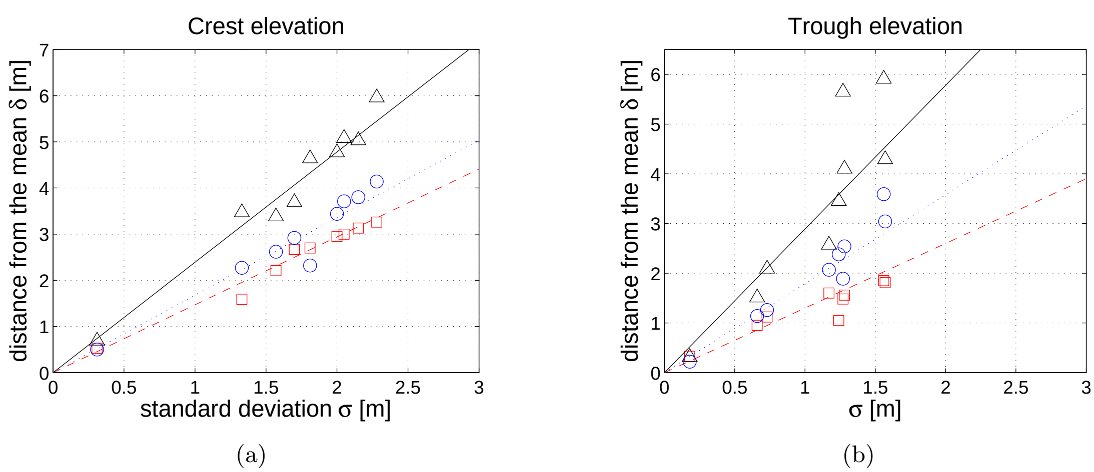

Figure 5.3: The Δ_5, Δ_{95} and the Δ_{99} of crest elevation and trough elevation for each study area plotted against the standard deviation σ. $\square = \Delta_5$ $\bigcirc = \Delta_{95}$ $\triangle = \Delta_{99}$ The linear fits are the average values of *a*, *b* and *c*.

if a linear relationship exists for the δ values of the extreme values and the corresponding standard deviation. Figure 5.2(b) shows that the variation of the data around the fits is larger than was seen for the crest elevation. This is also observed in Table 5.4. The variation in a_{η_c} values vary between 0.85 and 1.53, with an average of 1.30. The b_{η_c} values show a wide variation between 1.22 and 2.30, with an average of 1.79. The variation in the plots of the Δ_{99} values is even wider between 1.75 and 4.45 and in Figure 5.3(b) can be seen that the Δ_{99} markers are situated widely around the fit, with a slope $c_{\eta_c,avg}$ of 2.89, trough the data.

Table 5.4: Extreme values of the trough elevation

Area	Δ_5	Δ_{95}	Δ_{99}	σ	μ	δ_5	δ_{95}	δ_{99}	$a_{\eta t}$	$b_{\eta t}$	$c_{\eta t}$	$E_{\eta t}$
	[m]	**[m]**	**[m]**	**[m]**	**[m]**	**[m]**	**[m]**	**[m]**	[-]	[-]	[-]	[-]
R0302C	0.30	5.74	8.06	1.56	2.15	1.85	3.59	5.91	1.19	2.30	3.79	0.52
R0302D	0.29	4.39	5.95	1.28	1.85	1.56	2.54	4.10	1.22	1.98	3.20	0.61
R0303C	0.34	3.71	7.47	1.27	1.82	1.48	1.89	5.65	1.17	1.49	4.45	0.78
R0304D	0.37	5.22	6.47	1.57	2.18	1.81	3.04	4.29	1.15	1.94	2.73	0.60
R0305A	0.90	4.33	5.40	1.24	1.95	1.05	2.38	3.45	0.85	1.92	2.78	0.44
R0305B	0.43	4.10	4.60	1.17	2.03	1.60	2.07	2.57	1.37	1.77	2.20	0.77
Average									1.16	1.90	3.19	0.62
TWIN01	0.27	2.65	3.48	0.73	1.39	1.12	1.26	2.09	1.53	1.72	2.85	0.89
TWIN02	0.16	2.25	2.62	0.66	1.11	0.95	1.14	1.51	1.44	1.73	2.29	0.83
Average									1.48	1.73	2.57	0.86
Ecomorf 3	0.52	1.07	1.17	0.18	0.85	0.33	0.22	0.32	1.83	1.22	1.72	1.50
Total averages									1.30	1.79	2.89	0.77

5.6 Sand wave asymmetry

The distribution of the extreme values of the sand wave asymmetry show most values for E above one (Table 5.5). This means that the values Δ_5 are more distant from the mean value μ than the Δ_{95} values. Between the long crested and short crested areas, there is no difference observed.

Table 5.5 shows that for all the three extreme values the variation from the linear fit is quite small. For the Δ_5 values the a_A varies between 1.42 and 1.90, with a mean of 1.73. The b_A, for the Δ_{95} values, varies between 1.28 and 1.49, with a mean of 1.41. The distance between the mean and the Δ_5 values are larger than the distance between the mean and the Δ_{95} values. The highest 1% of values seems to be well represented by the fit trough the data in Figure 5.4(a). The values for c_A vary between 1.53 and 1.91. The average value $c_{A,avg}$ equals 1.73. Figure 5.4(a) shows that the fits trough the Δ_5 values and Δ_{99} values is the same. The small variation in the a_A, b_A and c_A values makes them useful to estimate the extreme values of sand wave asymmetry.

5.7 Overview

The average value of a_Δ is 1.50 and the average value of b_Δ is 1.80. The average distance of the Δ_{99} values to the mean c_Δ has an average value of 2.59. Van der Mark et al. (2007)

Table 5.5: Extreme values of the sand wave asymmetry

Area	Δ_{15}	Δ_{95}	Δ_{99}	σ	μ	δ_5	δ_{95}	δ_{99}	a_A	b_A	c_A	E_A
	[-]	[-]	[-]	[-]	[-]	[-]	[-]	[-]	[-]	[-]	[-]	[-]
R0302C	-0.50	0.65	0.80	0.36	0.11	0.61	0.54	0.69	1.69	1.49	1.91	1.14
R0302D	-0.47	0.64	0.79	0.35	0.15	0.62	0.49	0.64	1.78	1.41	1.84	1.27
R0303C	-0.48	0.66	0.81	0.36	0.16	0.64	0.50	0.65	1.79	1.40	1.82	1.28
R0304D	-0.39	0.74	0.82	0.37	0.22	0.61	0.52	0.60	1.67	1.42	1.64	1.17
R0305A	-0.51	0.58	0.73	0.41	0.07	0.58	0.51	0.66	1.42	1.25	1.61	1.14
R0305B	-0.49	0.61	0.72	0.38	0.05	0.54	0.56	0.67	1.60	1.66	1.98	0.96
Average									1.66	1.44	1.80	1.16
TWIN01	-0.36	0.81	0.88	0.35	0.31	0.67	0.50	0.57	1.90	1.42	1.62	1.34
TWIN02	-0.54	0.77	0.87	0.40	0.21	0.75	0.56	0.66	1.89	1.41	1.66	1.34
Average									1.89	1.41	1.64	1.34
Ecomorf 3	0.20	0.67	0.71	0.15	0.48	0.28	0.19	0.23	1.86	1.26	1.53	1.47
Total averages									1.73	1.41	1.73	1.23

analysed the Δ_{95} values for bedform height, bedform length, crest elevation and trough elevation for river dunes for laboratory flumes and field data. For 95% of the values found for the bedform height minus the mean bedform height versus the standard deviation a linear relationship is also found by Van der Mark et al. (2007). The average value found for the slope ($\delta_\Delta/\sigma_\Delta$) in their fit is 1.7, which is close to the $b_{\Delta,avg}$ determined in this study. So extreme value of bedform height for both the sand waves and the river dunes can be estimate based on the mean value and the standard deviation using Equation 5.9. Based on the higher variation in values the accuracy is considered lower for the estimation of the highest 1%.

For the sand wave length the extreme values can also be estimated with the mean values, the standard deviation and the values for $a_{L,avg}$, $b_{L,avg}$ and $c_{L,avg}$. These average values are respectively 1.27, 1.93 and 2.89. For the estimation of the largest sand wave lengths (Δ_{99}) the estimator will be less suited, because of the wider spread around the fit. Van der Mark

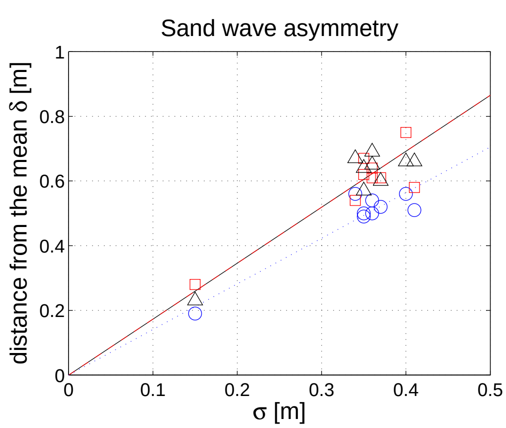

(a)

Figure 5.4: The Δ_5, Δ_{95} and the Δ_{99} of sand wave asymmetry for each study area plotted against the standard deviation σ. $\square = \Delta_5$ $\bigcirc = \Delta_{95}$ $\triangle = \Delta_{99}$ The linear fits are the average values of *a*, *b* and *c*.

et al. (2007) found a slope δ_L/σ_L in the fit trough the Δ_{95} values of the bedform length of 1.9. This value corresponds with the value we found. So the relation between the 95% value minus the mean bedform length and the standard deviation seems to correspond for sand waves and river dunes. Part of the data acquired by Van der Mark et al. (2007) consist of flume data, which make this result even more remarkable.

For 95% of the values found for the crest elevation minus the mean bedform height versus the standard deviation a linear relationship is also found by Van der Mark et al. (2007). The value for the slope ($\delta_{\eta_c}/\sigma_{\eta_c}$) of the fit trough the data is 1.7. In this study the value for the average b_{η_c} determined by $\delta_{\eta_c}/\sigma_{\eta_c}$ is 1.65. So again quite close to the value determined by Van der Mark et al. (2007). The 5% value and the 99% value for the crest elevation can also be determined based on the linear relation found. So the highest elevations towards the mean bed level can now be estimated, which is very important for, for example, navigation.

The relationship in this study between the $\Delta 95$ values and the standard deviation σ of the trough elevation seem to deviate from the relationship found by Van der Mark et al. (2007). The value of b_{η_t} in this study is 1.79 and is close to the value of 1.7 found by Van der Mark et al. (2007). So the extreme values for the trough elevation of sand waves have more or less the same relation with the standard deviation as the river dunes. The value of $a_{\eta t}$ and $b_{\eta t}$ can be used to determine the corresponding extreme values which is useful for the construction of pipelines and cable on the North Sea bed. The 99% values cannot be estimated accurately for the trough elevation, since the variation is too large.

The value for the relation E between the highest Δ_{95} and lowest Δ_5 extreme values is able to give insight in the type of sand waves analysed. For the sand wave height, crest elevation and the asymmetry the values found for E show no large differences between the short crested areas and the long crested areas. For the sand wave length and the trough elevation we observe a significant difference between the E values of the short crested areas and the long crested areas. So the E values may be used to indicate the sort of sand wave field without plotting a plan view.

Chapter 6

Discussion

In this chapter we discuss the data, methodology and tools used and the subjectivity of the choices made. We follow the steps which were made to determine the results of the study. We will summarise the steps in the used method and determine if our method can be turned into a tool for users in the North Sea area. Finally we will discuss the applicability by giving an example how the method is useful to dredgers.

6.1 Data

The used bathymetry data is obtained in 2003 and can be considered as snap shots. It is unknown in what season the measurements were carried out. There is no knowledge about the period in which the data is obtained and this makes it uncertain if the results of this study are always applicable in a year. We state in Section 1.1.1 that sand waves are subject to seasonal changes and storms. So if the bathymetry data is obtained in winter, the sand wave heights may be relatively lower compared to the summer. At this moment seasonal influences cannot be determined, so information on the period is needed to improve the quality of the results.

Specific information on dredging in the TWIN areas is not found, but only the quantity dredged in the total Dutch continental shelf is found (RWS-Noordzee, 2004) or sand mining locations discussed (Hoogewoning and Boers, 2001). More detailed information about dredging is needed to determine if there is a difference between the stochastic characteristics in dredged areas and the stochastic characteristics in areas where dredging does not take place. In this study the information on dredging is not sufficient and differences between the Noordhinder and TWIN area can only be assumed to be caused by dredging activities.

6.2 Methodology

In the used method some subjective choices are made in order to determine stochastics of the sand wave dimensions. Also some assumptions had to be made and there may be uncertainties in results found after one step, which are used in a next step in the data processing process.

Definitions
Many studies were carried out into sand waves, but no standard definition of geometric properties of sand waves exists. The question arises whether this is possible, as every study has

a different approach and certain definitions may suit one study better than another. In this study a choice is made for certain definitions to describe the geometric properties of sand waves analysed. These choices are based on a detrended longitudinal bed elevation profile and the definitions of every single sand wave are related to that detrended BEP.

Choosing another definition may lead to slightly different results. For example, Van der Mark et al. (2007) show that the standard deviation σ in bedform length defined as the distance between two troughs may differ from the standard deviation σ defined as the distance between two crests.

Orientation of sand wave field
In this study the orientation is defined using a part of the digipol method (RIKZ, 1997) implemented in Matlab. We determine in each data point in the bathymetry data the gradient vector $|\overrightarrow{G}|$ and project this vector as L on a line with a certain angle α. The highest total gradient L_{tot} is determined for a whole area and the corresponding angle α_{max} is considered the orientation of the sand wave field. This orientation is assumed to be valid for every longitudinal bed elevation profile. This may not be valid for every longitudinal profile extracted from the data. Therefore the areas were split up in smaller subareas with each the same amount of data points (∼50,000). The subareas of the used data sets showed a similar value for the highest gradient as the whole area. The results of the method also corresponded with the visual judgement of the direction of a sand wave. An advantage of the method is the possibility to use it for data sets with any grid size, as long as the data sets consist of *xyz* values. A small disadvantage is the amount of calculation needed. For one area it takes half a day to determine the gradient for the total area and the subareas. With a state of the art PC the calculation time will probably reduce significantly.

The results of the method show an orientation of the sand wave field that correspond with a visual judgement of the area (Figures 2.11 to 2.13). For each data set the orientation of the subareas and the complete area are more or less similar. Some small deviations can be seen in the plots of the angle α and the dimensionless gradients. It was shown that if the wrong direction is used the sand wave length is influenced. For the small deviations in the angle these deviations in sand wave length are quite small. For the mean sand wave value of 216 m in the Ecomorf 3 area a deviation in the angle of 5° means a deviation in the sand wave length of 0.83 m. The calculated orientation of the whole area is therefore assumed to be applicable to be used in order to find longitudinal bed elevation profiles in an area. A deviation of 0.83 m on 216 m is considered negligible. Sand wave asymmetry is not influenced, since A is defined by the stoss side L_s of the sand wave, the lee side L_l and the distance from trough to trough L_t. The values for L_s, L_l and L_t become larger when another orientation is used and their relationship stays the same.

Pluymaekers et al. (2007) determine in their study the orientation of sand dunes in the Western Scheldt in the Netherlands using a different method. They draw profiles of equal length trough a grid point at regular angle intervals. The angle of the profile with the highest number of local extrema gives the dune orientation. The method of Pluymaekers et al. (2007) is applicable in this study, but the scale of a sand wave field leads to many extrema for each profile. Pluymaekers et al. (2007) determine the orientation for one profile in one grid point.

This may lead to overlap of profiles drawn trough different grid points. In this study we determine the orientation for the whole surface and we do not come across this problem.

Bed elevation profiles
The orientation of the sand wave field is used to draw longitudinal bed elevation profiles (BEPs) trough the data. We use xy locations in the grid and assign a value z to it. Since the profiles are drawn trough the data under an angle we did not assign every Δy a value to the bed elevation, but we used the derived $\Delta y'$. The value of one grid cell will often be assigned twice to the BEP by using Δy. The distance $\Delta y'$ turns out to be an accurate translation from the grid to BEPs for small values of the orientation α, because no grid cell is passed over in this way.

For higher values for the orientation, this method passes over grid cells (Figure 6.2). Since the size of the grid cells in this study are small compared to the dimensions of the sand waves, the BEPs are still very accurate even for high values for the orientation α. To decrease the size of the grid cells may not be possible or take up too much time and therefore too expensive. Also a smaller grid would not necessarily improve the accuracy.

The bed elevation z assigned to a xy location is the value for a total grid cell in the bathymetry data and is not the exact value of the bed elevation at that location. It actually is the highest value for a grid cell of $5\,\text{m} \times 5\,\text{m}$ around the xy location. So there is small uncertainty in the values for the bed elevations assigned to the longitudinal bed elevation profile. The size of the grid cells are relatively small and the inaccuracy described in this paragraph is considered insignificant.

A subjective choice made in this study is the choice in the amount of longitudinal bed elevation profiles taken from the data sets. The longitudinal bed elevation profiles are taken from the data set every 5 times the grid size Δx. This choice is considered reasonably justified.

Trend line
The choice of trend line may influence the results significantly. In this study a linear trend

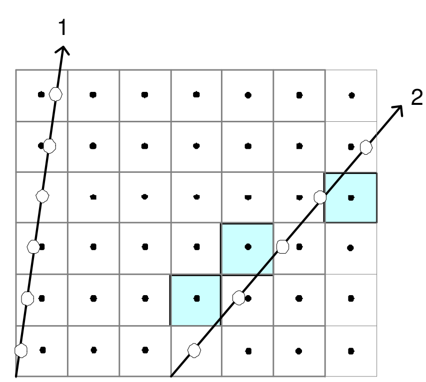

Figure 6.1: Two BEPs drawn through a grid with different orientation. In the first all gird cells are included, but the second passes over some grid cells it crosses. These grid cells are highlighted in grey.

line is used, since the mean bed level can be represented by a linear line for most BEPs. The linear trend line is described by the first order polynomial: $y = ax + b$. It is imaginable that there are fluctuations in the mean bed level that cause deviations in the results when a linear trend line is used. These deviations may be corrected by using a moving average trend line. In this study the use of a moving average was at first not applicable and afterwards it was briefly analysed. It turned out that half the data was lost by the use of it, while the influence on the results was very small.

So the benefits of a moving average trend line are recognised, but the linear trend line is considered sufficient. Also the inclusion of as much as possible data is considered to be important in this study.

Filter line
The smallest bedforms are already filtered because of the grid size of the bathymetry data of 5 m. Megaripples reach lengths up to 10 m, so they still need to be filtered out. The filter line in the BTT is very useful to determine the correct crossings with the mean bed level and filter out the crossings of the megaripples. In this study the megaripples on the crest and troughs are not filtered out yet. The highest and lowest locations on the BEP between crossings are defined as crest and troughs. In a newer version of the BTT used in the study by Van der Mark et al. (2007) this is adjusted and the highest and lowest values of the filtered BEP is used to determine the crests and troughs. The influence of this method is quite small, as the maximum the height of the megaripples is about 10 cm (Table 1.1).

Total vertical difference
We determined (Table 3.6) that the PDF of the sand wave height in the Ecomorf 3 area corresponds quite well with the normal distribution. Generally in a normal distribution 95% of the observations fall within 2 standard deviations of the mean, that is, between $\mu - 2\sigma$ and $\mu + 2\sigma$. This means that the δ_{95} is equal to 2 times the standard deviation σ.

Based on the data we determine how the Δ_{95} is determined for the sand wave height in Ecomorf 3. The value of δ_{95} in this study is 0.58. So for the sand wave height in the Ecomorf 3 area 95% of the observations fall within 0.58/0.36 = 1.61 standard deviations of the mean, that is, between $\mu - 1.61\sigma$ and $\mu + 1.61\sigma$. This is quite different than is found for normal distributions. The total vertical difference returns the probability distribution with the best fit, but this does not mean that the probability distribution with the best fit corresponds to the data distribution. For sand wave height in the Ecomorf 3 area it was already stated that the Weibull distribution is a better fit for the tail of the PDF.

6.3 Applicability

Currently the method used in this study is not very user friendly, because of the number of steps for which multiple proceedings have to be taken before the next step can be implemented. The total method exists of six steps:

1. The data (in *xyz* extension) can directly be processed by the *digipol* script and gives as output total gradient values L for each angle α.

2. With the angle for the highest gradient α_{max} it is manually determined what the x and y values for the BEP are.

3. The xy of the BEP are fitted over a grid with z values in a Matlab script resulting in xyz defined BEPs

4. A Matlab script is used to change the xyz BEPs into another extension, so the BEPs can be implemented in the BTT.

5. The BTT returns the BEPs as data sets of all the geometric properties for every single BEP

6. Another Matlab script is used to combine the data from the BEPs to one data set for a study area.

In contrast to the complete method, the BTT is already user friendly. In order to make the total method used widely applicable all the steps should be integrated and applicable like the BTT. Another option may be a shell build around the Matlab scripts.

So how can users in the North Sea area use the results of this study? We illustrate this by giving the applicability for dredgers as an example and we deepen this example. A dredger considers the distance between the water level to the crest of the sand wave as the water depth. A minimum allowed water depth is determined in order to guarantee navigation safety. In this study we consider sand waves in relation to the mean bed level and not to the water surface. Therefore the minimum allowed water depth should be transferred into a maximum allowed crest elevation based on the mean bed level.

We determined a linear relationship between the mean value μ for crest elevation and the standard deviation σ. By dividing the two we determined that the coefficient of variation C is more or less a constant:

$$C_{\eta_c} = |\frac{\sigma}{\mu}| = 0.61$$

$$\sigma = 0.61\mu$$

We showed that it is possible to determine the standard deviation when the mean value for the crest elevation in a certain area is known. Table 3.1 shows that the Beta distribution and the Weibull distribution have low S values for the PDFs of the crest elevations and can be used as an indication how the crest elevation is distributed. To estimate the extreme values the Weibull distribution is more suitable as it is a better fit for the tail of the distribution.

To estimate the actual extreme values a linear relationship is determined for the data distribution between the standard deviation σ and the distance (δ_{95}) between the mean value μ and the Δ_{95} value. Dividing the δ_{95} value by the standard deviation leads to a constant b:

$$b = \frac{\delta_{95}}{\sigma}$$

This constant enables us to estimate the Δ_{95} value, based on the mean and the standard deviation of the data. We combine Equation 5.2 with Equation 5.5:

$$\delta_{95} = \Delta_{95} - \mu$$

$$b = \frac{\Delta_{95} - \mu}{\sigma}$$

The standard deviation can also be estimated based on the coefficient of variation C_{η_c} as is shown in Chapter 4. So the standard deviation σ is expressed in the mean value μ:

$$\sigma = C\mu$$

And this expression makes:

$$b = \frac{\Delta_{95} - \mu}{C\mu}$$

$$C\mu b = \Delta_{95} - \mu$$

Now we can determine the Δ_{95} value by:

$$\Delta_{95} = C\mu b + \mu$$

$$\Delta_{95} = (Cb + 1)\mu \tag{6.1}$$

And with the constant value for $C_{\eta_c} = 0.61$ and $b_{\eta_c} = 1.65$ we are able to estimate the Δ_{95} for the crest elevation:

$$\Delta_{95} = (0.61 \cdot 1.65 + 1)\mu = 2.01\mu$$

The user is now able to determine the the Δ_{95} value.

After determining the mean bed level and the minimum allowed water depth a dredger needs to be able to determine a maximum crest elevation. This value can can have any value. For every Δ value an estimator, based on the mean value, as Equation 6.1 can be determined with the bathymetry data. The extreme values can be estimated accurately based on only a few measurements in order to determine the mean value of the geometric properties. The question rises how many sand waves need to be measured in order to determine an adequate value for the mean value.

In the same way as Equation 6.1 we can determine:

$$\Delta_5 = -(Ca + 1)\mu \tag{6.2}$$

$$\Delta_{99} = (Cc + 1)\mu \tag{6.3}$$

For every Δ value an estimator as in Equation 6.1, Equation 6.2 and Equation 6.3 can be determined. The accuracy of the latter is lower than for the first two.

By determining a corresponding percentage for every Δ value makes it for the the dredger possible, after determining a maximum crest elevation, to know the percentage of crest elevation higher than the determined maximum η_c. Figure 6.3 shows a plot of the crest elevation η_c to the Δ values. This is a sketch of what an estimator for all the data sets for the crest elevation may look like. Every dot represent a certain Δ_i value with a corresponding crest elevation $\eta_{c,i}$. The corresponding percentage of crest elevations is smaller than the crest elevation $\eta_{c,i}$.

Equation 6.1 is tested with the used bathymetry data and the results are shown in Table 6.1. When both the mean value μ and the standard deviation σ are used the result is more accurate than the estimated Δ_{95} based on only the mean value. This is because for the $\Delta_{95,\mu\sigma}$ the real standard deviation is used and not the estimated standard deviation based on 0.61μ. All the differences between the estimated and the measured Δ_{95} values are below 0.5 m except for the R0302D area. To improve the accuracy of this method more data is needed. With more data the coefficient of variation C and the b value in Equation 6.1 will be more accurate and therefore also the result of the estimator. The large difference in the result for the long crested Ecomorf 3 area are due to the fact that 0.61μ is determined for short crested areas.

Table 6.1: The measured Δ_{95} values and the estimated Δ_{95} values. The Δ_{95} is the measured value. The $\Delta_{95,\mu\sigma}$ value is estimated with use of both the mean value and standard deviation. The $\Delta_{95,\mu}$ value is only estimated with the use of the mean value.

Area	Δ_{95} [m]	$\Delta_{95,\mu\sigma}$ [m]	$\Delta_{95,\mu\sigma}$- Δ_{95} [m]	$\Delta_{95,\mu}$ [m]	$\Delta_{95,\mu}$- Δ_{95} [m]
R0302C	7.33	7.08	-0.25	7.08	-0.25
R0302D	5.42	6.09	0.67	6.22	0.80
R0303C	6.01	5.90	-0.12	6.20	0.19
R0304D	7.83	7.45	-0.38	7.40	-0.43
R0305A	7.19	7.05	-0.14	7.52	0.33
R0305B	7.33	7.00	-0.33	7.26	-0.07
TWIN01	5.12	5.09	-0.03	5.01	-0.11
TWIN02	4.01	3.93	-0.08	3.50	-0.51
Ecomorf 3	1.42	1.43	0.01	1.85	0.43

The dredger is now able to determine the percentage of sand waves that need to be dredged, but has no exact knowledge about the surface with a value above the maximum crest elevation η_{max}. The results of this study will have to be linked to the bed surface in order to determine

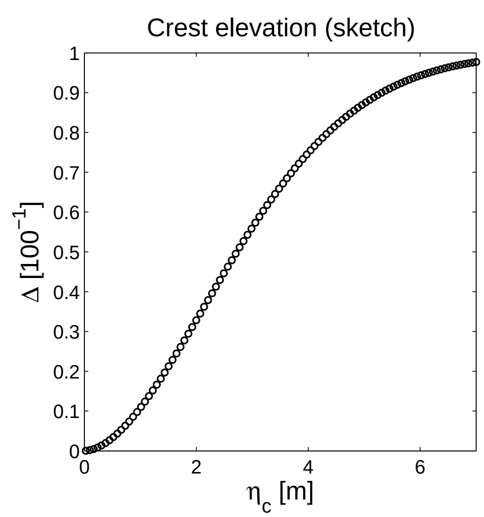

Figure 6.2: Sketch of the Δ values and corresponding crest elevations η_c.

the surface that needs to be dredged. With measurements of the study areas the BTT can be used to determine the surface and the amount of the bed sediment that needs to be dredged when a minimum water level is determined. With these results a relation between the results in this study may be established to be able to estimate the amount that needs to be dredged based on the mean water level.

An implementation can be added to the BTT when the η_{max} is determined as shown in Figure 6.3. The length of the crossings of the η_{max} level can be determined and the assumption is made that the shape of a BEP does not change until the next BEP. In this study this distance is 25 m. The distance between the width (Figure 6.3) multiplied with the distance to the next BEP gives an estimation of the surface that needs to be dredged. This can be done for every crest elevation that exceeds the maximum as is shown in Figure 6.3 and for every longitudinal bed elevation.

In the latest version of the BTT (Van der Mark and Blom, 2007) the slope in the sand waves is also determined. Based on this slope and the width in Figure 6.3 the triangular grey peak can be calculated. The surface of this peak multiplied by the distance between two BEPs determines the amount of sediment that needs to be dredged.

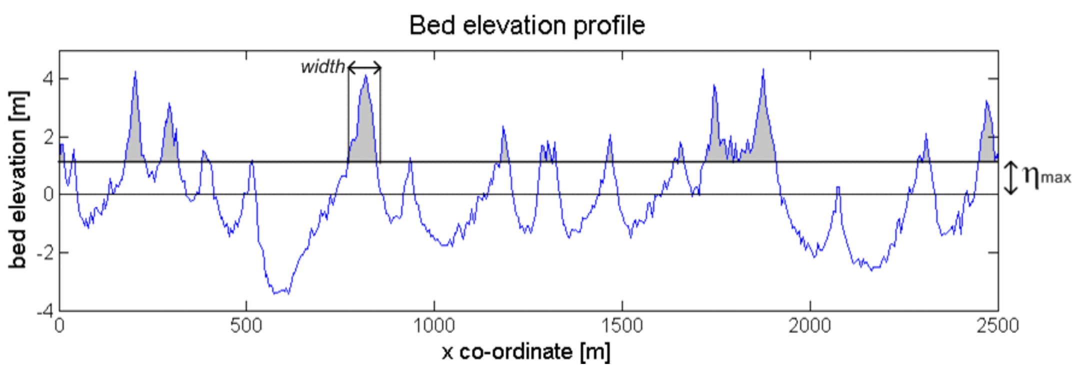

Figure 6.3: Longitudinal bed elevation profile with η_{max} crossings. The grey area is the amount of the sand waves above the η_{max} level.

For each study area we can determine the surface and the amount of data that needs to be dredged for certain values for η_{max}. If the ratio $\eta_{max}/\eta_{c,avg}$ and the corresponding amount of data that needs to be dredged is the same for each study area, than we are able to estimate the amount of dredging needed in a unknown area for which a certain η_{max} is determined.

Chapter 7

Conclusions

This thesis concerns the stochastic characteristics of geometric properties of sand waves in the North Sea. The problem statement, as introduced at the beginning of this thesis, is formulated as follows:

Little knowledge exists on the stochastic characteristics of geometric properties of sand waves in the North Sea. Furthermore not much is known about the extreme values of geometric properties of sand waves.

In this chapter we answer the research questions.

What do the different actors within the North Sea area need to know about the stochastic characteristics of sand waves and their extreme values?
Current models for sand waves can predict the development of regular patterns. The predicted waves are all equal in size and shape. However insight in the differences in size and shape and the dynamic behaviour of sand waves is helpful to users. The extreme values of, especially, the crest elevation and trough elevation are of interest as these interfere with activities as navigation and pipelines. Migration, growth rate and other dynamics of sand waves turned up in each conversation with users. Information on how variations in shape, wavelength and height correlate to these dynamics is valuable. With knowledge on such correlations information on dynamics can be obtained from single measurements instead of multiple measurements in space or time.

Users within the North Sea area need to know whether extreme values can be estimated accurately based on only a few measurements in space or time and whether the determined stochastic characteristics of geometric properties of sand waves are correlated with the hydraulic conditions they are situated in.

How do we analyse the North Sea data?
This research question is divided into several subquestions listed below. Data sets of locations are selected where sand waves are found and are suitable for the extraction of longitudinal profiles. The data sets have to consist of *xyz* data in order to be applied in this study. This means three columns with a x coordinate and a y coordinate and a depth value z. In this

study data sets from areas with short crested sand waves and an area with long crested sand waves are analysed.

How do we define geometric properties of sand waves?
Before geometric properties are defined the longitudinal bed elevation profile has to be detrended. We detrend the longitudinal bed elevation by subtracting the BEP by the trend line. We define the geometric properties based on this detrended longitudinal bed elevation profile and the definitions of geometric properties of every single sand wave are related to that detrended BEP. Sand wave height Δ_l is defined as the vertical distance between a crest and subsequent trough. Sand wave length L_c is the distance between two crests. Crest elevation η_c is the vertical distance from crest to the detrended mean bed level and trough elevation η_t is the vertical distance from trough to detrended mean bed level. Asymmetry A of the sand waves is defined by the difference between the length of the stoss side of a sand wave and the length of the lee side of a sand wave divided by the sand wave length, defined as the distance between two troughs.

How do we define longitudinal profiles in an area?
First an orientation of the whole sand wave field is determined using an implementation in Matlab of a part of the *digipol* method. The highest total gradient L_{tot} and the corresponding angle α_{max} are the outcomes of the Matlab tool. With the defined orientation α_{max} a profile can be determined with a step size $\Delta y'$ along the profile with a certain measure in x and y direction. The longitudinal bed elevation profile now consists of certain x and y values. These x and y values are fitted over a grid with bed elevation values and for every step size $\Delta y'$ the corresponding bed elevation z is assigned to the x and y values. The longitudinal bed elevation profiles are now defined over a distance with size step $\Delta y'$ and bed elevation z taken from the bathymetry data. In a data set every 25 m in x direction the next BEP is drawn.

The uncertainty of the assigned z values is not considered significant, as the scale of the size of the grid cells is much smaller than the size of the sand waves. The same applies to the uncertainty that occurs when the BEP passes over grid cells due to a high value for α_{max}.

How do we define the trend line in the longitudinal profiles?
A linear trend line, described by the first order polynomial is used as trend line in the profile and is defined as $y = ax + b$. The values for a and b are derived from the data by a Matlab function. The trend line is applicable to every bed elevation profile. In this study most BEPs are well represented with a linear trend line, but for some other BEPs with a more irregular pattern a moving average trend line may suit better. Higher order polynomial trend lines are not suited to be used as trend line.

How do we filter the measured data?
The smallest bedforms are filtered by the grid size of $5\,\text{m} \times 5\,\text{m}$. A moving average is fitted over the longitudinal bed elevation profile to filter out the biggest megaripples. This filter line is a smooth version of the original profile and filters out the crossings of the megaripples with the mean bed level, so correct up-crossings and down-crossings can be determined. These crossings are used to determine the geometric properties of the sand waves.

How can available software tools be altered in order to be used in this study?
In this study several software tools have been used to analyse and process the data. Not all of them were ready to use and therefore needed some adjustments. Many standard Matlab functions as well as small Matlab scripts are developed and used in this study, but two major larger tools used in this study were developed by others. One of these tools is the *digipol* implementation and is used to determine the orientation of the sand wave field. The tool was created to analyse single beam echo sounding bathymetry data, but turned out to be just as useful for multi beam bathymetry data. No significant adjustments are necessary to use the tool.

The bedform tracking tool (BTT) is originally developed for river dunes, but successfully determined bedform characteristics in the longitudinal bed elevation profiles in this study. The sand wave asymmetry could easily be determined in the profiles by adding a simple expansion in the BTT. The output of the tool consists of data sets with the values for each individual sand wave. Geometric properties analysed are the sand wave height, sand wave length, crest elevation, trough elevation and sand wave asymmetry. In the process of analysing and using the BTT, all the adjustments are implemented. This process was not very complex, because the BTT is quite user friendly. However the BTT consist of multiple scripts, which all have to be adjusted in order to be applicable for sand waves.

What are the stochastic characteristics (mean value, standard deviation, shape of probability distribution) of geometric properties of sand waves?
For every analysed data set, a lot of stochastic characteristics are determined. This leads to a great amount of stochastic data. For all this data the mean values and standard deviations can be calculated and the coefficient of variation can be determined. The mean values for the long crested sand waves differ from the mean values found for the short crested sand waves. The same is the case for the standard deviation. The spread in the long crested sand waves is observed to be smaller than for the long crested sand waves.

The shape of the probability distributions that correspond best with the data are almost symmetrical for the geometric properties of the long crested sand waves and asymmetrical for the short crested areas. The PDFs for the short crested areas are all skewed to the left, except for the sand wave asymmetry. The asymmetry of the PDF of the sand wave asymmetry A shows that the shape of the sand waves is not sinus-like. Also the PDF of the long crested sand wave asymmetry are asymmetrical.

Are the different geometric properties in the available data set from the North Sea distributed according to a known probability distribution?
For each analysed geometric property the probability density function is determined and they are analysed in order to determine if they are distributed according to a known probability distribution. In Table 3.6 an overview is given of all the areas with the probability distribution corresponding best with the data.

In literature the Kolmogorv-Smirnov test is used to determine if a data set is distributed according to a certain probability distribution. In this study it is shown that the KS test not always performs as one would expect.

Based on the total vertical difference S between the cumulative density functions of the data and the probability distributions, the probability distributions with the best fit are determined (Table 3.6). For some data sets the normal distribution turned out to be the best fit, even when a skewness can be observed. In than case the mass of the distribution corresponds best with the normal distribution and the tail of the distribution corresponds best with a asymmetrical probability distribution.

Is there a relation between the standard deviation and the mean value for different geometric properties of sand waves, like was found for river dunes?
A linear fit is found between the mean value and the standard deviation. This means that the coefficient of variation C is a more or less a constant and can be used to estimate the standard deviation of a data set based on the mean value. The mean value for the sand wave height of a data set multiplied with the coefficient of variation leads to the standard deviation of the data set. The C_{avg} can be used as an estimator for the geometric properties (sand wave height, sand wave length, crest elevation, trough elevation and asymmetry) of the short crested sand wave fields analysed. The estimator is defined as:

$$\sigma = C\mu$$

The accuracy of the estimation differs per geometric property and is the highest for the sand wave length and sand wave height. For the other geometric properties a larger range of C values is observed. For the sand wave asymmetry the coefficient of variation showed the widest variation in values and will estimate values for the standard deviation less accurate based on the mean and average coefficient of variation. The coefficient of variation of the Ecomorf 3 area differs from the short crested values and as no other long crested areas are available it cannot be determined if a constant coefficient of variation can be found for long crested sand waves.

We observe a relation between the sand wave length and the sand wave height for the short crested Noordhinder areas. The sand wave length can be estimated by multiplying the sand wave height by 54. To determine if these correlations can be seen for the long crested area more data is needed. For all the short crested areas we observe that the values of the crest elevations are 1.72 times larger than the values for the trough elevations. So values for the crest elevation and the trough elevation cannot be referred to as amplitude.

Is there a relationship between the above stochastic characteristics and the extreme values of geometric properties of sand waves?
A relation is found between the mean value μ, the standard deviation σ and the distances (δ_5 and δ_{95}) between the extreme values (Δ_5 and Δ_{95}) and the mean μ. For each study area and geometric property the δ_5 and δ_{95} are divided by the standard deviation σ and constant values are found (a and b). With the constants a and b we can estimate the Δ_5 and Δ_{95} value based on the mean value μ and the standard deviation σ. As the coefficient of variation C based on the mean an the standard deviation is a constant as well, only mean value has to be measured in an area:

$$\Delta_{95} = (Cb + 1)\mu$$

$$\Delta_5 = -(Ca + 1)\mu$$

For both the long crested sand waves as the short crested sand waves this linear relation is found. Also for every geometric property this relation is determined for the lowest 5% percent of the values and the highest 5% percent. Of course the highest 5% is the most useful value to be able to estimate. The accuracy may improve when more data is analysed. The relation E between δ_5 and δ_{95} values can be used as to determine if the sand waves in an area are long crested or short crested.

Chapter 8

Recommendations

In this study many data was available, but only one data set consists of long crested sand waves. It turned out that short and long crested sand wave were hard to compare, however this statement is only grounded on one long crested data set. So more data sets of long crested sand waves will help to find out the differences between the two types of sand waves.

We observed that dredging has its effect on the result of the study. Because we do not know the locations or the amount of dredging in the areas, it is hard to estimate the impact of dredging on the stochastic characteristics of sand wave. More information on dredging will help to determine the influence of dredging on the stochastic characteristics of sand waves. Also the stochastic characteristics of short crested sand wave can be better determined, because now there may still be dredging activities in the Noordhinder areas.

The used bathymetry data consists of snap shots of different areas. The same areas should be measured under different circumstances as wind, surface waves, seasonal variations and tidal currents are all of influence on the sea bed. With different measurements in time these influences can be studied.

In new studies into the stochastic characteristics of the geometric properties, one should select study areas based on hydraulic conditions and grain size. With different measurements in space the influences of the hydraulic conditions and grain size can be studied.

The moving average line should be studied as trend line if more data is available and the need of including complete longitudinal bed elevation profiles is less high than in this study.

As the mean value μ is used to estimate the coefficient of variation C and the extreme values it is important to be able determine how many sand waves have to be measured in order to have a reasonable value for μ. This will probably differ for long crested sand waves and short crested sand waves and may differ for the different geometric properties. With more data and better estimators for the coefficient of variation C and the extreme values it should be studied if more can be said about the accuracy of the estimators.

Currently the total method is not user friendly for users in the North Sea area. To make the total method used widely applicable all the steps should be integrated as was done for the

BTT or a shell should be built around the Matlab tools.

The stochastic characteristics of sand waves need to be linked to bed surface information in order to be able to estimate the surface that needs to be dredged after the maximum crest elevation is known. A first intention is described in this thesis.

The latest version of the bedform tracking tool (Van der Mark and Blom, 2007) allows the user to determine the slope of the bedforms. This feature should be studied as it may be of interest for the construction of pipelines and cables in the North Sea. It is very interesting if the slope of the lee or stoss side is related to for instance the mean sand wave height or another stochastic characteristic. Also the slope could then be estimated based on only a few measurement in space or time.

Bibliography

Annambhotla, V. S. S., Sayre, W. W., and Liversy, R. H. (1972). Statistical properties of Missouri River bedforms. *Journal of the waterways, harbors and coastal engineering division ASCE*, 98:489–510.

Ashida, K. and Tanaka, Y. (1967). A statistical study of sand waves. *In: Proceedings of the 12th IAHR congress*, pages 103–110. Fort Collins, Colorado.

Barnard, P. L., Hanes, D. M., Rubin, D. M., and Kvitek, R. G. (2006). Giant sand waves at the mouth of san francisco bay. *Eos*, 87(29):285–289.

Bijker, R. (2006). Personal communication. ACRB, Lemmer, The Netherlands.

Brown, E., Colling, A., Pard, D., Philips, J., Rothery, D., and Wright, J. (2002). *Waves, tides and shallow-water processes*. The Open University, Milton Keynes, England, 2nd edition.

Cheong, F. and Shen, H. W. (1976). The intervals between successive zero crossings of sand bed profiles. *In: Proceedings 2nd International IAHR Symposium on Stochastic hydraulics*, pages 245–265. Lund, Sweden.

Crickmore, M. J. (1970). Effect of flume width on bedform characteristics. *Journal of the hydraulics division, ASCE*, 96:473–496.

DelftCluster (2003). Eco-morphodynamics of the seafloor. Theme 3: Coast and River.

Dorst, L. L. (2006). Personal communication. Hydrographic Service, Royal Netherlands Navy, The Hague, The Netherlands.

Gabel, S. L. (1993). Geometry and kinematics of dunes during steady and unsteady flows in the Calamus River, Nebraska, USA. *Sedimentology*, 40:237–269.

Havenbedrijf Rotterdam, N. V. (2006). Haven in cijfers 2005. www.port.rotterdam.nl.

Hoogewoning, S. and Boers, M. (2001). Fysische effecten van zeezandwinning, Rapport RIKZ/2001.050. National Institute for Coastal and Marine Management, Ministry of Transport, Public Works and Water Management, North Sea Directorate.

Hulscher, S. J. M. H. (1996). Tidal-induced large-scale regular bed form patterns in a three-dimensional shallow water model. *Journal of Geophysical Research*, 101(C9):20727–20744.

Hulscher, S. J. M. H. and Van de Brink, G. M. (2001). Comparison between predicted and observed sand waves and sand banks in the north sea. *Journal of Geophysical Research*, 106(C5):9327–9338.

IHB (2005). *Manual on hydrography, Publication M13*, 1st edition. International Hydrographic Bureau, Monaco.

Knaapen, M. A. F. (2005). Sandwave migration predictor based on shape information. *Journal of Geophysical Research*, 110.

Knaapen, M. A. F. (2006). Quality assessment tool for sand wave models. Twente University, Enschede, The Netherlands.

Knaapen, M. A. F. and Hulscher, S. J. M. H. (2002). Regeneration of sand waves after dredging. *Coastal Engineering*, 46:277–289.

Leclair, S. F., Bridge, J. S., and Wang, F. Q. (1997). Preservation of cross-strata due to migration of subaqueous dunes over aggrading and non-aggrading beds: comparison of experimeental data with theory. *Geoscience Canada*, 24(1):55–66.

Mahmood, K. and Ahmadi-Karvigh, H. (1976). Analysis of bed profiles in sand bed canals. *In: Proceedings Rivers '76*, pages 489–510. ASCE Waterways, Harbors and Coastal Engineering Division Specialty Conference.

Mathworks (2001). Statistics Toolbox User's Guide. The MathWorks Inc., url: http://www.mathworks.com.

McCave, I. N. (1971). Sand waves in the north sea off the coast of holland. *Marine Geology*, 10(3):199–225.

Morelissen, R., Hulscher, S. J. H. M., Knaapen, M. A. F., Németh, A. A., and Bijker, R. (2003). Mathematical modelling of sand wave migration and the interaciton with pipelines. *Continental Shelf Research*, 48:197–209.

Nelson, C. H., Baraza, J., and Maldonado, A. (1993). Mediterranean undercurrent sandy contourites, gulf of cadiz, spain. *Sedimentary Geology*, 82:103–131.

NIST/SEMATECH (2006). e-Handbook of Statistical Methods. National Institute of Standards and Technology (NIST) and SEMATECH Inc., url: http://www.itl.nist.gov/div898/handbook/ (March, 2007).

Németh, A. A. and Hulscher, S. J. M. H. and, D. V. H. J. (2003). Offshore sand wave dynamics, engineering problems and future solutions. *Pipeline & Gas Journal*, April:67–69.

Németh, A. A., Hulscher, S. J. M. H., and De Vriend, H. J. (2002). Modelling sand wave migration in shallow shelf seas. *Continental Shelf Research*, 22:2795–2806.

Nordin, J. H. (1971). Statistical properties of dune profiles. *Geological survey professional paper*, 562-F. U.S. government Printing Office, Washington.

Nordin, J. H. and Algert, C. F. (1966). Spectral analysis of sand waves. *Journal of the hydraulics division, ASCE*, 92:95–114.

Pluymaekers, S., Lindenbergh, R. C., Simons, D., and De Ronde, J. G. (2007). A deformation analysis of a dynamic estuary using two-weekly MBES surveying. *Proceedings Oceans'07 (In press), Aberdeen, United Kingdom.*

RIKZ (1997). RWS National Institute for Coastal and Marine Management (RWS RIKZ), Gebruikershandleiding, Digipol V1.0, Hoofdstuk 4 Interpolatie procedure. The Hague, The Netherlands.

RWS-Noordzee (2004). Regionaal Ontgrondingsplan Noordzee, 2004. Rijswijk, The Netherlands.

Shen, H. W. and Cheong, H. F. (1977). Statistical properties of sediment bed profiles. *Journal of the hydraulics division, ASCE*, 103:1303–1321.

Squarer, D. (1970). Friction factors and bedforms in fluvial channels. *Journal of the hydraulics division, ASCE*, 96:995–1017. Fort Collins, Colorado.

Stolk, A. (2000). The role of sand waves in the management of the Netherlands Continental Shelf. *In proceedings of Marine Sandwave Dynamics*, pages 199–200. Lille, France, 23 & 24 March 2000.

Stolk, A. (2006). Personal communication. Rijkswaterstaat, North Sea Directorate, Rijswijk, The Netherlands.

Stolk, A. (2007). Personal communication. Rijkswaterstaat, North Sea Directorate, Rijswijk, The Netherlands.

Tobias, F. C. (1989). Morphology of sand waves in relation to current sediment and wave data alont hte Eurogeul, North Sea. *Rep. GEOPRO 1989*. Department of Physical Geography, University of Utrecht, The Netherlands.

Van de Meene, J. W. H. and Van Rijn, L. C. (2000). The shoreface-connected ridges along the central Dutch coast, part 2: morphological modelling. *Continental Shelf Research*, 20:2325–2345.

Van der Mark, C. F. and Blom, A. (2007). A new and widely applicable tool for determining the characteristics of bedform dimensions. CiT Report, Twente University, Enschede, The Netherlands.

Van der Mark, C. F., Blom, A., Hulscher, S. J. M. H., Leclair, C. F., and Mohrig, D. (2005). On modelling the variability of bedform dimensions. *River, Coastal and Estuarine Morphodynamics: RCEM 2005*, pages 831–841.

Van der Mark, C. R., Blom, A., and Hulscher, S. J. M. H. (2007). Variability in bedform characteristics using flume and river data. *In press*. 8 p., University of Twente, Water Engineering and Management, Enschede, the Netherlands.

Van der Veen, H. H., Hulscher, S. J. M. H., and Knaapen, M. A. F. (2006). Grain size dependancy in the occurence of sand waves. *Ocean Dynamics*, 56:228–234.

Van Dijk, T. A. G. P. and Kleinhans, M. G. (2005). Processes controlling the dynamics of compound sand waves in the North Sea, Netherlands. *Journal of Geophysical Research*, 110.

Van Maren, D. S. (1998). Sand Waves - A state-of-the-art review and bibliography. North Sea Directorate, Ministry of Transport, Public Works and Water Management, Rijswijk, The Netherlands.

Wang, W. C. and Shen, H. W. (1980). Statistical properties of alluvial bed forms. *In: Proceedings of the 3rd international symposiom on stochastic hydraulics*, pages 371–389. Tokyo, Japan.

Wüst, J. C. (2004). Data-driven probabilistic predictions of sand wave bathymetry. *In: Marine Sandwave and River Dune Dynamics, MARID 2004*, pages 338–344. Enschede, The Netherlands.

Wüst, J. C. (2007). Personal communication. AVV Transport Research Centre, Rijkswaterstaat, Rotterdam, The Netherlands.

Yang, C. T. and Sayre, W. W. (1971). Stochastic model for sand dispersion. *Journal of the hydraulics division, ASCE*, 97:265–288.

Appendix A

Plan views and gradients

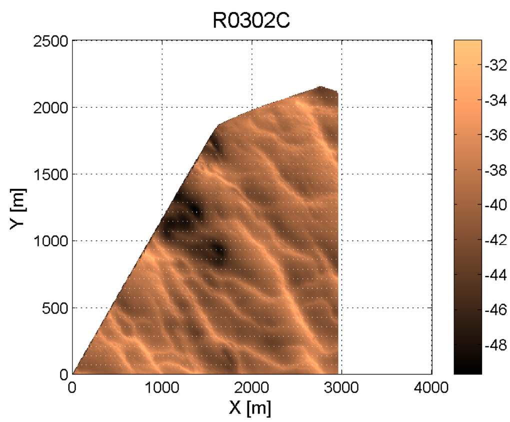

(a)

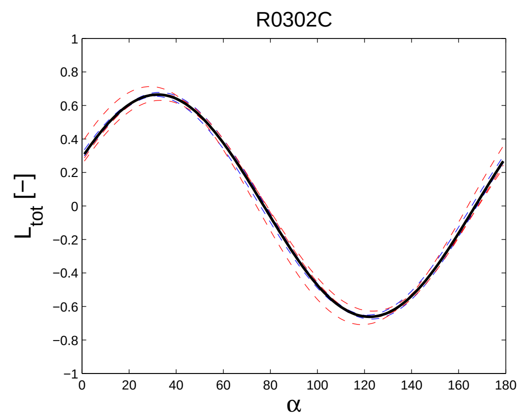

(b)

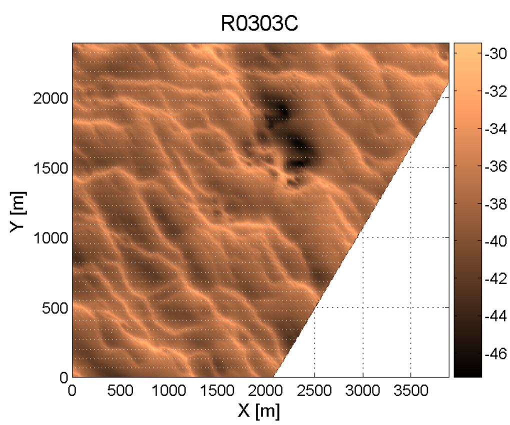

(c)

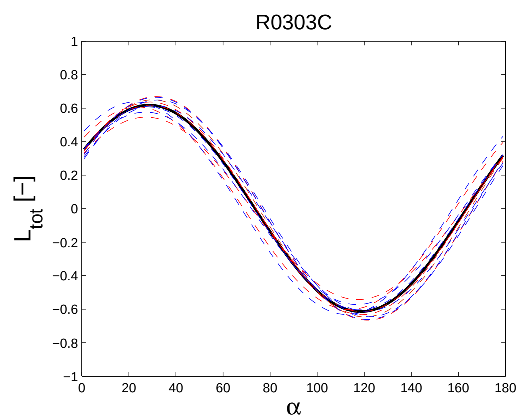

(d)

Figure A.1: Study areas in the Noordhinder area and a plot of the dimensionless gradient.

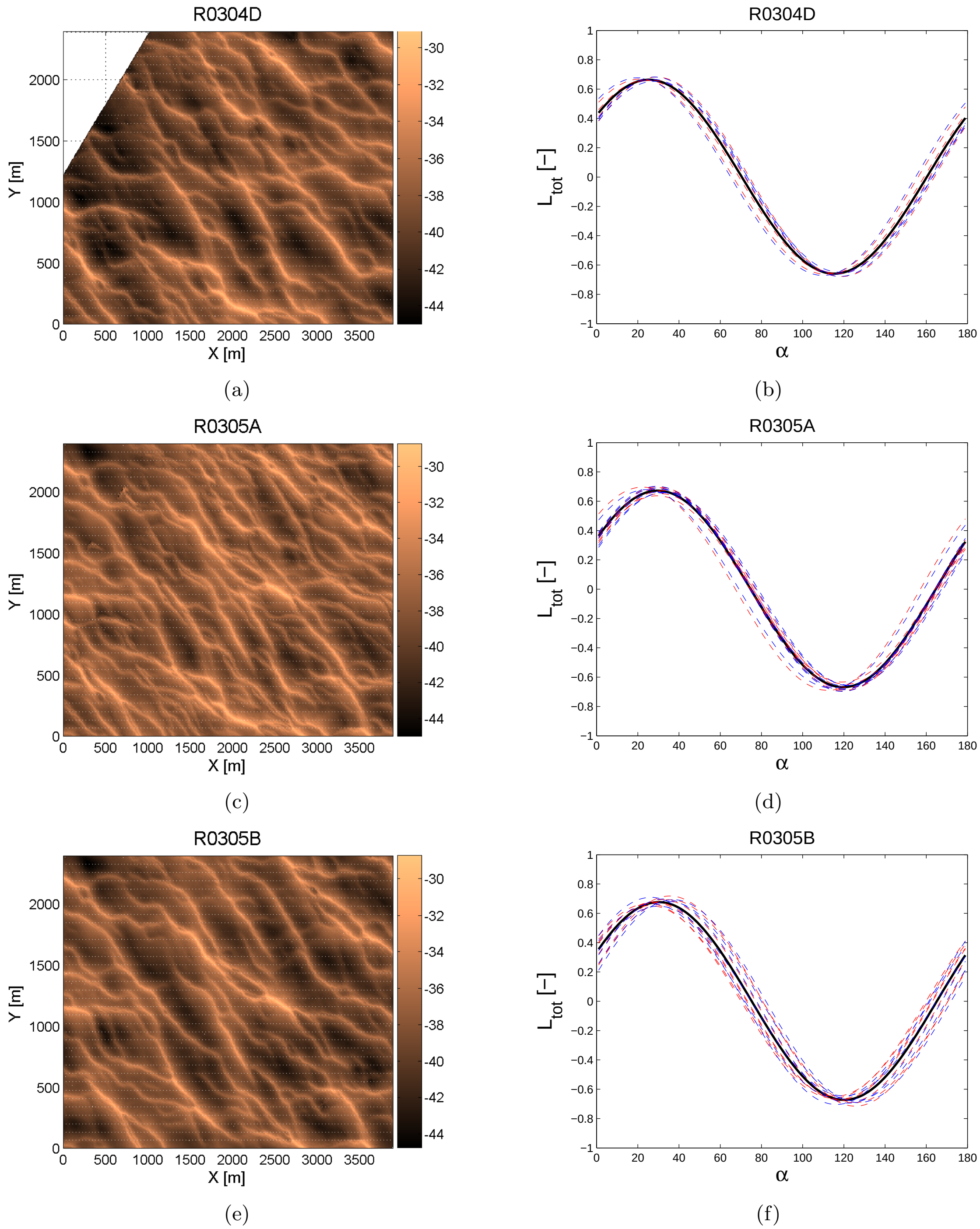

Figure A.2: Study areas in the Noordhinder area and a plot of the dimensionless gradient.

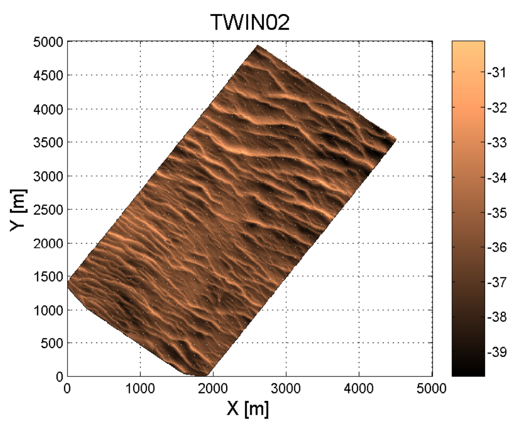

(a)

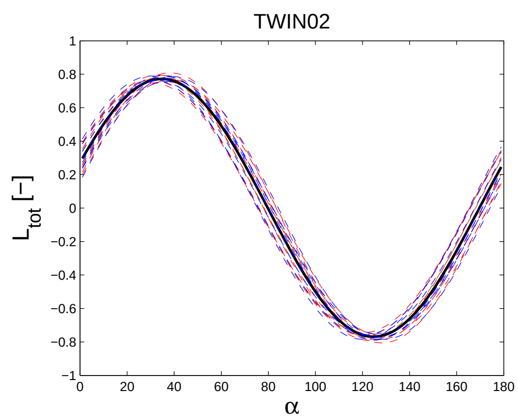

(b)

Figure A.3: Study area 02 in the TWIN area and a plot of the dimensionless gradient.

Appendix B

PDFs of sand wave height

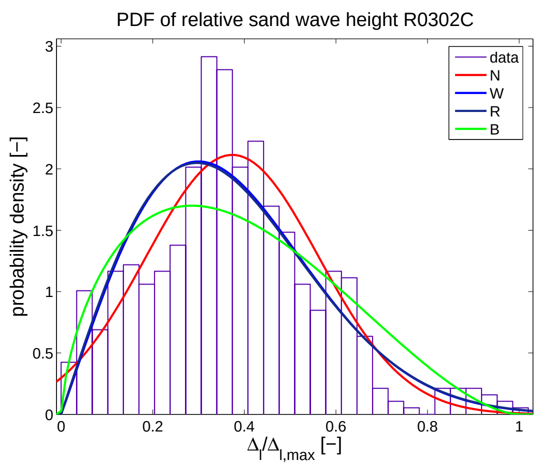

(a)

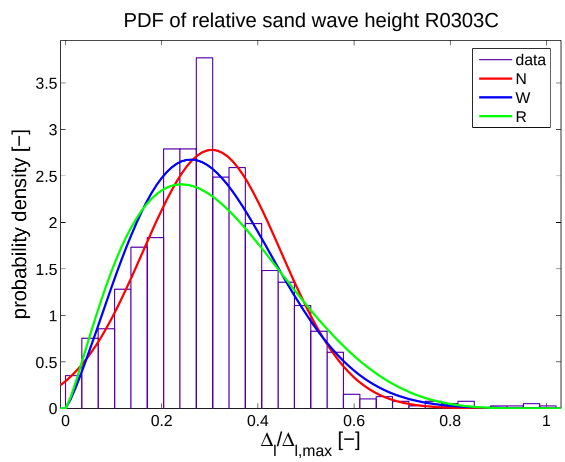

(b)

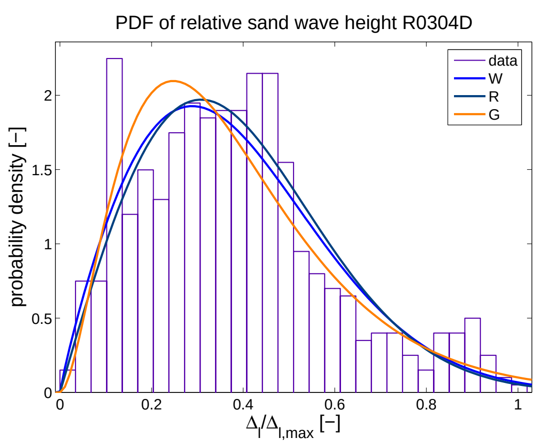

(c)

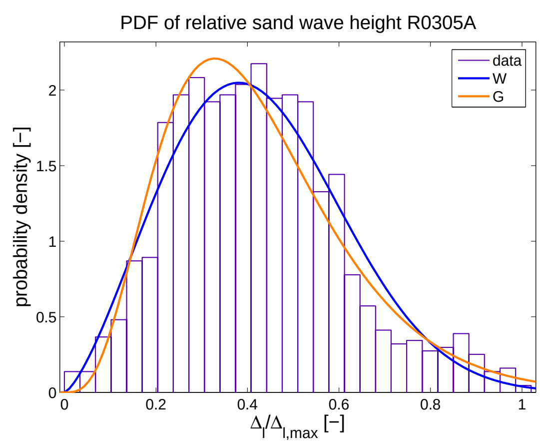

(d)

Figure B.1: Sand wave height in the Noordhinder area. PDFs of the relative sand wave height (Δ_l^*)

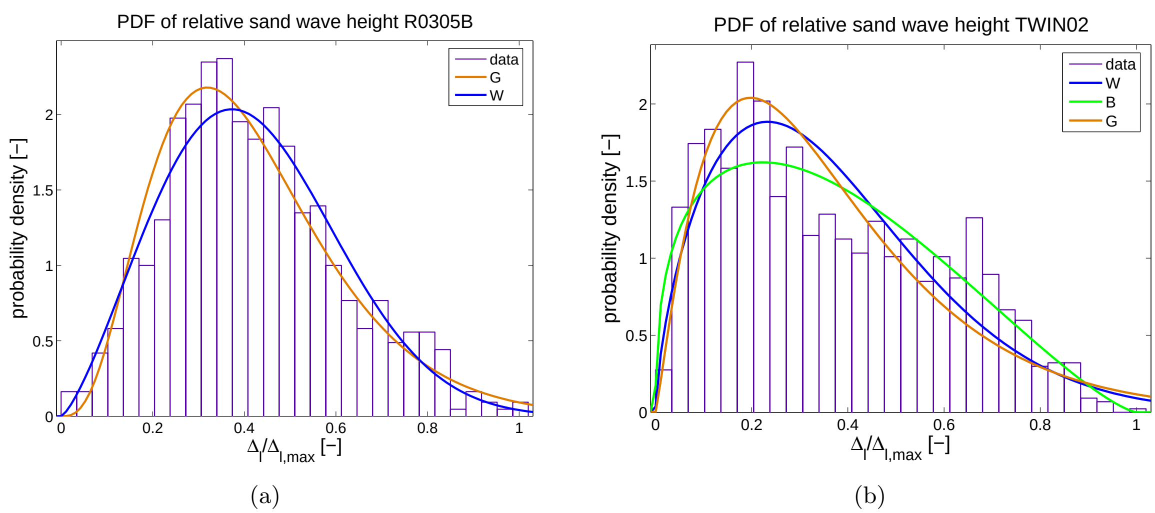

Figure B.2: Sand wave height in the Noordhinder area and TWIN area. PDFs of the relative sand wave height (Δ_l^*).

Appendix C

PDFs of sand wave length

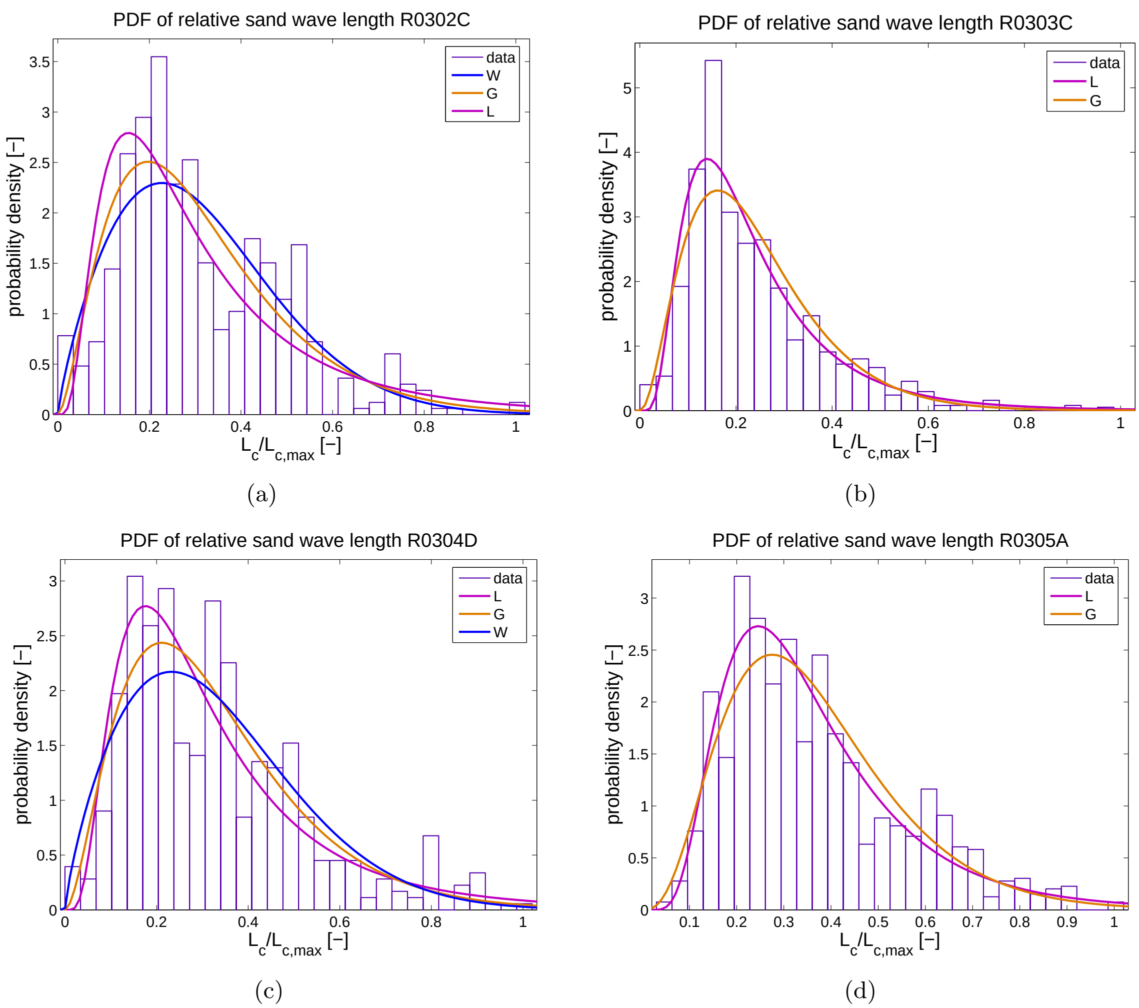

Figure C.1: Sand wave length in the Noordhinder area. PDFs of the relative sand wave height (L_c^*)

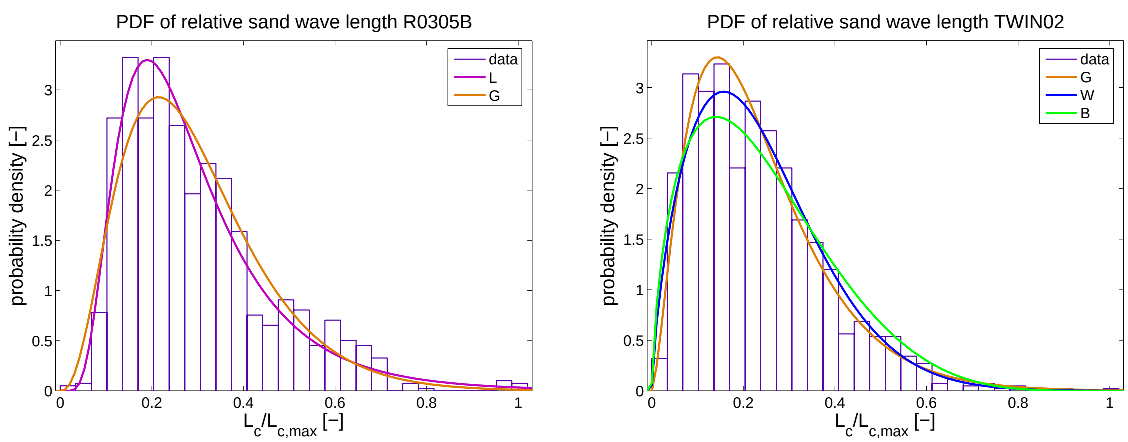

(a) (b)

Figure C.2: Sand wave length in ta Noordhinder area and TWIN area. PDFs of the relative sand wave height (L_c^*)

Appendix D

PDFs of crest elevation

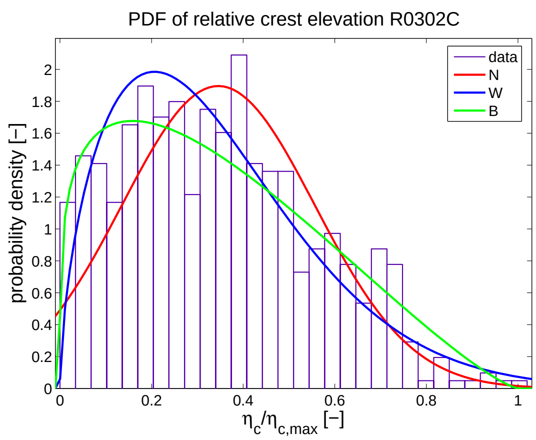

(a)

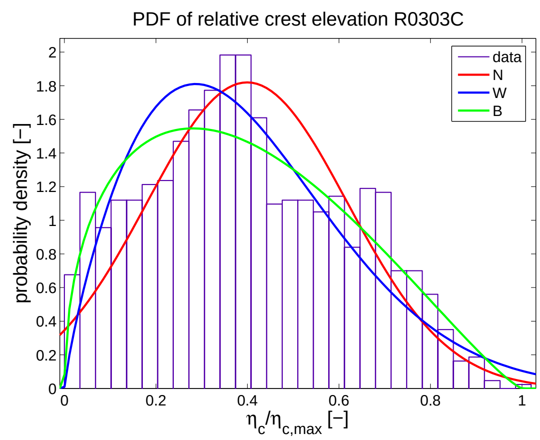

(b)

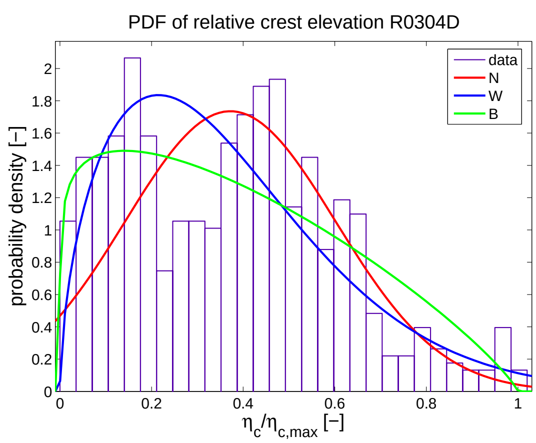

(c)

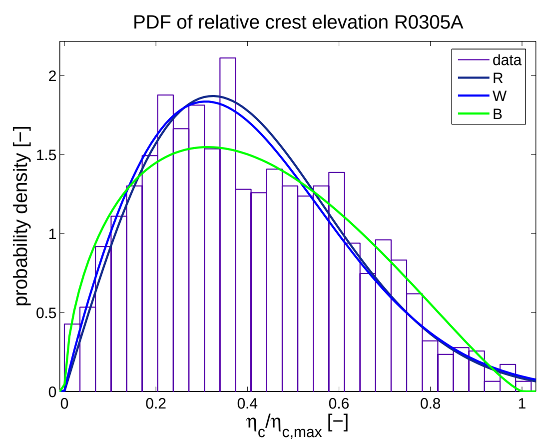

(d)

Figure D.1: Crest elevation in the Noordhinder area. PDFs of the relative crest elevation (η_c^*).

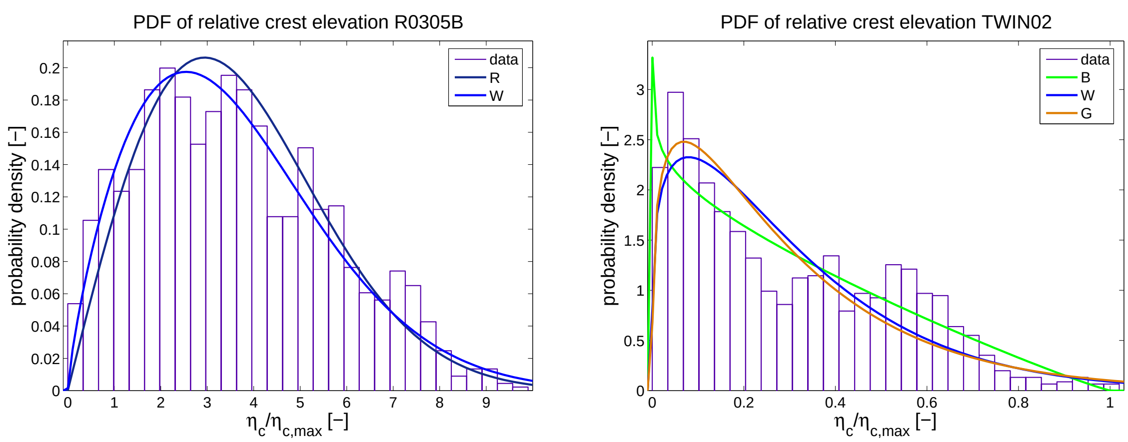

(a) (b)

Figure D.2: Crest elevation in the Noordhinder area and TWIN area. PDFs of the relative crest elevation (η_c^*).

Appendix E

PDFs of trough elevation

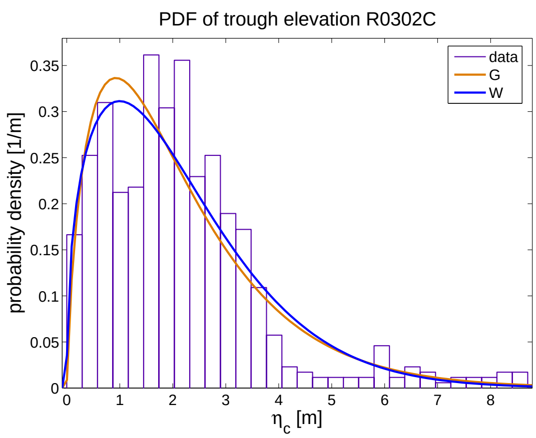

(a)

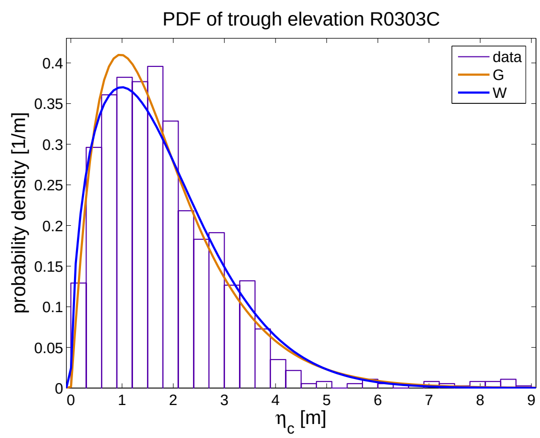

(b)

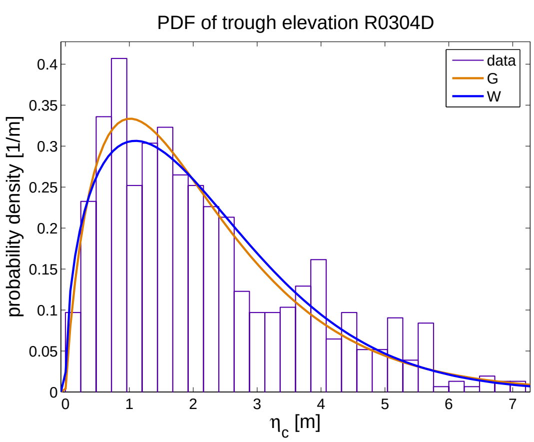

(c)

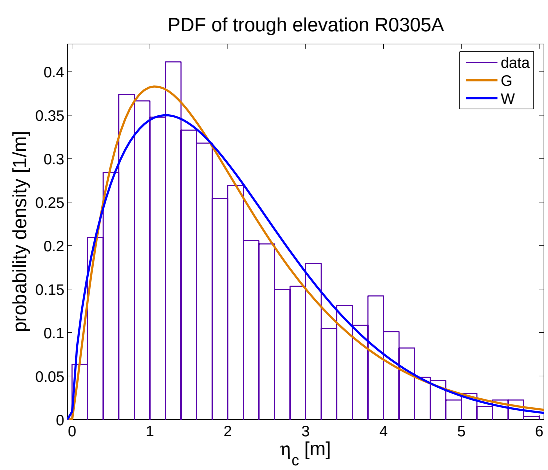

(d)

Figure E.1: Trough elevation in the Noordhinder area. PDFs of the relative trough elevation (η_t^*).

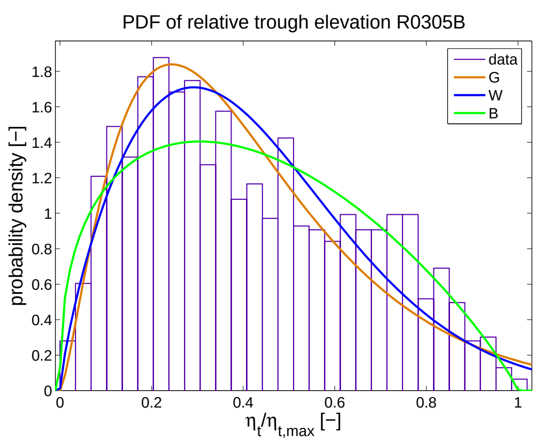

(a)

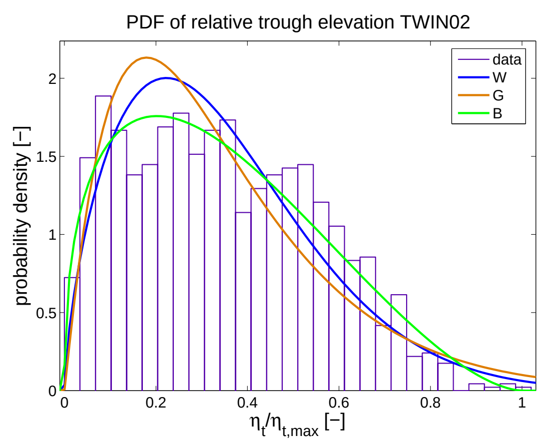

(b)

Figure E.2: Trough elevation in the Noordhinder area and TWIN area. PDFs of the relative trough elevation (η_t^*).

Appendix F

PDFs of sand wave asymmetry

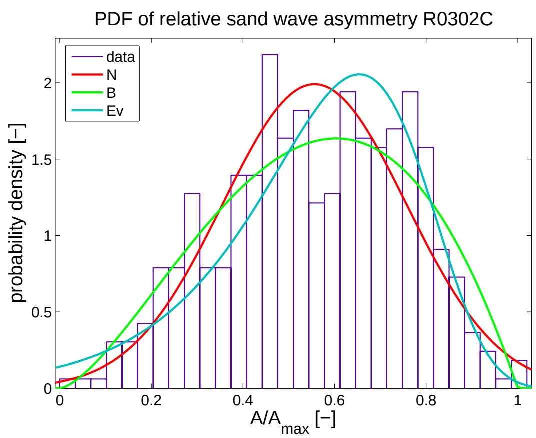

(a)

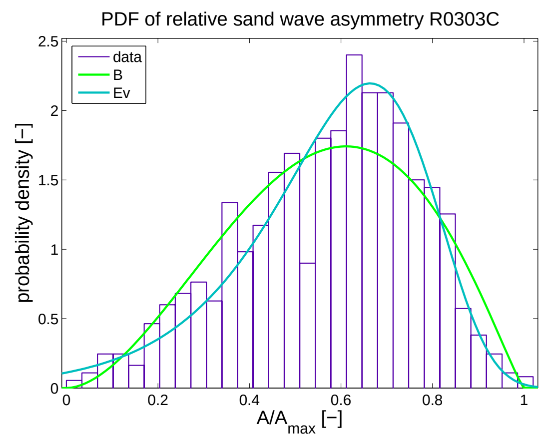

(b)

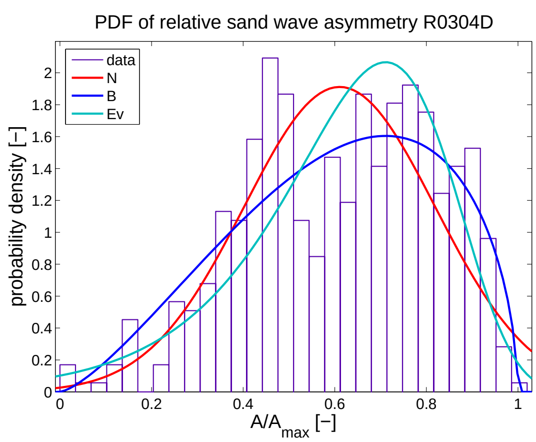

(c)

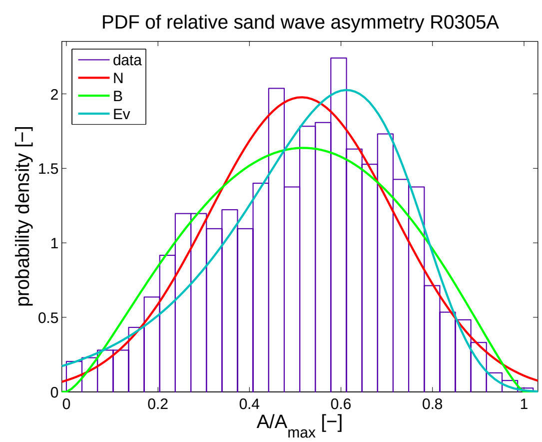

(d)

Figure F.1: Sand wave asymmetry in the Noordhinder area. PDFs of the sand wave asymmetry A at different locations.

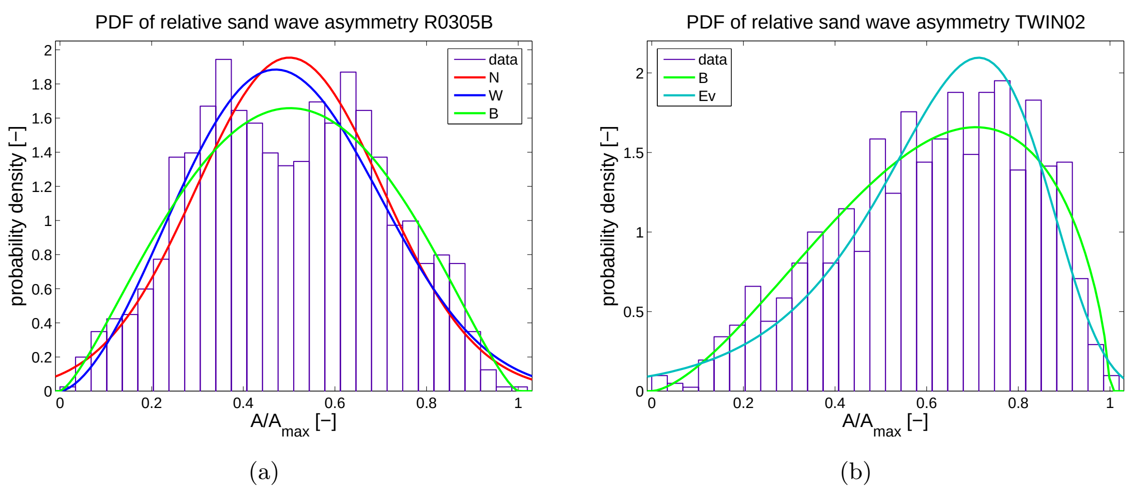

Figure F.2: Sand wave asymmetry in the Noordhinder area and TWIN area. PDFs of the sand wave asymmetry A at different locations.